MONOGRAPH

13th European Young Engineers Conference 2025

Scientific Club of Chemical and Process Engineering „Venturi”

Faculty of Chemical and Process Engineering
Warsaw University of Technology

Warsaw University of Technology

GOOD Solution

Monograph

13th European Young Engineers Conference
Warsaw, 7-9th April 2025

EYEC Monograph

All papers reviewed by the Scientific Committee

This monograph has been issued for the thirteen edition
of the European Young Engineers Conference which
was held 7 – 9 April 2025 at the Faculty of Chemical
and Process Engineering, Warsaw University of Technology

Warsaw 2025 · Eleventh volume
ISBN 978-83-953822-5-3

Contents

Introduction

We are thrilled to present the upcoming edition of the European Yong Engineers Conference, which offers a unique opportunity for young researchers to connect, collaborate and exchange ideas in a vibrant academic setting. We are proud to see that the EYEC continues to grow in popularity, attracting both our long-standing participants and many new faces taking their first steps in the world of scientific research. As we worked throughout the year to organize this conference, we have strived to make it an even more engaging and enriching experience than before.

We hope the lectures from our distinguished Special Guests have enabled you to broaden your knowledge or sparked new research interests. Whether you're delving deeper into familiar fields or discovering new areas of study, we believe the talks and discussions will offer invaluable insights. We look forward to seeing you next year at the European Young Engineers Conference, where we will once again come together to share groundbreaking ideas and innovations.

Additionally, we would like to extend our heartfelt appreciation to the members of the Scientific Committee who worked diligently to ensure the highest quality of submitted papers. Your invaluable assistance and guidance are greatly valued by all of us, the organizers and young scientists alike. We would like to express our sincere gratitude to the Dean and the authorities of the Faculty of Chemical and Process Engineering for their unwavering support for this initiative from the very beginning and encourage us to continue it.

We warmly invite you to actively participate in both the formal scientific sessions and the more informal networking opportunities, which will allow you to build valuable connections with fellow researchers. We hope that this year's event will be a catalyst for new ideas, collaborations, and innovative research that will shape the future of engineering and science.

~ Organizing Committee

1 Special Guests

1.1 Prof. József Kalmár

Jozsef Kalmár*,1

1. Department of Inorganic and Analytical Chemistry, University of Debrecen, Debrecen, Hungary

e-mail: kalmar.jozsef@science.unide.hu

Dr. József Kalmár earned his Ph.D. in 2013 and worked for two years as a research chemist in the R&D division of TEVA Pharmaceutical Works. He joined the faculty of the University of Debrecen in 2014, where he currently serves as a habilitated associate professor. Since then, he has established a new research direction focusing on application-related structure-property-function relationships in porous nanostructured materials. Under his supervision, several new functional aerogels have been prepared and characterized. His team has investigated the mechanisms of hydration-induced structural changes in aerogels (Acta Biomater. 2020, Appl. Surf. Sci. 2020, ACS Appl. Mater. Interf. 2021, Adv. Mater. Interf. 2023), sorption equilibria (Dyes Pigm. 2016, Int. J. Mol. Sci. 2022), catalytic reactions (Appl. Surf. Sci. 2021, Appl. Surf. Sci. 2022), surface complexation of metal ions (ACS Appl. Nano Mat. 2020, Chemosph. 2021, Appl. Surf. Sci. 2022) and drug delivery systems (Carbohydr. Polym. 2018, Chem. Eng. J. 2024). The team's innovative mechanistic approach has been recognized by the EU Aerogel Community, resulting in regular invitations to participate in joint EU consortium projects.

Abstract: Aerogels – Understanding the relationship between the structural characteristics and the properties of the known lowest density porous solids

Keywords: *aerogel, structural characterization, hydration, NMR, SANS*

Aerogels have exceptionally high porosities (up to 99%), highly permeable micro- and/or mesoporous structures, high specific surface areas in the mesoporous region (up to 1000 $m^2 \cdot g^{-1}$), and low densities (below 0.1 $g \cdot cm^{-3}$). Aerogels are widely researched for biomedical applications (e.g. drug delivery systems, wound healing and tissue regeneration scaffolds) and environmental engineering applications (e.g. sorbents for pollutants). Therefore, understanding the fundamental structural characteristics in their dry and wet states, together with the mechanism of hydration of the backbone and the consequent modification of the aerogel structure is essential for establishing structure-properties-functions relationships. Dry aerogel structures are characterized by highly interconnected and permeable pore systems. The hydration of aerogels is usually accompanied by significant structural changes, which can cause volume reduction, the stiffening of the aerogel, and, in extreme cases, the collapse of the pores.

Dry aerogels are usually characterized by scanning electron microscopy (SEM), N_2 sorption porosimetry, infrared spectroscopy (IR) and solid-state nuclear magnetic resonance spectroscopy (NMR). The wetting mechanisms of aerogels are investigated using liquid phase NMR spectroscopy and small angle neutron scattering (SANS) techniques. NMR relaxometry is informative on the extension of the hydration sphere of the backbone. The geometry and the size of water droplets in the solid backbone can be measured by NMR cryoporometry. The self-diffusion properties of water can be measured by gradient stimulated echo (PGSTE) NMR spectroscopy, giving information on the permeability of the hydrated pore network. SANS experiments reveal the hydration induced rearrangement of the aerogel backbone and the consequent alteration of the fractal properties of the porous structure [1-5].

The fundamental hydration mechanisms of the archetypical silica aerogel, and the anomalous hydration of silica-gelatin and silica-casein hybrid aerogels are discussed. An example is also given for structural changes during the hydration of a biopolymer, i.e. Ca (II)-alginate aerogel.

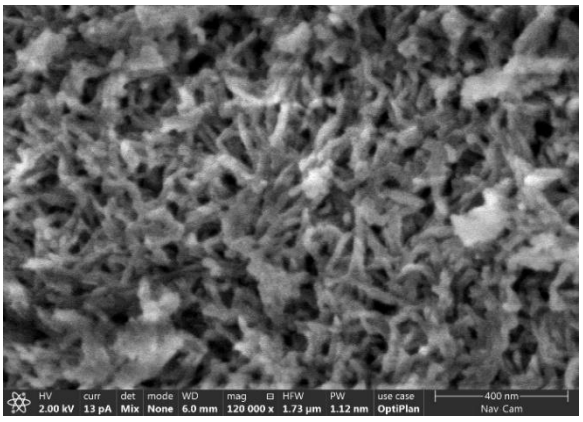

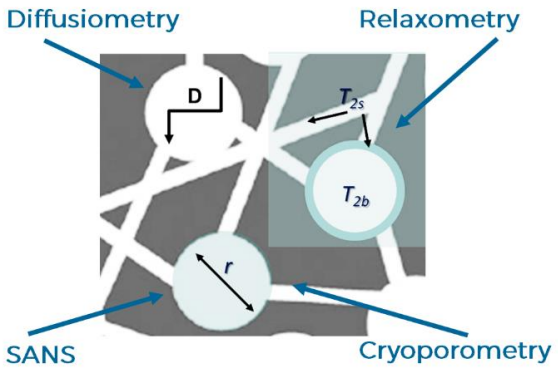

References

[1] P. Veres, et.al. Colloids Surf. B 152, 229-237. (2017)

[2] M. Kéri, et.al. Acta Biomater. 105, 131-145. (2020)

[3] I. Lázár, et.al. Appl. Surf. Sci. 531, 147232. (2020)

[4] A. Forgács, et.al. ACS Appl. Mater. Interfaces 13(2), 2997-3010. (2021)

[5] P. Paraskevopoulou, et.al. ACS Appl. Nano Mater 4(10), 10575–10583. (2021)

1.2 Assoc. Prof. Kenji Sugimori

Kenji Sugimori*,1

1. FACULTY OF MEDICINE, TOHO UNIVERSITY, TOKYO, JAPAN

e-mail: kensan19551207@gmail.com

Born on December 7, 1955, Dr. Sugimori is an esteemed biologist with a distinguished career at Toho University Faculty of Medicine in Tokyo. He holds a BSc in Hygiene Science from Kitasato University, specializing in virology (measles).

His research focuses on microorganisms that inhabit special environments such as hot springs and crater lakes, and he conducts research on microorganisms that live in environments with high temperatures and strong acidity. He discovered a new type of bacteria in near-boiling hot spring water.

Recently, Dr. Sugimori has been exploring Fango Therapy—a hot spring-based wellness treatment using thermophilic algae extracts. As Chairman of the Spa Fango Healthy Ageing Society, he educates therapists in this innovative field. His dedication earned him an award from Japan's Minister of the Environment for achievements in hot spring science (2016). He had more than 100 lectures and published more than 40 papers about the bacteria living in the extreme environments and their background of their living, he has also chaired multiple international conferences and held teaching positions at various universities.

Abstract: The useful effects for human body used by Fango, maturated with hot spring water

KEYWORDS: *Fango, Fangotherapy, Biofango®, thermal effect, pain relief*

Background and Objectives:

Fango therapy is a medical treatment method in Europe that uses peloids aged in hot spring water. We focused on the fango practiced in Abano, Italy, and improved it into Biofango®, a "Japanese-style fango" made from natural hot spring water and aged peloids. In this presentation, we will report on the verification of the various medical effects of fango, including its thermal effect.

Materials and Methods:

The subjects' surface body temperature and blood flow rate were checked to compare hot tap water bathing, hot spring water bathing, and Biofango® treatment. True Fango (Biofango®) and imitation Fango (made with flowed hot tap water) were compared with the data of deep body temperature (DBT), changes in pulse (CP), changes in stroke volume index (CSVI) and changes in diastolic blood pressure (CDBP).

We also checked about physical findings and skin symptoms on the body and face with a questionnaire survey on true and imitation Fango treatment.

The pain relief effect of osteoarthritis on the knee by Biofango® treatment were investigated using crossover study with randomly selecting 2 groups (A group; Biofango® group, B group; usual treatment destination group) of 43 men and women (over 50 years old) who had osteoarthritic knee disease.

Results and Conclusion:

Biofango® was observed to have a thermal effect that maintains normal blood pressure and blood flow, in contrast to hot spring baths and tap water baths, which increase blood pressure. In addition, a comparison of real Fango and imitation Fango showed that real Fango was effective in data on deep body temperature (DBT), pulse rate change (CP), stroke volume index (CSVI), and diastolic blood pressure (CDBP), and also demonstrated a sufficient thermal effect (significant difference ($p<0.05$) in the thermal effect data over 7 days) and did not place a burden on the body's blood pressure.

The pain relief effect of osteoarthritis on the knee showed significant improvement effect in the Fangotherapy compared to usual treatment, and pain reduction effect was recognized.

1.3 Assoc. Prof. Katarzyna Siuzdak & Assoc. Prof. Katarzyna Grochowska from Science Misson

Katarzyna Siuzdak*,1, Katarzyna Grochowska *,1

1. INSTITUTE OF FLUID-FLOW MACHINERY, POLISH ACADEMY OF SCIENCE, GDANSK, POLAND

e-mail: kontakt@science-mission.pl

Assoc. Prof. Katarzyna Siuzdak

She leads the Department of Physical Aspects of Ecoenergy at one of the units of the Polish Academy of Sciences in Gdansk. During her studies, she combined biotechnology with technical physics, later earning a PhD in chemical technology. She completed an internship in France and obtained a habilitation in technical sciences. She is a recipient of the Start Fellowship from Foundation for Polish Science, the Ministry of Science and Higher Education of Poland Scholarship, and the Prof. W. Nernst Award. She has authored over 100 publications and book chapters, as well as patents. In 2022, she was listed among the 22 Polish women to watch, according to Forbes Women.

Assoc. Prof. Katarzyna Grochowska

She works at the Department of Physical Aspects of Ecoenergy at PAN in Gdansk. She graduated in biomedical physics, and during her studies, she took courses at the Faculties of Mathematics, Physics, and Computer Science, Chemistry, and Biology at the University of Gdansk, as well as at the Medical University of Gdansk and Gdansk University of Technology. She earned a PhD in mechanics, completed seven international research internships in countries such as Germany, Portugal, and Croatia, and obtained her habilitation in materials engineering. She has authored over 70 research articles, 5 book chapters, as well as patents and utility models. She has received numerous awards, including the Polish Intelligent Development Award and the Fulbright STEM Impact Award.

Since 2021, both scientists have been popularizing science online through their Instagram account @science_mission, which in 2023 was recognized in the "Popularizer of Science" competition and won the POP-SCIENCE award at the Silesian Science Festival in Katowice. Their work can be explored on their website: https://science-mission.pl/.

2 Scientific Commission

2.1 Assoc. Prof. Donata Konopacka-Łyskawa

FACULTY OF CHEMISTRY, GDANSK UNIVERSITY OF TECHNOLOGY, GDANSK, POLAND

Donata Konopacka-Łyskawa is an Associate professor at the Faculty of Chemistry, Gdańsk University of Technology. Since 2024 she has been the Head of the Department of Process Engineering and Chemical Technology. She obtained her PhD degree (2000) in Chemical Technology from the Faculty of Chemistry at Gdańsk University of Technology, and her DSc (habilitation) degree (2020) from the Faculty of Chemical Technology and Engineering at West Pomeranian University of Technology in Szczecin. In 2002 she completed an internship at Grupement de Recherches de Lacq (TotalFinaElf, Lacq Research Center) in France. Her research interests are focused on processes in multiphase systems: particles precipitation in a gas-liquid system, hydrolysis and fermentation of lignocellulosic biomass, and carbon dioxide capture technologies. She is the author and coauthor of several dozen scientific publications, a chapter in the Encyclopedia of Colloid and Interface Science, two patents, and numerous papers presented at national and international conferences.

2.2 Beata Butruk-Raszeja, PhD

FACULTY OF CHEMICAL AND PROCESS ENGINEERING, WARSAW UNIVERSITY OF TECHNOLOGY, WARSAW, POLAND

Beata Butruk-Raszeja, BEng PhD obtained her PhD in chemical engineering from Warsaw University of Technology (WUT) in 2013. Currently she is an assistant professor at WUT, where she teaches courses on cell culture and biomedical nanotechnology. Her research focuses on blood– material interactions, bioactive coatings, tissue engineered vascular grafts and 3D bioprinting.

2.3 Rafał Anyszka, PhD

INSTITUTE OF POLYMER AND DYE TECHNOLOGY, FACULTY OF CHEMISTRY, LODZ UNIVERSITY OF TECHNOLOGY, LODZ, POLAND

Rafal Anyszka is currently busy designing a high-performance rubber for the Mars environment in the frame of Marie Sklodowska-Cure Action project RED 4 MARS. The project is realized in collaboration between the Lodz University of Technology, the University of Twente and The University of Akron. Rafal Anyszka got his Ph.D. in 2014 at the Lodz University of Technology, designing ceramifiable elastomer composites for fire protection systems. Afterwards, he was involved in the development of sulfur-derived polymers and sulfur concretes. In 2017 he started Postdoc projects at the University of Twente, designing molecular Velcro systems for silica-rubber coupling and surface-functionalized nano-silica for high-voltage DC polypropylene insulation composites. His expertise covers rubber composites and surface functionalization of mineral fillers. He is passionate about Space exploration and designing new materials for extraterrestial use.

2.4 Agnieszka Markowska-Radomska, PhD

FACULTY OF CHEMICAL AND PROCESS ENGINEERING, WARSAW UNIVERSITY OF TECHNOLOGY, WARSAW, POLAND

Agnieszka Markowska-Radomska, PhD works at the Faculty of Chemical and Process Engineering at Warsaw University of Technology (WUT). Her scientific interests lie in exploring the potential of liquid dispersed systems, particularly multiple emulsions, as advanced multifunctional carriers for the encapsulation and

delivery of active agents. Her research encompasses experimental investigations (release study) and modelling of mass transfer within emulsion systems. Currently, she is focused on developing innovative carriers tailored for anti-cancer therapeutic applications. Dr. Markowska-Radomska also explores the role of liquid dispersed systems in environmental protection, particularly in separation processes such as the extraction of heavy metal ions and the removal of organic compounds using emulsion liquid membranes (ELMs).

2.5 Marcin Odziomek, PhD

FACULTY OF CHEMICAL AND PROCESS ENGINEERING, WARSAW UNIVERSITY OF TECHNOLOGY, WARSAW, POLAND

Marcin Odziomek received his PhD in Chemical Engineering in 2014 and started work as an assistant professor at WUT in 2015. He currently heads the Laboratory of Process Equipment at the Faculty of Chemical and Process Engineering. His research interests focus on the processes of aerosol formation in devices intended for medical purposes, aerosol dynamics, physical modelling of the effects of inhaled aerosols on the respiratory system and new concepts in pulmonary inhalation drug delivery. More recently, his work has also been on using aerosols to improve the efficiency of combustion processes in the energy sector. During his work, he led three projects funded by public resources, participated in research grants funded by the industry, and was a member of the International Society for Aerosols in Medicine (ISAM). He received an individual Award from the Rector of Warsaw University of Technology for scientific and educational achievements and a scholarship from the Marshal of the Mazowieckie voivodeship.

2.6 Krzysztof Wojtas, PhD

FACULTY OF CHEMICAL AND PROCESS ENGINEERING, WARSAW UNIVERSITY OF TECHNOLOGY, WARSAW, POLAND

Krzysztof Wojtas works for Warsaw University of Technology as an Assistant Professor at the Faculty of Chemical and Process Engineering. His research is currently focused on the application of computational fluid dynamics, supplemented with population balance, to predict the course of industrial processes and in biomedical research, to predict phenomena accompanying blood flow in the human cardiovascular system.

Krzysztof finished both his MEng (2011) and PhD (2017) in chemical engineering at the Warsaw University of Technology. His doctoral dissertation was focused on the identification, analysis and description of relations between flow, mass exchange (mixing) and the course of complex chemical reactions occurring in jet reactors. In 2018, Krzysztof joined the Department of Chemical Engineering at Loughborough University as a Research Associate, where he conducted mixing process simulations to identify key process parameters in the scale-up of polymer resin production in automotive industry. Afterwards, in 2019, he joined the Division of Separation Processes at Faculty of Chemical and Process Engineering WUT.

Since his employment at WUT, Dr Wojtas has been awarded several grants regarding application of population balance to both homogenization process modeling and biomedical research, to estimate the risk of primary and secondary arterial stenosis associated with coronary artery disease. His commitment is also recognized by students—he was awarded Individual Rector's Award for outstanding teaching. In addition to his research and teaching activities, Dr Wojtas shares his knowledge and experience also by working with many Polish companies, including ANWIL S.A., Polpharma Biologics Warsaw Sp. z o.o., SAWEX S.A.

3 Scientific committee

Kamil Czelej, PhD	WARSAW UNIVERSITY OF TECHNOLOGY, POLAND
Nikou Hamzehpour, PhD	UNIVERSITY OF MARAGHEH, IRAN
Artur Małolepszy, PhD	WARSAW UNIVERSITY OF TECHNOLOGY, POLAND
Krzysztof Wojtas, PhD	WARSAW UNIVERSITY OF TECHNOLOGY, POLAND

4 Organizing committee

The thirteenth edition of the European Young Engineers has been organized by the following members of the Scientific Club of Chemical and Process Engineering "Venturi", students and researchers of The Faculty of Chemical and Process Engineering:

Grzegorz Bernacki, BSc	Main Coordinator
Maria Marecka	Coordinator of the Logistics Section
Maria Rewolińska	Coordinator of the Contact Section
Monika Klimek, MSc	Coordinator of the Monograph Section
Izabela Kazimierczak	Coordinator of the Monograph Section Vice-chairwoman of Scientific Club of Chemical and Process Engineering "Venturi"
Zuzanna Kupniewska	Coordinator of the Sponsorship Section Chairwoman of Scientific Club of Chemical and Process Engineering "Venturi"
Martyna Musiatowicz, BSc	Coordinator of the Social Media Section

Rafał Czajka, BSc	Jakub Lewandowski, MSc	Karolina Traczyk
Zuzanna Dąbała	Adrian Malinowski	Aleksandra Sawczuk
Adam Grzybowski	Kinga Matejczuk	Amini Seyedshoja, MSc
Laura Derwiszyńska	Aleksandra Pisarek, MSc	Dominika Siekiera
Wiktoria Kucharska	Kamil Pruchniak, BSc	Maria Ziółkowska

5 Monographic articles

5.1 Kinetic studies of new photoinitiating systems to obtain high-performance dental resins dedicated to 3D printing.

Jakub Pietraszewski[1], Monika Topa-Skwarczyńska*, Karolina Kozanecka, Filip Petko, Mariusz Galek, Joanna Ortyl

1. Faculty of Chemical Engineering and Technology, Cracow University of Technology, Cracow, Poland

e-mail: monika.topa-skwarczynska@pk.edu.pl

KEYWORDS: *photopolymerization, photoinitiating systems, 3D printing*

Abstract

Many photoinitiators on the market rely on UV light, which can be limiting for manufacturing techniques that use visible light sources. This study addresses the need for more versatile photoinitiators that can work effectively with visible light sources, commonly found in modern 3D printers.

The aim of this study was to develop and test new two-component photoinitiating systems capable of initiating radical photopolymerization under visible light. This research sought to create high-performance resin formulations for 3D printing applications in the dental industry. To evaluate the performance of these new systems absorbance study and real-time FT-IR spectroscopy were used, providing key insights into the polymerization kinetics of the compositions. To assess the photodegradation of the new systems, photolysis studies were conducted.

This work shows that these new systems significantly improve reactivity, delivering high conversion rates and low induction times, which are critical for achieving consistent and high-quality prints. The adaptability and compatibility with visible light sources offer high print quality, stability, and durability, making these systems a viable alternative to traditional UV-based initiators. Overall, this study contributes to advancing the use of radical photopolymerization in 3D printing and highlights the potential of new photointiating systems as resins with high performance for the dental industry.

Introduction

In 3D printing for dental applications, UV light has traditionally been used to cure photosensitive resins due to its ability to quickly initiate polymerization. However, it has several limitations; it is unable to deeply penetrate the resin, leading to incomplete curing of intricate designs, as well as the fact that prolonged exposure to UV light can degrade resin and be harmful to the operator's health as well as the patient's (e.g. when curing dental fillings inside a patient's mouth) (Bagheri & Jin, 2019). This is one of the main reasons why the industry should shift towards safer light wavelengths from the visible spectrum, like 405 nm (Grimm, 2024). Visible light penetrates deeper into the resin, improving the structural integrity of the print and ensuring more uniform curing. The shift also aligns with the modern advancements in photochemistry and resin formulations, where new photoinitiating systems that require higher wavelength light spectra are readily made, like the ones explored in this study (Bennett, 2017).

Radical photopolymerization is a chemical process induced by light, in which a photoinitiator (photosensitive material) absorbs light and generates free radicals that initiate a chain reaction of photopolymerization (Christmann et al., 2019). The general stages of this process are initiation, propagation and termination. During the first step, initiation, absorption of UV or visible light by the photoinitiator occurs. This mechanism splits light into reactive free radicals that are capable of interacting with monomers, such as methacrylates used in this study, forming active centers. During the next phase, propagation, the active centers react with surrounding monomer molecules, facilitating polymerization of polymer chains. During the final stage, termination, the polymerization process stops when two active centers react with each other, when an active center encounters an inhibitor of the process or when simply there is no more material in the system (Chen et al., 2016, "VAT photopolymerisation: Additive Manufacturing").

The process of radical polymerization is used in a wide range of industries, like painting, optics and electronics (Min et al., 2015). In this work, the process was studied with the dentistry industry in mind, where its fast and precise chain formation enables the curing of resins inside a patient's mouth. In addition, radical photopolymerization is greatly utilized in 3D printing of crowns, inlays, bridges, and dental models, where the process is capable of fabricating complex geometries with fine details and minimal material waste, compared to traditional manufacturing methods (Abdul-Monem, 2020).

3D VAT printing is an additive manufacturing method, where the liquid photopolymer is cured layer by layer by light, usually building the object an entire layer at a time in a vat. Digital Light Processing (DLP) is a 3D VAT printing method that uses a digital projector to cure photosensitive. The projector has a digital micromirror device (DMD) that reflects light to create precise and complex geometric patterns, enabling prints that are high in resolution, with fine details and

smooth surfaces, making it ideal for dental printing (Chaudhary et al., 2022). Compared to other popular 3D VAT methods, like stereolithography (SLA), where the layer is cured by a laser in a path, DLP is particularly advantageous in terms of the speed of printing; and compared to Liquid Crystal Display (LCD), where the printer uses a fixed-resolution LED panel, DLP offers higher resolution and better accuracy. Overall, DLP technology is a versatile and efficient option for industries like dentistry that require high quality, precise and structurally solid prints with a low printing time (Weng et al., 2023, "VAT photopolymerization").

In 3D printing for dental applications, UV light has traditionally been used to cure photosensitive resins due to its ability to quickly initiate polymerization. However, it has several limitations; it is unable to deeply penetrate the resin, leading to incomplete curing of intricate designs, as well as the fact that prolonged exposure to UV light can degrade resin and be harmful to the operator's health as well as the patient's (e.g. when curing dental fillings inside a patient's mouth) (Bagheri & Jin, 2019). This is one of the main reasons why the industry should shift towards safer light wavelengths from the visible spectrum, like 405 nm (Grimm, 2024). Visible light penetrates deeper into the resin, improving the structural integrity of the print and ensuring more uniform curing. The shift also aligns with the modern advancements in photochemistry and resin formulations, where new photoinitiating systems that require higher wavelength light spectra are readily made, like the ones explored in this study (Bennett, 2017).

A base molecule and molecules with six different compounds were synthesized. The new photoinitiating systems studied in this work addressed several of the problems described as well as the challenges associated with the traditional photoinitiators, which are limited absorption in the visible light spectrum, inefficient polymerization kinetics, and low resolution in 3D printing (Shao et al., 2014). Comprehensive experiments were conducted to evaluate the new systems. Absorbance measurements were examined to determine their compatibility with the targeted light sources, while Real-Time FT-IR spectroscopy was utilized to study the kinetics and conversion rates of radical photopolymerization. The practical efficacy of the systems in 3D printing were validated via a 3D VAT DLP Lumen X+ printer. Each experiment was conducted to explore the potential of the new systems to obtain high-performance resins dedicated to 3D printing in dental applications.

Methods

Spectrophotometric analyses were conducted using a SilverNova spectrometer, paired with a tungsten-deuterium lamp as the UV-Vis light source, both of which were produced by StellarNet INC. Absorbance spectra were obtained from solutions contained in a quartz cuvette with a precise optical path length of 1 centimeter. Absorbance measurements were performed to evaluate the optical properties of the solution across the UV-Vis spectrum. The use of the quartz cuvette with a constant optical path length ensured accuracy and consistency of the measurements.

The system kinetics and the final conversion rates of the polymer compositions were analyzed in real time using Fourier-Transform Infrared Spectroscopy (FT-IR). Measurements were conducted with the Nicolet™ i10 spectrometer from Thermo Scientific, equipped with a horizontal attachment to enable instantaneous monitoring of the photopolymerization process. During the analysis, samples were irradiated using a M405L4 Vis-LED from ThorLabs INC. at 20 mW·cm^2 (1000 mA) light intensity. The measurements were captured using OMNIC software, with exposure of the sample starting 10 seconds after data recording. The radical systems with a UDMA/TEGDMA blend were measured in samples in ring form (thickness of 1.4 mm) and polypropylene film (thickness of 25 μm). Conversion rates were determined using Equation 3.1.1, based on changes in the monitored band area (A_{After}), relative to the initial area (A_{Before}), with the targeted bandwidths at 6164 cm^{-1} and 1634 cm^{-1} for the 1.4 mm and 25 μm film thickness samples respectively.

$$C_{FT-IR}\,[\%] = \left(1 - \frac{A_{After}}{A_{Before}}\right) \cdot 100\ \% \qquad (3.1.1)$$

where:

A_{Before} – area of the absorbance peak characteristic for appropriate monomer and type of photopolymerization before curing,

A_{After} – area of the same absorbance peak after the polymerization process.

The test prints were carried out on a DLP printer, LumenX+ from CELLINK. The printing process utilized a specialized build plated coated with polydimethylsiloxane (PDMS) to enhance adhesion and facilitate layer separation. A single layer height of 100 um was maintained, 65% of maximum optical power was used, equating 28 mW·cm^{-2}. Various layer irradiation times were explored. The Lumen X+ printer was chosen as it is specifically designed for high-resolution 3D printing of biocompatible materials, offering precise control over layer thickness and light exposure, making it ideal for dental application.

Photolysis studies were done on the best-performing systems to assess its stability under continuous exposure to 405 nm light. Measurements were conducted with the StellarNET SilverNova spectrometer. The samples were irradiated for a specified duration

of 30 minutes, and their structural integrity was monitored to identify any signs of degradation.

The newly developed photoinitiating systems used in this study are based on a series of seven synthesized molecules, all sharing a common molecular core structure with variations introduced through different substituents. This design aims to explore how the substituents influence the photophysical and photochemical properties of the molecules. The substituents include a methyl group (-CH_3), a methoxy group (-OCH_3), a thiomethyl group (–SCH_3), a nitrile group (–CN), a fluoro group (–F), and a trifluoromethyl group (–CF_3). Each substituent changes various properties of the system such as light absorption, radical generation efficiency, and compatibility with resin formulations, providing insight into the relationship between molecular structure and photoinitiation behavior. The compounds with their substituents and their acronyms were presented in Table 5.1.1 Substituents of the molecules used in this study with their acronyms.

Table 5.1.1 Substituents of the molecules used in this study with their acronyms.

Acronym	Substituents
PHT06-102	-H
PK04-003	-CH_3
PHT18-103	-OCH_3
PHT18-133	-SCH_3
PHT18-145	-CN
PK03-007	-F
Pk03-006	-CF_3

Outside of the studied new molecules, other materials used in the study were as such; monomers undergoing photopolymerization according to radical mechanism were urethane dimethylacrylate (UDMA, Sigma Aldrich) mixed with triethylene glycol dimethacrylate (TEGDMA, Sigma Aldrich) in a 7:3 ratio. A traditional commercial photoinitiator IOD (Lambson Ltd.) was used as component of the photoinitiating system for radical polymerization. Methyldiethanolamine (MDEA, Fluorochem) is an amine co-initiator that was used to boost the photopolymerization process and radical generation. The chemical formulas of the respective substances used in the study were presented in Figure 5.1.1.

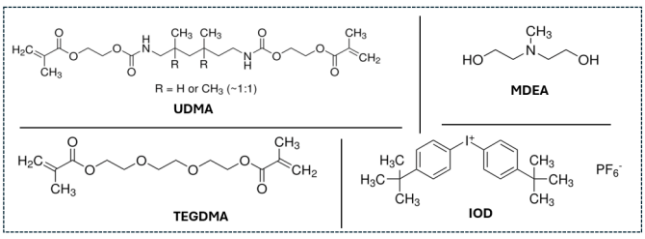

Figure 5.1.1. The chemical formulas monomers and co-initiators used in the study.

Results

Spectroscopic analysis of the new compounds focused on absorbance measurements to evaluate their light absorption spectrum. Pure acetonitrile was used as the solvent for the absorption spectrum. 1mg of the new molecules were dissolved in 3 ml of acetonitrile for absorbance and photolysis measurements. This allowed us to check their compatibility with long-wavelength light sources, especially those within the light spectrum at around 405 nm. The experiments revealed that the new molecules exhibit strong absorption in the 350 to 420 nm range, being in the visible light spectrum and containing 405 nm wavelength. This characteristic aligns with the light wavelengths in modern printers, ensuring efficient activation in them while printing. The photoinitiators' absorbance spectra were displayed in Figure 5.1.2.

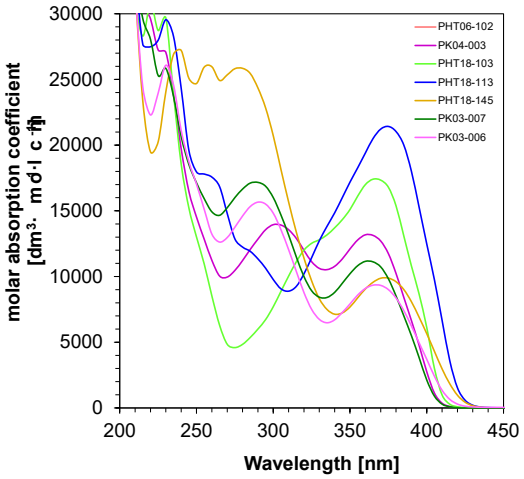

Figure 5.1.2 Absorption spectra of the new compounds.

Photolysis studies were performed to assess the stability of the best-performing photoinitiating system under 405 nm light exposure. This experiment revealed that the system maintained their structural integrity and exhibited minimal degradation over extended irradiation, highlighting its durability and reliability.

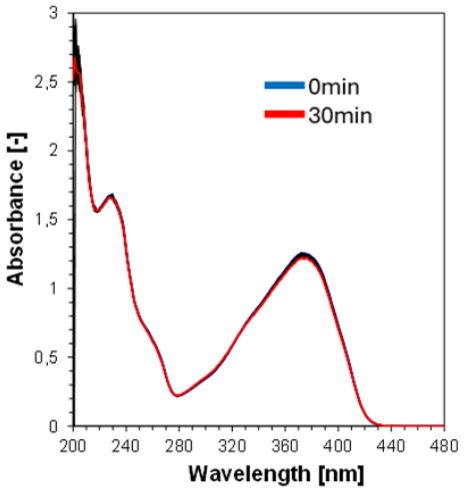

Figure 5.1.3 Photolysis of PHT18-133 (1%$_{w/v}$) in ACN u der 405 nm light, exposure time 30 minutes.

Real-Time FT-IR analysis was employed to study the photopolymerization kinetics of the newly synthesized photoinitiating systems, providing insights into their efficiency and conversion rates under visible lights. The systems measured in this study were compositions of 1 mg of the new compound, 1 g of UDMA/TEGDMA monomer blend (in 7:3 weight ratio) and 3 mg of IOD. They were exposed to a 405 nm LED diode at 20 mW·cm^{-2} light beam, simulating the condition in typical modern 3D printing applications. In Figure 5.1.3 ring sample of 1.4 mm thickness was monitored to see band changes at 6134 cm^{-1}, associated with the depletion of double bonds. The sample demonstrated rapid initiation from 10 to 60 seconds after irradiation, as well as high progression of polymerization, achieving high conversion rates up to 70%. In Figure 5.1.4, polypropylene film sample of 25 µm thickness was monitored to see band changes at 1634 cm^{-1}, associated with the depletion of double bonds. The sample demonstrated rapid initiation from 10 to 40 seconds after irradiation, as well as high progression of polymerization, achieving high conversion rates up to 50%. The results indicate effective utilization of visible light energy, highlighting the high reactivity of the radical photopolymerization process in these systems with low induction times and steady reaction progress. As shown, the substituents in the compounds' structures influence conversion rates and the compound with the highest achieved conversion rates was for the PHT18-133 with the thiomethyl group (–SCH_3) substituent. This data further validates the kinetics of these systems when exposed to visible light sources at 405 nm, emphasizing their potential for improving the performed in high-resolution 3D printing in dental applications.

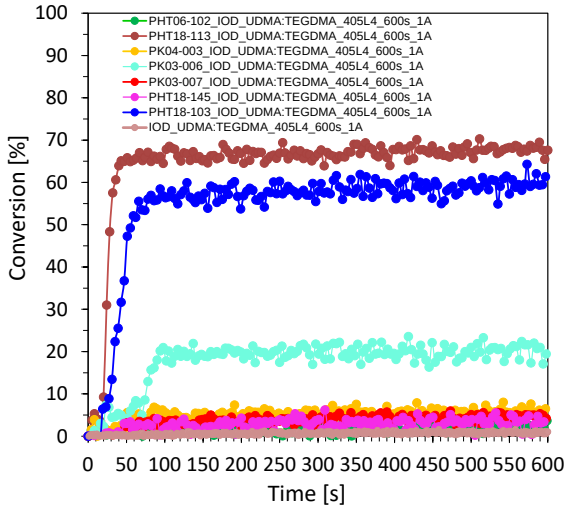

Figure 5.1.4 Kinetic profiles presenting real time photopolymerization process of radical reactive systems in UDMA/TEGDMA composition with IOD 0.3% w/w and different new compounds at 0.1%$_{w/w}$. A 1.4 mm thick sample exposed to 20 mW·cm^{-2} light beam at 405 nm for 600 seconds.

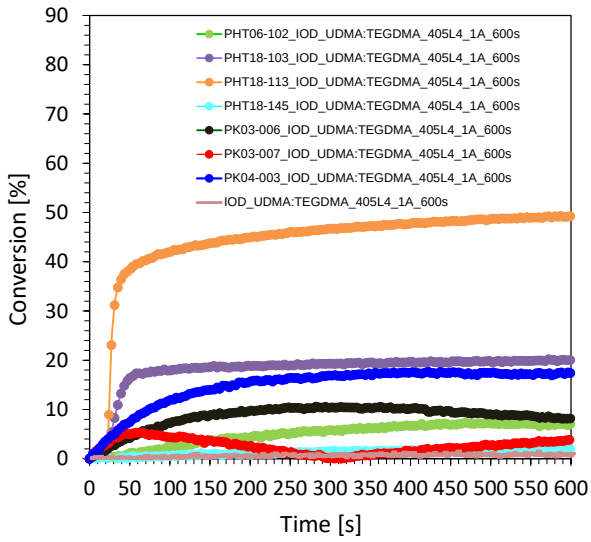

Figure 5.1.5 Kinetic profiles representing real time photopolymerization processes of radical reactive systems in UDMA/TEGDMA composition with IOD 0.3%$_{w/w}$ and different new compounds at 0.1%$_{w/w}$. A 25 µm thick sample exposed to 20 mW·cm^{-2} light beam at 405 nm for 600 seconds.

The photoinitiating system deemed most promising for 3D printing applications was PHT18-133, based on FT-IR and absorbance results. Strong absorbance at 405 nm wavelength and high conversion rates during photopolymerization enabled precise curing of the resin, leading to production of high-quality 3D objects. Using the DLP Lumen X+, three prints were achieved in Figure 5.1.5, Figure 5.1.6 and Figure 5.1.7. The printed objects had the same layer thickness and light beam intensity, but different light exposure times. The system's compatibility with visible light and great reactivity in radical photopolymerization shows it as a promising candidate for use in the dental industry, advancing the development of dental restoration.

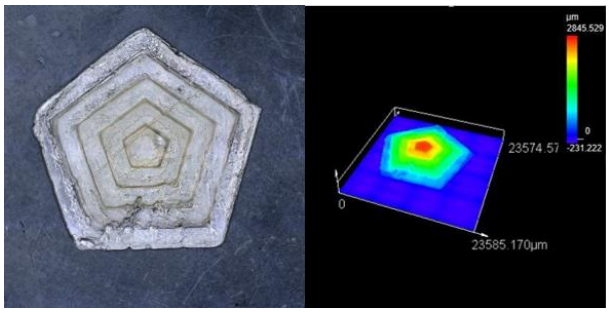

Figure 5.1.6 OLYMPUS microscope photos of a PHT18-113 (0.1%$_{w/w}$), IOD (0.3%$_{w/w}$), UDMA: TEGDMA (1 g) system in a 3D printed object on Lumen X+. Irradiation power 65%, light beam 28 mW·cm^{-2}, bottom layer light exposure time 40 s, layer exposure time 10 s, layer height 100 µm. On the left, a microscope photo of the printed object; on the right, a rendered 3D height model of the printed object.

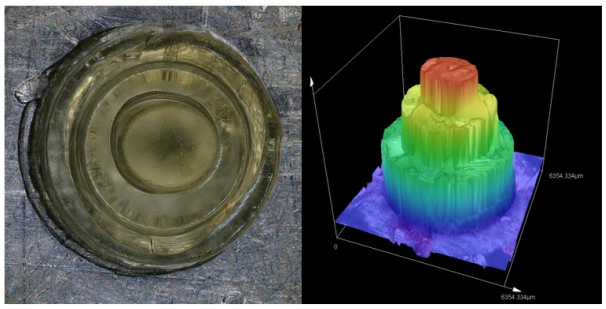

Figure 5.1.7 OLYMPUS microscope photos of a PHT18-113 (0.1%$_{w/w}$), IOD (0.3%$_{w/w}$), UDMA: TEGDMA (1 g) system in a 3D printed object on Lumen X+. Irradiation power 65%, light beam 28 mW·cm^{-2}, bottom layer light exposure time 50 s, layer exposure time 10 s, layer height 100 µm. On the left, a microscope photo of the printed object; on the right, a rendered 3D height model of the printed object.

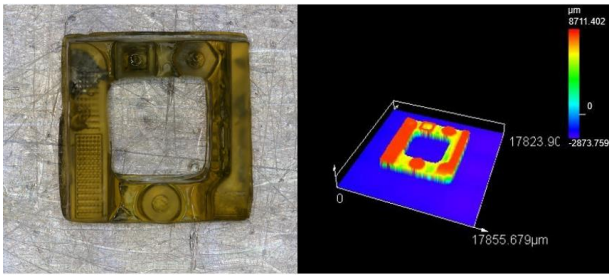

Figure 5.1.8 OLYMPUS microscope photos of a PHT18-113 (0.1%$_{w/w}$), IOD (0.3%$_{w/w}$), UDMA: TEGDMA (1 g) system in a 3D printed object on Lumen X+. Irradiation power 65%, light beam 28 mW·cm^{-2}, bottom layer light exposure time 53 s, layer exposure time 7 s, layer height 100 µm. On the left, a microscope photo of the printed object; on the right, a rendered 3D height model of the printed object.

Discussion

The absorbance measurements displayed strong alignment with 405 nm wavelength, which is the standard in common printers nowadays (Ciocan et al., 2024). Real Time FT-IR analysis further confirmed and underlined the systems' ability for efficient radical generation and photopolymerization. As shown in Figure 5.1.3 and Figure 5.1.4, the newly developed photoinitiating systems demonstrated significantly higher conversion rates at 405 nm in real-time FT-IR analysis compared to the traditional UV-based photoinitiator IOD. This indicates superior kinetics under visible light conditions. The enhanced performance of these systems highlights their potential as safer and more energy-efficient alternatives to conventional UV-based initiators in 3D printing applications.

The interpretation of the kinetics of the new photoinitating systems in radical photopolymerization process highlights the critical role of molecular structure in influencing polymerization efficiency and reactivity under visible light. The substituents attached to the base molecule play a crucial role in influencing the systems' efficiency by altering the electronic environment of the molecule, which directly impacts radical generation and polymerization kinetics. The thiomethyl group (–SCH_3) was found to lead to the highest conversion rates, likely due to its strong electron-donating properties, which enhance radical generation and stability. The methoxy group (–OCH_3), another electron-donating substituent, also demonstrated high efficiency, though slightly less than the thiomethyl group, suggesting subtle differences in their influence. In contrast, electron-withdrawing groups such as cyano (–CN) and fluoro (–F) likely reduced radical generation efficiency by stabilizing the excited-state molecule, slowing initiation and polymerization kinetics. The variations in substituents directly influenced the system's ability to generate radicals, control initiation rates, induction times, and sustain polymer growth, with the most effective photoinitiating system being PHT18-133, with an electron-donating thiomethyl group (–SCH_3) as its substituent. The results emphasize the critical relationship between a photoinitiator's chemical structure, spectral properties and kinetic behavior. Preliminary photolysis experiments were conducted to evaluate the stability of the new photoinitiating systems when exposed to 405 nm light, showcasing their photostability under prolonged irradiation, further supporting their suitability for applications in 3D printing and dental environments.

This study is an introductory work of the new synthesized compounds, upon which further and more advanced research about 3D printing and kinetics in the dental industry can be conducted. This investigation allowed us to select the most promising and effective photoinitiating systems. Future research could focus on their long-term stability or degradation under extended exposure to light or human saliva.

This work mainly focused on exploring the photoinitiators in the visible light spectra around 405 nm wavelength, while future studies could explore their broader compatibility with visible light spectrum. Only DLP 3D printing technology was explored, so investigation into other popular printing methods could provide deeper insight into the new systems.

Conclusion

In this work, photoinitiating systems suitable for radical photopolymerization processes were developed. Moreover, this study highlights the development of novel photoinitiating systems for radical photopolymerization under visible light for dental applications. They achieved rapid photopolymerization kinetics, characterized by minimal induction times and high conversion rates. These systems demonstrated great performance in practical applications, that is, in DLP 3D printing, achieving high resolution prints with stable structures. They showed significant potential for demanding applications in the dental industry, enabling efficient and versatile manufacturing processes.

Acknowledgements

Kinetic research and 3D printing was funded by National Centre for Research and Development in Poland under the Lider Program, grant number LIDER13/0156/2022. Moreover, spectroscopic study was conducted as part of the program OPUS LAP, grant number 2020/39/I/ST5/03556

References

Abdul-Monem, M. M. (2020). Naturally derived photoinitiators for dental and biomaterials applications. European Dental Research and Biomaterials Journal, 1(02), 72–78. https://doi.org/10.1055/s-0040-1721313

Bagheri, A., & Jin, J. (2019). Photopolymerization in 3D printing. ACS Applied Polymer Materials, 1(4), 593–611. https://doi.org/10.1021/acsapm.8b00165

Bennett, J. (2017). Measuring UV curing parameters of commercial photopolymers used in additive manufacturing. Additive Manufacturing, 18, 203–212. https://doi.org/10.1016/j.addma.2017.10.009

Chaudhary, R., Fabbri, P., Leoni, E., Mazzanti, F., Akbari, R., & Antonini, C. (2022). Additive manufacturing by Digital Light Processing: A Review. Progress in Additive Manufacturing, 8(2), 331–351. https://doi.org/10.1007/s40964-022-00336-0

Chen, M., Zhong, M., & Johnson, J. A. (2016). Light-controlled radical polymerization: Mechanisms, methods, and applications. Chemical Reviews, 116(17), 10167–10211. https://doi.org/10.1021/acs.chemrev.5b00671

Christmann, J., Ley, C., Allonas, X., Ibrahim, A., & Croutxé-Barghorn, C. (2019). Experimental and theoretical investigations of free radical photopolymerization: Inhibition and termination reactions. Polymer, 160, 254–264. https://doi.org/10.1016/j.polymer.2018.11.057

Ciocan, L. T., Vasilescu, V. G., Pantea, M., Pi ūru, S. M., Imre, M., Ripszky Totan, A., & Froimovici, F. O. (2024). The evaluation of the Trueness of dental mastercasts obtained through different 3D printing technologies. Journal of Functional Biomaterials, 15(8), 210. https://doi.org/10.3390/jfb15080210

Engineering Product Design. (2024, June 27). VAT photopolymerization. Engineering Product Design. https://engineeringproductdesign.com/knowledgebase/vat-photopolymerization/

Grimm, M. (2024). Durability of photopolymers in 3D printing with SLA and DLP. Jellypipe. https://www.jellypipe.com/en/blog-news/durability-of-photopolymers-in-3d-printing/

Min, L. J., Edgar, T. Y., Zicheng, Z., & Yee, Y. W. (2015). Biomaterials for bioprinting. 3D Bioprinting and Nanotechnology in Tissue Engineering and Regenerative Medicine, 129–148. https://doi.org/10.1016/b978-0-12-800547-7.00006-0

Shao, J., Huang, Y., & Fan, Q. (2014). Visible light initiating systems for photopolymerization: Status, development and challenges. Polymer Chemistry, 5(14), 4195–4210. https://doi.org/10.1039/c4py00072b

Sinocure Chemical Group. (n.d.). From Traditional UV to Innovative Photochromic Systems and LED Integration. Sinocure Chemical Group Co.,Ltd. https://www.sinocure-chem.com/2024/09/11/from-traditional-uv-to-innovative-photochromic-systems-and-led-integration/

VAT photopolymerisation: Additive Manufacturing. Loughborough University. (n.d.). https://www.lboro.ac.uk/research/amrg/about/the7categoriesofadditivemanufacturing/vatphotopolymerisation/

Weng, Z., Huang, X., Peng, S., Zheng, L., & Wu, L. (2023). 3D printing of ultra-high viscosity resin by a linear scan-based VAT photopolymerization system. Nature Communications, 14(1). https://doi.org/10.1038/s41467-023-39913-4

5.2 Investigations into the influence of the type of 3D printers available on the market and their parameters on the resolution and shrinkage of the obtained printouts.

Jakub Pietraszewski[1], Monika Topa-Skwarczyńska*, Karolina Kozanecka, Filip Petko, Mariusz Galek, Joanna Ortyl

1. Faculty of Chemical Engineering and Technology, Cracow University of Technology, Cracow, Poland

e-mail: monika.topa-skwarczynska@pk.edu.pl

KEYWORDS: *polymer materials, 3D printing, printing resolution, polymerization shrinkage*

Abstract

3D printing is an additive material manufacturing method that is widely used in many industries, such as dentistry or medical device manufacturing due to its ability to produce parts with extremely high resolution and detail. Accuracy, resolution and stability of 3D printed structures are critical factors in 3D-VAT printing applications, where high precision is often required for detailed parts and functional prototypes. However, these factors can vary with different printing parameters and the type of 3D printer used. The discrepancy between them can be a challenge for consistent 3D printing with high detail and structural integrity. Therefore, it is important to optimize printing parameters (layer exposure time and power) so that the resulting product has excellent resolution and low polymerization shrinkage, which directly affects the quality and dimensions of the resulting product.

This study analyzed how different types of 3D printers and printing parameters such as layer cure exposure time, layer height and varying incident light intensity on the layer affect the resolution, dimensional fidelity and shrinkage of 3D printed objects from light-curing resins. Standard resins dedicated to 3D-VAT printing were used in the study.

The results obtained allowed us to conclude that the type of 3D printer used, and the printing parameters set for it significantly affect the resolution and polymerization shrinkage of the final product. By exploring the various 3D printer models and the various parameters used in the process, this work provides valuable insight into optimizing 3D VAT printing.

Introduction

Three-Dimensional (3D) Printing is a technology that has been recently rising in popularity in science, various industries as well as in the general populace. It is also called additive manufacturing, which describes its purpose - creation of three-dimensional objects from digital designs, by manufacturing additional material layer by layer to build up a print (Iftekar et al., 2023; Shahrubudin et al., 2019). This makes it unlike traditional manufacturing methods, which often rely on subtractive techniques, like grinding and cutting, or moulding the material ("Additive vs. subtractive manufacturing"). 3D printing allows for precise customization, reduced material waste and fast prototyping of complex geometries. Due to its efficiency and versatility, this technology has become a valuable asset in both science and industry (Srinivasan et al., 2021). In scientific research, 3D printing plays a crucial role in developing prototypes. Because of its ability to create intricate designs with high precision on a small scale, it is commonly used in biomedical fields, like dentistry or regenerative medicine (Li et al., 2022). In industry, 3D printing enables on-site production of case-specific apparatus and localized fabrication (Tripathi et al., 2022). This improves system and product performance, as well as aligning with sustainability goals by minimizing material waste and energy consumption. Along with its continuous evolution, 3D printing technology is expected to be more in use in all areas of science, industry, and life in the upcoming years (Nadagouda et al., 2021).

A particularly noteworthy method of 3D printing is 3D VAT printing, also called vat photopolymerization. It is an additive manufacturing method that utilizes a vat with a light transmitting film bottom that contains a liquid monomer. The monomer undergoes photopolymerization under a light beam, creating an object layer by layer. (Shaukat et al., 2022) Since the creation of 3D VAT printing, there have been many new printing technologies created. The most widespread and important ones have been explored in this study to investigate how the different technology would affect the shrinkage and print resolution, so the overall quality of the print.

Among the most promising and popular technologies within 3D VAT printing are Digital Light Processing (DLP) and Liquid Crystal Display (LCD). Both of them utilize light to cure a liquid monomer but there are differences in their mechanisms and key characteristics (Caussin et al., 2024).

Despite its applications and potential, 3D printing faces various challenges, especially when it comes to achieving high-quality objects. One of the most common problems is called shrinkage, which is the reduction of the desired object dimensions during printing, leading to dimensional inaccuracies and distortion. It occurs as materials solidify and cool down during creation, for that reason it is especially prevalent in photopolymerization-based printing methods, where there are noticeable changes in the temperature during the process because of the reaction progress (Tran et al., 2024). Warping is another frequent problem. It is a distortion where parts of the print curl or deform,

due to internal stresses building up during printing because of rapid cooling or inconsistent thermal gradients in the print. This makes it especially problematic in printing of large or flat structures (Boissonneault, 2024). The next common problems are generally called layer adhesion defects, for example poor inter-layer bonding. These defects can weaken the overall structure of the print and are often caused by insufficient curing in layers and low print temperatures. Surface imperfections, like visible layer lines or surface roughness reduce functional quality as well as the aesthetic value of the printed object. They can result from poor calibration of the 3D printer as well as printer model limitations, like low-quality settings. Material contamination, such as dust or debris in the resin vat, and inconsistent light exposure can cause uneven curing or voids in the printed object (Ramian et al., 2021; Francis, 2024). These challenges in 3D printing highlight the need for optimized parameters and frequent maintenance to minimize defects and ensure high-quality 3D prints.

In this article, we present the impact of printing parameters such as layer height, light exposure time and light beam intensity, as well as the type of printers (and their technologies) used on print resolution and accuracy. The printers investigated were the LCD printer Anycubic Photon Mono M7 PRO and the DLP printer Lumen X+.

Methods

An iodonium salt photoinitiator was used as a base molecule for resin in this study of 3D printers. The photoinitiator was dissolved in monomers undergoing photopolymerization according to radical mechanism (generation of reactive free radicals initiated by light, thus triggering the polymerization of monomers into a solid polymer network through a chain reaction). These were urethane dimethylacrylate (UDMA, Sigma Aldrich) mixed with triethylene glycol dimethacrylate (TEGDMA, Sigma Aldrich) in a 7:3 ratio. Their chemical formulas were presented in Figure 5.2.1.

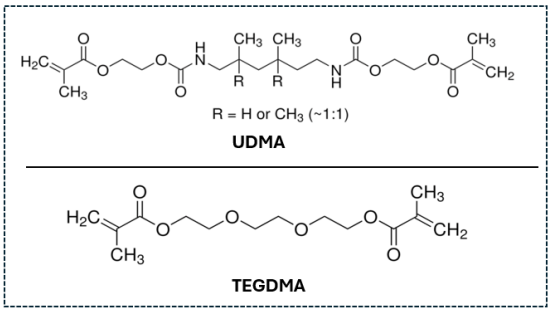

Figure 5.2.1. The chemical formulas of monomers used in this study.

In this study, two distinct 3D printers were used: Anycubic Photon Mono M7 PRO and Lumen X+, each offering unique advantages for high-resolution VAT photopolymerization. The optical power of each was measured using the ThorLabs PM160 power meter with a photodiode sensor. The optical power measurements were conducted to compare the printing settings as well as to study the kinetics of the systems in Real-Time Fourier-Transform Infrared Spectroscopy (FT-IR). The Nicolet™ i10 spectrometer from Thermo Scientific, fitted with a horizontal accessory, was used to facilitate real-time observation of the photopolymerization process. Samples were exposed to light from a M405L4 Vis-LED provided by ThorLabs INC., operating at various light intensities, equating those in the 3D printers studied in this work, that is 7 mW·cm^{-2} and 23 mW·cm^{-2}. Data acquisition was managed through OMNIC software, with sample irradiation commencing 10 seconds after the start of the recording. The systems with an UDMA/TEGDMA blend were measured in samples in polypropylene film (thickness of 25 μm). Conversion rates were determined using Equation 3.2.1, based on changes in the monitored band area (A_{After}), relative to the initial area (A_{Before}), with the targeted bandwidth at 1634 cm^{-1}.

$$C_{FT-IR}\,[\%] = \left(1 - \frac{A_{After}}{A_{Before}}\right) \cdot 100\,\% \qquad (3.2.1.)$$

where:

A_{Before} – area of the absorbance peak characteristic for appropriate monomer and type of photopolymerization before curing,

A_{After} – area of the same absorbance peak after the polymerization process.

For the 3D printing tests, 2 types of printers were used: the LCD printer, Anycubic Photon Mono M7 PRO and the DLP printer, Lumen X+. The LCD printer emitted light of 7 mW·cm^{-2} light beam intensity. The printing parameters set for this printer were 10 μm layer height, 25 bottom layers exposed to light for 100 seconds each, and the rest of the layers exposed to light for 50 seconds each. The LCD printer emitted light of 23 mW·cm^{-2} light beam intensity. The printing parameters set for this printer were 50 μm layer height, 2 bottom layers exposed to light for 70 seconds each, and the rest of the layers exposed to light for 22 seconds each.

To ensure consistency in the findings and facilitate comparison of the results, each print was based on the same digital model composed of three simple geometric shapes: a pyramid, a cuboid, and a cylinder, all of which were placed on a rectangular strip. The model is displayed in Figure 5.2.2. The shapes were selected because of their distinct geometrical features, allowing for comprehensive evaluation of print quality. The pyramid, with sharp angles and tapering structure, tested the printers' ability to reproduce fine details. The cuboid provides insight into dimensional accuracy, surface flatness and roughness, while the cylinder tested the printers' capacity to produce smooth, curved surfaces.

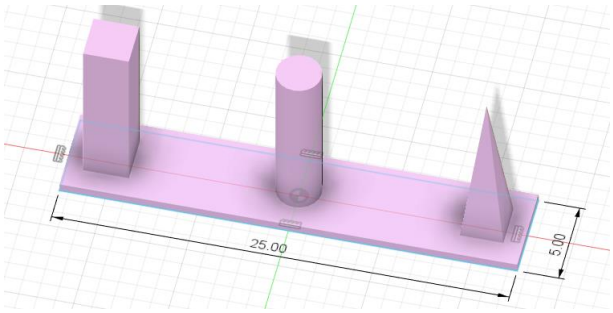

Figure 5.2.2. The 3D model that was used to test printing.

The printed objects needed to be captured in high quality photos. The Olympus DSX1000 – High Resolution Model digital microscope was employed for detailed imagining and analysis as it offers exceptional high-resolution optical system for digital imagining. The microscope features a wide magnification range from 20x to 9637x, enabling precise examination of features of the print, like microsufaces. It boasts a Z axis accuracy of 1 µm, making it ideal for examining small-scale structures, as well as resin and printer quality. The system's motorized stage allows for smooth, automated navigation, while the integrated DSX software provides versatile tools for measurement, image stitching and 3D reconstruction. This digital microscope delivers comprehensive insights into sample morphology and texture.

Results

Real-Time FT-IR analysis was employed to study photopolymerization kinetics to provide insights into efficiency and conversion rates under visible lights of the resin in conditions akin to those in the 3D printers. In Figure 5.2.3, polypropylene film sample of 25 µm thickness was monitored to see band changes at 1634 cm^{-1}, associated with the depletion of double bonds. The samples demonstrated rapid initiation; the sample with 23 $mW \cdot cm^{-2}$ (400mA) at 5 seconds after irradiation, and the one with 7 $mW \cdot cm^{-2}$ (100mA) at 10 seconds after irradiation. High progressions of polymerization were noted, achieving high conversion rates of 40% for the 23 $mW \cdot cm^{-2}$ (400mA) sample and 45% for the 7 $mW \cdot cm^{-2}$ (100mA) sample. The results indicate effective utilization of light energy, highlighting the high reactivity of the photopolymerization process in these conditions with low induction times and quick reaction progress.

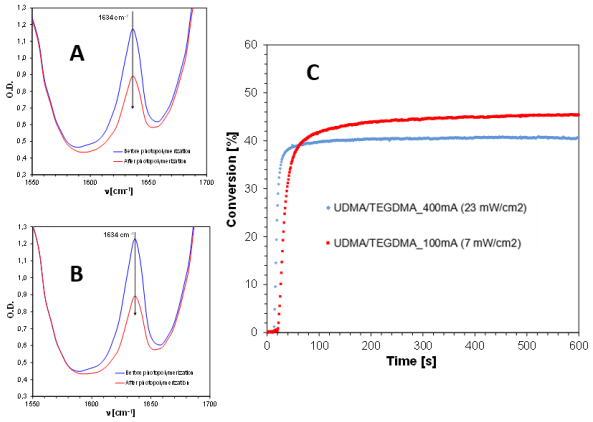

Figure 5.2.3. Before and after polymerization bands for 23 $mW \cdot cm^{-2}$ **(A)** and 7 $mW \cdot cm^{-2}$ **(B)** light beams; kinetic profiles presenting real time photopolymerization process **(C)** of radical reactive systems. 25 µm thick samples exposed to 7 $mW \cdot cm^{-2}$ (100 mA) or 23 $mW \cdot cm^{-2}$ (400mA) light beam at 405 nm for 600 seconds.

Digital imaging and surface analysis were utilized to evaluate the quality and authenticity of the prints produced by both 3D printers (Figure 5.2.4), providing critical insights into their performance. The Lumen X+ print experienced slight warping on its base, while the Anycubic Photon Mono M7 Pro did not.

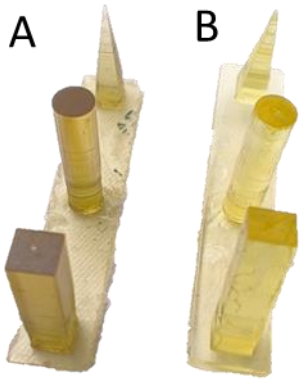

Figure 5.2.4. Prints from Anycubic Photon Mono M7 Pro (A) and Lumen X+ (B).

The analysis presented notable differences in shrinkage and resolution between the two technologies. Print from Anycubic Photon Mono M7 Pro, the LCD printer (Figure 5.2.5, left column), was printed with 10 µm thick layers, while that from the DLP Lumen X+ printer (Figure 5.2.5, right column) was printed with 50 µm thick layers. The LCD printed demonstrated higher resolution, with finer details and more precise reproduction of intricate features, attributed to its 6.8 x 24.8 µm XY resolution. However, the print showed slightly greater shrinkage in the X axis, while having better resolution in the Y axis of the print, which was expressed as shrinkage of the print (Table 5.2.1). In contrast, the Lumen X+ exhibited

Table 5.2.1 Dimensions and percentage shrinkage of the printouts.

	Model (mm)	LCD		DLP	
		Dimensions (mm)	Shrinkage (%)	Dimensions (mm)	Shrinkage (%)
Length	25	24,39	2,43%	24,65	1,39%
Width	5	4,84	3,13%	4,70	5,92%

slightly lower resolution in the Y axis but better in the X axis. As can be seen in the photos of the prints (Figure 5.2.4), the LCD printer achieved smoother finish of the print, thanks to its lower layer thickness of 10 µm.

The dimensions of the printouts were compared with the model dimensions (Figure 5.2.2) to calculate the percentage shrinkage of the print, that is, how much from the model the dimensions of the print are off. The length of the print was the long side of the rectangular strip, and the width was the short side. The data was displayed in Table 5.2.1.

The bottom layer of the pyramid was also measured using an electronic caliper with 0.005mm accuracy. The model length was 2.50 mm, while as shown in Figure 10, the dimensions of the prints were different, highlighting polymer shrinkage of 11,6% (2.21 mm) for the DLP Lumen X+ printer and 10,0% (2.25 mm) for the LCD Anycubic Photon Mono M7 PRO.

Discussion

The FT-IR parameters were the same as those in the 3D printers, making it a great tool for optimizing as well as checking the polymerization kinetics progress. Real Time FT-IR analysis confirmed resin's ability for sufficient photopolymerization under those conditions. Optimizing parameters for 3D printing is crucial for advancing its applications across various industries like dentistry, where precision and material performance are especially important. Parameters such as light intensity, exposure time, and layer thickness directly influence the quality of the prints, including their surface finish, shrinkage, and warping. By optimizing these parameters, manufacturers can produce high-quality printouts with minimal printing defects. This study serves as a direct comparison of the type of printing technology employed as well as the printing parameters and their influence on the final printout's quality and resolution.

Anycubic Photon Mono M7 PRO is an LCD commercial 3D printer designed for precision and affordability, featuring a high-resolution 14K monochrome LCD screen, with XY axis resolution of 6.8x24.8 µm, allowing for fine details in small-scale prints. The printer supports a layer thickness in the range from 10 to 200 microns, making print model parameters very customizable. Its light source delivers uniform illumination at about 405 nm wavelength with an optical power of 7 mW·cm^{-2}. This printer is well-suited for applications requiring prototyping and intricate designs with high precision and quick completion time.

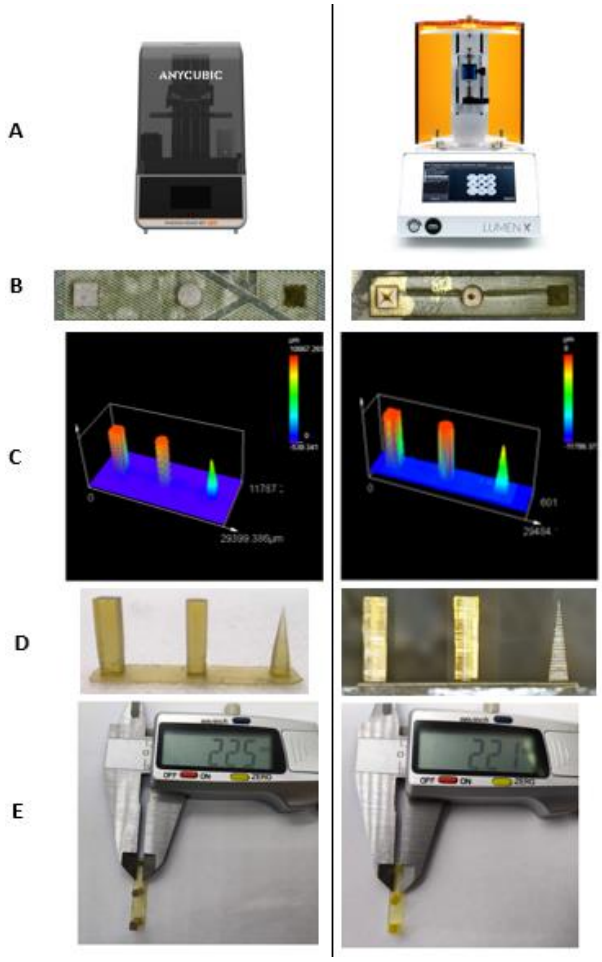

Figure 5.2.5 Compiled photos of the prints investigated in this study. Anycubic Photon M7 PRO on the left column, with printing parameters of 10 µm layer height, 25 bottom layers exposed to light for 100 seconds each, and the rest of the layers exposed to light for 50 seconds each. Lumen X+ on the right column, with printing parameters of were 50 μm layer height, 2 bottom layers exposed to light for 70 seconds each, and the rest of the layers exposed to light for 22 seconds each, (A) Photos of the printers used in the work, (B)Top view of the print, (C) 3D imaging of the print, (D) Side view of the print, (E)The dimension measurement of the bottom layer of the printed pyramid.

On the other hand, the Lumen X+ is a professional grade DLP printer built with bioprinting and microfluidic applications in mind, with XY axis resolution of 50 microns. The Z-axis resolution supports layer thickness as 100 and 50 microns, enabling high vertical accuracy. This printer employs a DLP projector as its light source, delivering uniform illumination at about 405 nm wavelength, with an optical power of 45 mW·cm^{-2} maximum output. The optical power can also be adjusted, making it ideal for research

applications. This printer is tailored for applications requiring biocompatibility and high precision, such as tissue and bone engineering or dental printing.

The main differences between these two printers lie in their light sources, intended applications and vertical accuracy. The Photon Mono M7 Pro's LC technology offers higher XY resolution, making it ideal for detailed prints for commercial use. In contrast, the Lumen X+ excels in professional and research applications, with the DLP technology ensuring uniform light projection while using specialized resins. This printer also delivers higher optical power by about 6 times at maximum power output than the LCD one. These differences highlight the versatility of 3D VAT printers in addressing various academic and industrial needs.

The analysis of shrinkage in this study provides valuable insights but is subject to certain limitations. Specifically, the shrinkage measurements were based on a single sample for each print, which, while informative, may not fully account for potential variability in the printing process. To achieve a more comprehensive understanding of shrinkage behavior, future investigations should involve multiple printouts under identical conditions. This approach would ensure greater statistical reliability, allowing for more concrete conclusions about the influence of printing parameters and technologies on dimensional stability.

This study is an introductory work for optimizing printing parameters and comparing various 3D printing technologies, mainly those used in the dental industry. Further research could focus on a wider variety of printing technologies and printing parameters, comparing them extensively. Additionally, future works can explore the integration of advanced or hybrid materials to enhance precision and functionality of 3D printer objects for dental applications.

Conclusion

In this work, the influence of different 3D printing technologies and their parameters on print resolution and shrinkage was investigated. The study demonstrated the distinct advantages of DLP and LCD technologies. Optimized printing conditions were shown to significantly enhance the dimensional stability and surface quality of prints. These findings serve as foundation for further advancements in 3D printing.

Acknowledgements

This research was funded by National Centre for Research and Development in Poland under the Lider Program, grant number LIDER13/0156/2022.

References

Boissonneault, T. (2024, April 5). 3D print warping (PLA, PETG, ABS): 6 simple fixes. Wevolver. https://www.wevolver.com/article/3d-print-warping

Caussin, E., Moussally, C., Le Goff, S., Fasham, T., Troizier-Cheyne, M., Tapie, L., Dursun, E., Attal, J.-P., & François, P. (2024). VAT photopolymerization 3D printing in Dentistry: A comprehensive review of actual popular technologies. Materials, 17(4), 950. https://doi.org/10.3390/ma17040950

Formlabs. (n.d.). Additive vs. subtractive manufacturing. Formlabs. https://formlabs.com/blog/additive-manufacturing-vs-subtractive-manufacturing/

Francis. (2024, August 2). Understanding warping in 3D printing: What causes warping? - solevant - software reviews. Solevant. https://solevant.com/what-causes-warping-in-3d-printing/

Iftekar, S. F., Aabid, A., Amir, A., & Baig, M. (2023). Advancements and limitations in 3D printing materials and technologies: A critical review. Polymers, 15(11), 2519. https://doi.org/10.3390/polym15112519

Li, B., Zhang, M., Lu, Q., Zhang, B., Miao, Z., Li, L., Zheng, T., & Liu, P. (2022). Application and development of modern 3D printing technology in the field of Orthopedics. BioMed Research International, 2022(1). https://doi.org/10.1155/2022/8759060

Nadagouda, M. N., Ginn, M., & Rastogi, V. (2021). A review of 3D printing techniques for environmental applications. Current Opinion in Chemical Engineering, 28, 173–178. https://doi.org/10.1016/j.coche.2020.08.002

Ramian, J., Ramian, J., & Dziob, D. (2021). Thermal deformations of thermoplast during 3D printing: Warping in the case of ABS. Materials, 14(22), 7070. https://doi.org/10.3390/ma14227070

Shahrubudin, N., Lee, T. C., & Ramlan, R. (2019). An overview on 3D printing technology: Technological, materials, and applications. Procedia Manufacturing, 35, 1286–1296. https://doi.org/10.1016/j.promfg.2019.06.089

Shaukat, U., Rossegger, E., & Schlögl, S. (2022). A review of multi-material 3D printing of functional materials via VAT photopolymerization. Polymers, 14(12), 2449. https://doi.org/10.3390/polym14122449

Srinivasan, D., Meignanamoorthy, M., Ravichandran, M., Mohanavel, V., Alagarsamy, S. V., Chanakyan, C., Sakthivelu, S., Karthick, A., Prabhu, T. R., & Rajkumar, S. (2021). 3D printing manufacturing techniques, materials, and applications: An overview. Advances in Materials Science and Engineering, 2021(1). https://doi.org/10.1155/2021/5756563

Tran, T. V., Long, D. C., & Van, C. N. (2024). The influence of printing materials on shrinkage characterization in metal 3D printing using material extrusion technology. Engineering, Technology & Applied Science Research, 14(4), 15356–15360. https://doi.org/10.48084/etasr.7758

Tripathi, S., Mandal, S. S., Bauri, S., & Maiti, P. (2022). 3D bioprinting and its innovative approach for biomedical applications. MedComm, 4(1). https://doi.org/10.1002/mco2.194

5.3 Impact of nanofillers on the kinetics of the photopolymerization process and the printing resolution of 3D photopolymerizable polymer resins with the study of the properties of nanocomposites produced using 3D-VAT printing technology.

Kamil Pulit[1], Małgorzata Noworyta, Magdalena Jankowska, Paweł Niezgoda, Joanna Ortyl*

1. Faculty of Chemical Engineering and Technology, Cracow University of Technology, Cracow, Poland

e-mail: joanna.ortyl@pk.edu.pl

KEYWORDS: *photopolymerization, 3D printing, nanofillers, nanocomposites, polymer materials*

Abstract

Photopolymerization is a critical process in the 3D printing of polymer resins, particularly in applications that demand high precision and intricate structures. Recently, the incorporation of nanofillers into photopolymerizable resins has garnered significant attention for their potential to enhance both material properties and printing performance. The addition of nanoparticles can influence polymerization kinetics, allowing for better control over the curing process and improving the mechanical, thermal, and optical properties of the final printed structures. This study explores how nanofillers impact the speed and efficiency of the photopolymerization process and their effect on achievable printing resolution, which is essential in fields such as microelectronics, biomedical devices, and high-precision manufacturing. The mechanical properties under tensile stress of the resulting nanocomposites, produced by integrating various nanofillers into the polymer resin matrix, were also investigated.

Introduction

Nanocomposites are materials that consist of at least two components, e.g. a polymer matrix and a dispersed phase, which can exist alone, but in combination they form a material with superior mechanical properties compared to the individual components of the composition, e.g. the polymer matrix itself (Barton et al. 2014). Nanofillers themselves are advanced materials with submicron grain sizes, oscillating at 10^{-9} m, which are a special variety of fillers used to modify the properties of polymers (Stabik, 2004; Fu et al. 2019; Shameem et al. 2021).

Nowadays, nanofillers are gaining prominence as a means to produce modern nanocomposites with exceptional mechanical properties, such as better tensile strength, lower polymerization shrinkage, or reduced material abrasion, which is used in various industries such as electronics (Zhu et al. 2024), automotive (Nichols, 2019), construction (Pilch et al. 2024), and biomaterials (Ahmad et al. 2017). In particular, technologies such as 3D-VAT printing have revolutionized the manufacturing process of modern nanomaterials, making it possible to create objects directly from digital CAD (Computer-Aided Design) models (Robakowska et al. 2023). These methods use light to initiate photopolymerization reactions (Jankowska et al. 2024), allowing a single layer to be formed as designed (Kalkal et al. 2021). The process proceeds layer by layer, allowing the fabrication of objects with complex shapes and high resolutions (He et al. 2023; Chen et al. 2024). Due to its energy-efficient nature, the photopolymerization process itself is considered environmentally friendly (Noworyta et al. 2023).

Also, an important direction in the development of new nanocomposites is the discovery of new photoinitiators that absorb light with a wavelength greater than 400 nm. This is due to the need to use cheaper and safer light sources for initiating the photopolymerization process that does not emit harmful UV radiation (Petko et al. 2023).

The results of this study indicate that the incorporation of tested nanofillers into the matrix of commercially available 3D printing resins significantly influences photopolymerization kinetics. Enhanced printing resolution and improved mechanical properties were observed with specific types of nanofillers. This study provides valuable insights into the role of nanofillers in optimizing both the photopolymerization process and the quality of 3D-printed structures, showcasing the promising potential of nanocomposites in industries requiring high-performance engineered materials.

Methods

Research materials

Three commercially available resins were used in the study:

- ANYCUBIC ABS-LIKE RESIN+ (ABS-LIKE) - the manufacturer assures that models printed with this resin show high performance and are suitable for drilling and tapping into them due to their similar properties to acrylonitrile-butadiene-styrene copolymer,
- ANYCUBIC UV TOUGH RESIN (UV TOUGH) - the manufacturer assures that objects made with this resin show no stress marks or bending of finished projects,
- ANYCUBIC WATER WASH RESIN+ (WATER WASH) - models printed with this resin show the ease of cleaning with water.

Inorganic nanofillers used in the study:
- titanium (IV) oxide (TiO_2) - particle size: <100 nm, manufacturer: Sigma-Aldrich,
- aluminum (III) oxide (Al_2O_3) - particle size: <50 nm, from manufacturer: Sigma-Aldrich,
- silicon (IV) oxide (SiO_2) - particle size: 10-20 nm, manufacturer: Sigma-Aldrich,
- hydroxyapatite ($Ca_{10}(PO_4)_6(OH)_2$) - particle size: 60 nm ± 10 nm, manufacturer: Sigma-Aldrich,
- halloysite nanoclay ($Al_2Si_2O_5(OH)_4 \cdot 2\,H_2O$) - particle size: nanotubes about 30 nm in diameter and up to 70 nm long, from manufacturer: Sigma-Aldrich,

Each of the tested nano-additives was added at 10% by weight to the commercial resin. According to the literature, already a small addition by weight of inorganic oxides such as Al_2O_3 or SiO_2 affects the change of mechanical properties of the composite, like abrasion resistance and hardness (Spychaj et al. 2007).

Real-Time FT-IR Photopolymerization Measurements

The kinetics of the photopolymerization process of polymer nanocomposites were measured using Fourier Transform Infrared Spectroscopy. The study was carried out using an i10 Nicolet™ spectrometer from Thermo Scientific, equipped with a specialized horizontal attachment (Figure 5.3.1), which made it possible to monitor the photopolymerization reaction directly in real time. During the measurements, a 405 nm L4 Vis-LED diode provided by Thorlabs Inc. was used to illuminate the samples. The intensity of the light on the sample was 0.2 $mW \cdot cm^{-2}$. The light radiation was directed to the samples using a 1.2-m-long, 0.5-cm-diameter optical fibre. The irradiation process was started each time 10 seconds after the start of measurement data recording. Measurements were made on 25 µm thick layers of samples inserted between polypropylene films to minimize the effects of oxygen inhibition. Data recording was carried out using OMNIC software, which ensured precise process control and result acquisition. The disappearance of the characteristic band corresponding to the frequency of double bonds between two adjacent carbons in the monomer molecules (1614 cm^{-1}) was monitored for each of the tested resins.

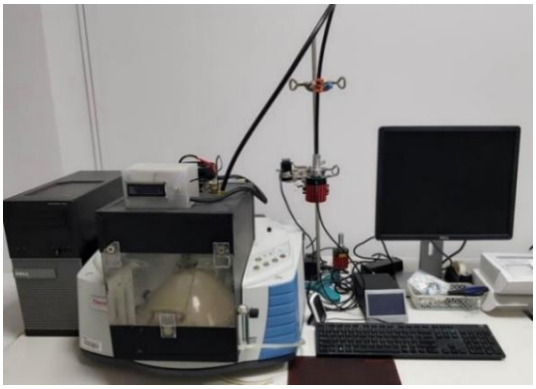

Figure 5.3.1 Thermo Scientific's i10 Nicolet™ spectrometer with specialized horizontal attachment.

3D Printing

An Anycubic Photon Mono X printer (Figure 5.3.2), operating with LCD technology, was used to produce the test prints. The printing parameters were set to 20 seconds of exposure for the first three layers and 4 seconds for subsequent layers, with each layer having a thickness of 100 µm. The printer's light output was measured using a PM160 optical meter from Thorlabs inc. and showed a result of 5.9 mW/cm^2. In the case of using TiO_2 and SiO_2 nano-additives, due to the limited light penetration, as well as the poor adhesion of the TiO_2 composition to the table and the high viscosity of the SiO_2 composition, the prints were unsuccessful, making it necessary to use aluminium (III) oxide, hydroxyapatite and halloysite nanoclay in the following sections of the work to study the effect of nano-additives on the resolution of 3D prints.

Figure 5.3.2 Anycubic Photon Mono X 3D printer (https://cn.anycubic.com/article/670.html)

Mechanical studies – tensile strength

Tensile tests were conducted using a Shimadzu machine and software (Figure 5.3.3). The tests were performed three times for each composition to ensure reproducibility of the results. Specially designed shapes shown in Figure 5.3.4 were used for the tests.

Figure 5.3.3 Shimadzu tensile strength testing machine.

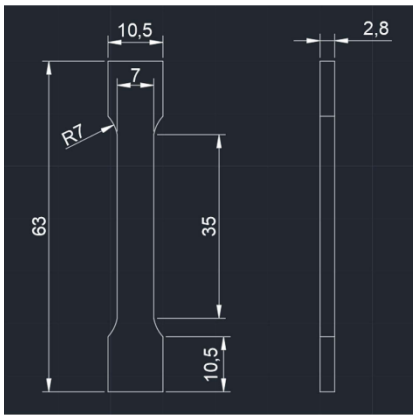

Figure 5.3.4 Dimensioned (in millimeters) design of the shape in AutoCAD 2023 software.

Optical Microscope Images

2D images and surface height maps of the 3D printed calibration cubes were taken using an Olympus DSX1000 optical microscope. Imaging was carried out under bright-field light (BF and MIX), where the light source, placed inside the eyepiece, fell perpendicularly on the surface of the sample.

Scanning Electron Microscope (SEM)

A study of the surface of the prints was carried out using an Apreo 2 S LoVac scanning electron microscope (Figure 5.3.5), which is an advanced tool that allows high-quality imaging of samples. Thanks to this technology, it was possible to study the microstructure and surface of the tested materials in detail.

Figure 5.3.5 Apreo 2 S LoVac scanning electron microscope (Thermo Fisher Scientific)

Results and Discusion

Real-Time FT-IR

A real-time FT-IR technique was used to verify the effect of nano-additives on the photopolymerization of individual commercial resins. By monitoring the characteristic band (Figure 5.3.6) for the monomers, the kinetics of photopolymerization was determined. In this case, the disappearance of the band height of 1614 cm^{-1} was monitored. The systems were irradiated for 300 seconds with a diode with a wavelength of 405 nm. Light of this length is commonly used in 3D printers using vat photopolymerization methods. With the addition of nanofillers to ABS-LIKE resin, all the determined conversions are higher than those of pure resin without nanofillers (Figure 5.3.7; Table 5.3.1). The highest conversion rate was achieved by the composition with TiO_2 additives, which showed a more than twofold increase in the final monomer conversion rate. For the UV TOUGH (Figure 5.3.8; Table 5.3.2) and WATER WASH (Figure 5.3.9; Table 5.3.2) resins, all of the nano-additives increased the final monomer conversion rate, except SiO_2, which caused an approximately twofold decrease in the conversion rate, as well as a 30-second induction time for the UV TOUGH resin and an almost complete disappearance of the photopolymerization process for the WATER WASH resin.

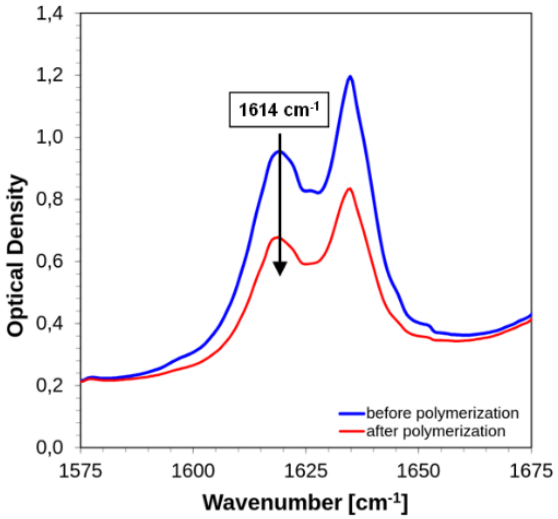

Figure 5.3.6 Example of characteristic band decay for determining the kinetics of the photopolymerization process.

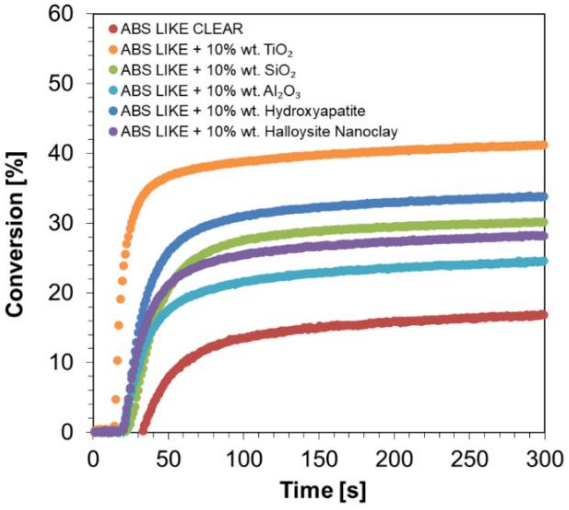

Figure 5.3.7 Kinetic profiles showing the photopolymerization process of pure ABS-LIKE resin and 10% wt. of the aforementioned composition of inorganic nano-fillers based on it at a current set on Thorlabs con-troller at 10 mA (0.2 mW· cm^{-2}) for Thorlabs 405L4 diode.

Table 5.3.1 Summary of the results of measurements of photopolymerization kinetics for ABS-LIKE resin and nanocomposites based on it.

Kinetic parameters of photopolymerization	**ANYCUBIC ABS-LIKE RESIN+**					
	CLEAR	10%$_{wt.}$ TiO_2	10%$_{wt.}$ SiO_2	10%$_{wt.}$ Al_2O_3	10%$_{wt.}$ hydroxyapatite	10%$_{wt.}$ Halloysite Nanoclay
Conversion (%)	17	41	3	25	34	28
Induction time (s)	2	4	13	9	10	1
Kinetic curve slope	0.4819	4.4411	0.9112	0.8827	1.5971	1.2830

Table 5.3.2 Summary of the results of measurements of photopolymerization kinetics for UV TOUGH resin and nanocomposites based on it.

Kinetic parameters of photopolymerization	**ANYCUBIC ABS-LIKE RESIN+**					
	CLEAR	10%$_{wt.}$ TiO_2	10%$_{wt.}$ SiO_2	10%$_{wt.}$ Al_2O_3	10%$_{wt.}$ hydroxyapatite	10%$_{wt.}$ Halloysite Nanoclay
Conversion (%)	19	35	9	30	34	25
Induction time (s)	7	3	28	9	6	7
Kinetic curve slope	1.1748	3.2663	0.2499	1.7638	1.8417	1.3821

Table 5.3.3 Summary of photopolymerization kinetics measurements for WATER WASH resin and nanocomposites based on it.

Kinetic parameters of photopolymerization	**ANYCUBIC ABS-LIKE RESIN+**					
	CLEAR	10%$_{wt.}$ TiO_2	10%$_{wt.}$ SiO_2	10%$_{wt.}$ Al_2O_3	10%$_{wt.}$ hydroxyapatite	10%$_{wt.}$ Halloysite Nanoclay
Conversion (%)	49	63	3	58	60	5
Induction time (s)	6	3	51	7	8	6
Kinetic curve slope	1.9345	6.9200	0.0558	3.2211	4.3053	3.2201

Table 5.3.4 Summary of calculated energies delivered per 1 cm² at a given time by the light source of the Anycubic Photon Mono X printer.

Time (s)	2	4	6	8	10	12	15	20	25	30
Energy E_0 (mJ·cm²)	11.8	23.6	35.4	47.2	59.0	70.8	88.5	118.0	147.5	177.0

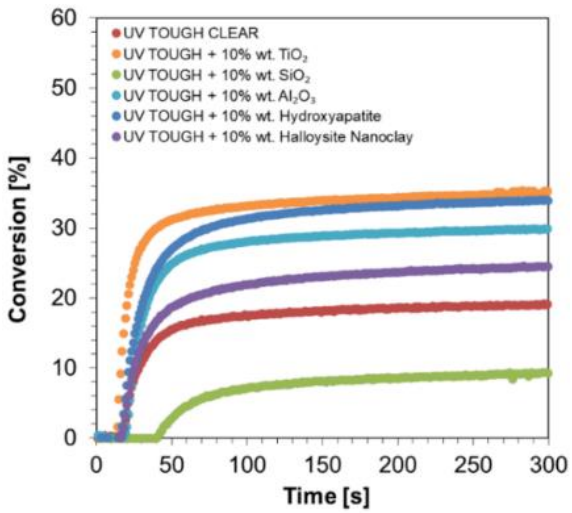

Figure 5.3.8 Kinetic profiles showing the photopolymerization process of pure UV TOUGH resin and 10%$_{wt.}$ of the aforementioned composition of inorganic nano-fillers based on it at a current set on Thorlabs' controller at 10 mA (0.2 mW·cm^{-2}) for Thorlabs 405L4 diode.

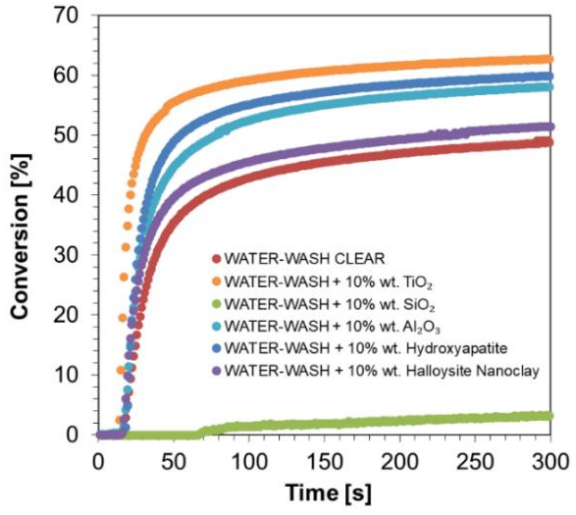

Figure 5.3.9 Kinetic profiles showing the photopolymerization process of pure WATER WASH resin and 10%$_{wt.}$ of the aforementioned composition of inorganic nano-fillers based on it at a current set on Thorlabs con-troller at 10 mA (0.2 mW·cm^{-2}) for Thorlabs 405L4 diode.

Jacob test

Before printing the 3D objects, Jacob's tests were performed to determine the minimum energy needed to cure the layer. The composition was poured into the printer vat without a table mounted, and then exposed to light within a 1 cm² square. After a 2-second exposure, the layer was removed, washed, dried and its thickness was measured with a micrometer screw. The process was repeated, gradually increasing the time to 4 s, 6 s, 8 s, 10 s, 12 s, 15 s, 20 s, 25 s and 30 s, respectively. Based on the collected data, the energy delivered per cm² at a given time was calculated (Table 5.3.4) and the dependence of the thickness of the cured layer on the delivered energy was plotted (Figure 5.3.10, Figure 5.3.11, Figure 5.3.12). Tests were carried out for commercial resins mixed with the nano-additives aluminium (III) oxide, hydroxyapatite and halloysite nanoclay. Using the determined trend lines, the minimum energy needed to cure the film and the penetration depth of the curing light were determined, and the results were summarized in Table 5.3.5.

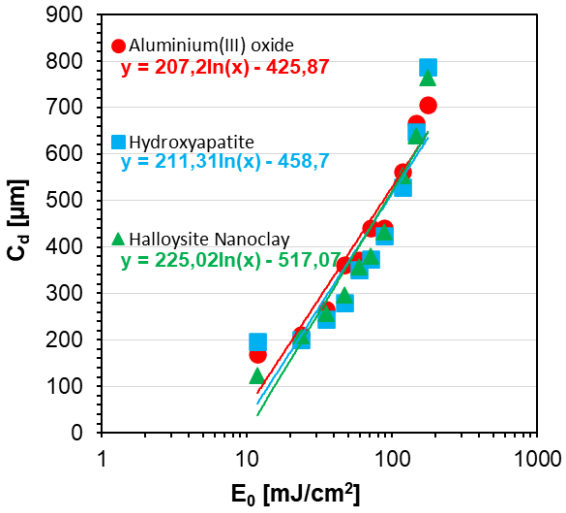

Figure 5.3.10 Plot of the dependence of cured film thickness (C_d) on delivered energy (E_0) for ABS-LIKE-based nanocompositions.

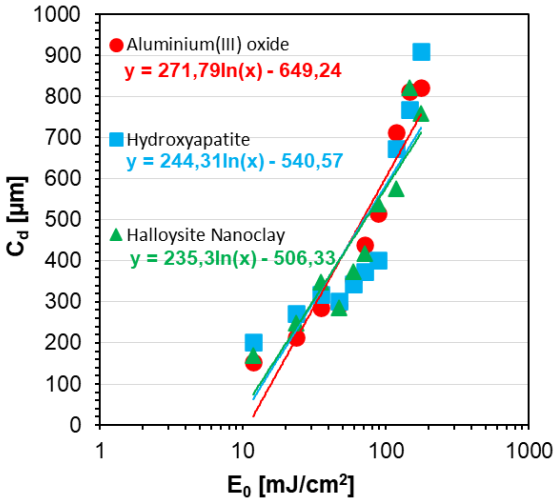

Figure 5.3.11 Plot of the dependence of cured film thickness (C_d) on delivered energy (E_0) for a UV TOUGH-based nanocompositions.

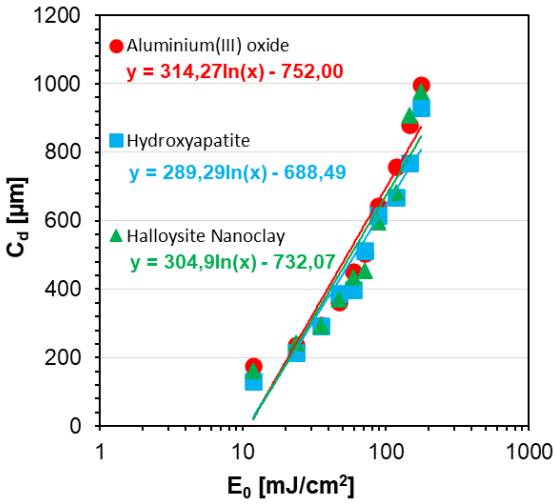

Figure 5.3.12 Plot of the dependence of cured film thickness (C_d) on delivered energy (E_0) for WATER WASH-based nanocompositions.

Table 5.3.5 Summary of calculated critical energies (E_C) of film curing and depth of penetration of curing light (D_p) for individual nanocompositions of aluminium (III) oxide (Al_2O_3). hydroxyapatite (HA) and halloysite nanoclay (HNc).

	ABS-LIKE			UV TOUGH			WATER WASH		
	Al_2O_3	HA	HNc	Al_2O_3	HA	HNc	Al_2O_3	HA	HNc
E_c (mJ)	7.8	8.8	10.0	10.9	9.1	8.6	10.9	10.8	11.0
D_p (µm)	196	190	211	252	224	224	289	270	282

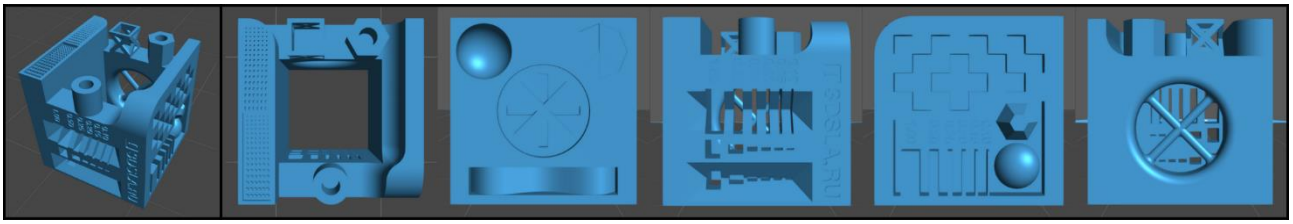

Figure 5.3.13 Cube model in CHITUBOX 1.9.4 software to evaluate the effect of nano-additives on the overall resolution of fabricated objects.

Applications - 3D Printing

Prints were made for the selected compositions using an Anycubic Photon Mono X printer. Two types of cubes measuring 1 cm x 1 cm x 1 cm were made: the first to evaluate the effect of nano-additives on the overall resolution of the fabricated objects (Figure 5.3.13), and the second to examine the quality and resolution of the individual print layers (Figure 5.3.14). In addition, special beams were printed for each tested composition to analyse the effect of nano-additives on the mechanical properties of the nanocomposites (Figure 5.3.4; Figure 5.3.15).

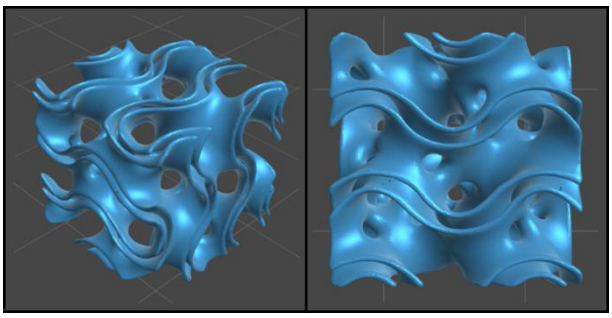

Figure 5.3.14 A gyroid cube model in CHITUBOX 1.9.4 software for evaluating the effect of nano-additives on the layer resolution of fabricated objects.

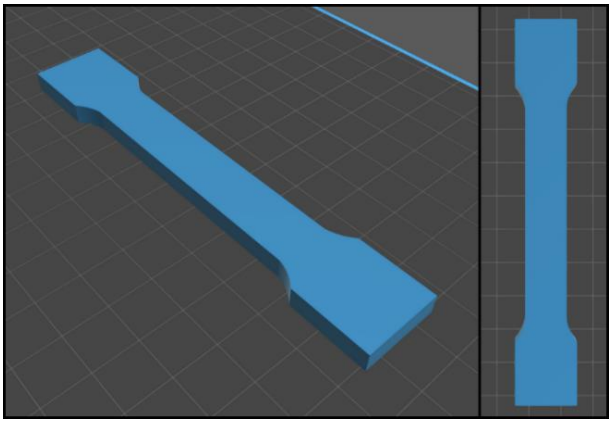

Figure 5.3.15 Beam model in CHITUBOX 1.9.4 software to study the effect of nano-additives on the mechanical properties of fabricated objects.

Optical Microscope Images

The printed cubes were photographed with an Olympus DSX1000 optical microscope to check their resolution. In each case, a change in the colour of the cubes can be observed compared to those without nanocomposites, and the surfaces of the nanocomposite cubes themselves appear more matte than glossy.

Cubes printed with ABS-LIKE-based nanocompositions (Figure 5.3.17, Figure 5.3.18, Figure 5.3.19) show comparable resolution to cubes made with pure ABS-LIKE resin (Figure 5.3.16). Small agglomerations of nanofillers can be observed on the walls of the same cubes, but they are most visible on the cube with addition of hydroxyapatite (Figure 5.3.18).

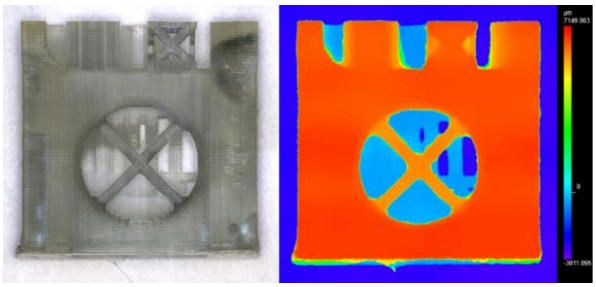

Figure 5.3.16 A photo of a printout of an ABS-LIKE resin cube without nano-additives under BF light and a heatmap of the same cube showing the height of the individual elements taken with a DSX1000 optical microscope.

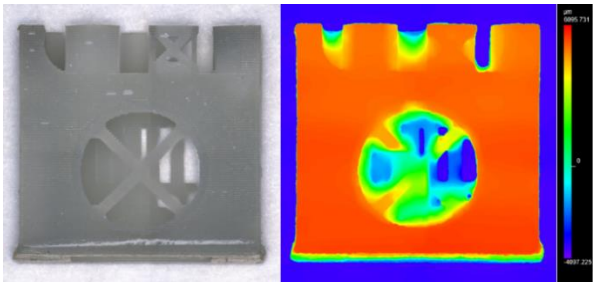

Figure 5.3.17 A photo of a printout of an ABS-LIKE resin cube with 10%$_{wt.}$ aluminium (III) oxide additive under BF light and a heatmap of the same cube showing the height of the individual elements taken with a DSX1000 optical microscope.

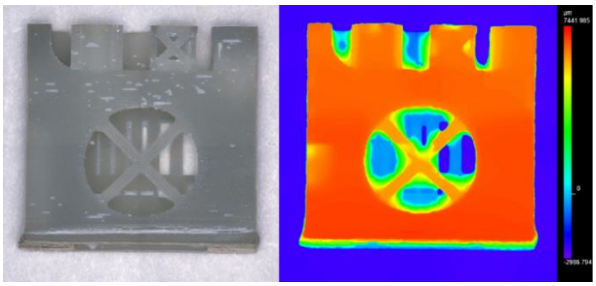

Figure 5.3.18 A photo of a print of an ABS-LIKE resin cube with 10%$_{wt.}$ hydroxyapatite additive under BF light and a heatmap of the same cube showing the height of the individual elements taken with a DSX1000 optical microscope.

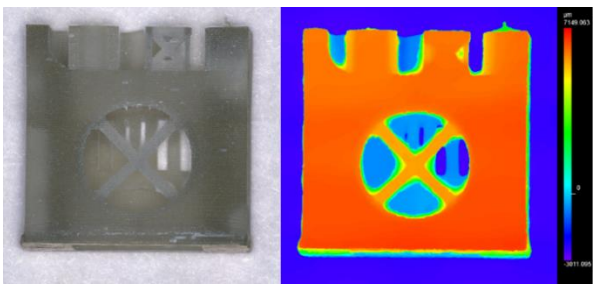

Figure 5.3.19 A photo of a printout of an ABS-LIKE resin cube with 10% wt. halloysite nanoclay additive under BF light, and a heatmap of the same cube showing the height of the individual elements taken with a DSX1000 optical microscope.

The quality of printed cubes from the UV TOUGH-based nanocompositions (Figure 5.3.21, Figure 5.3.22, Figure 5.3.23) are also comparable to that of cube printed from pure resin (Figure 5.3.20). In this case, however, the cube with the addition of hydroxyapatite (Figure 5.3.22) has agglomerations of the used nanofiller strongly visible on its surface, especially at the base of the cube.

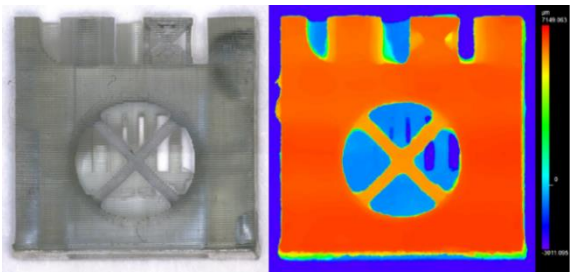

Figure 5.3.20 A photo of a UV TOUGH resin cube print without nano-additives under BF light and a heatmap of the same cube showing the height of the individual elements taken with a DSX1000 optical microscope.

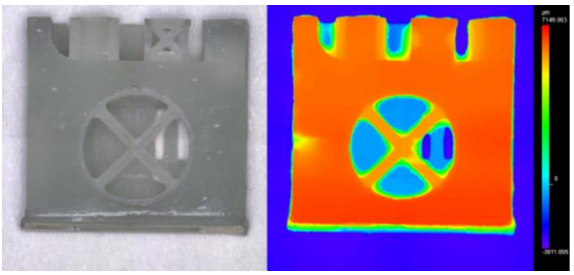

Figure 5.3.21 A photo of a UV TOUGH resin cube print with 10% wt. aluminium (III) oxide additive under BF light and a heatmap of the same cube showing the height of the individual elements taken with a DSX1000 optical microscope.

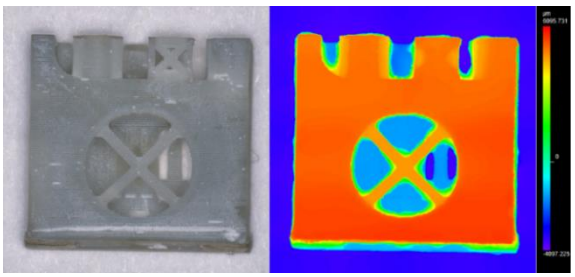

Figure 5.3.22 A photo of a UV TOUGH resin cube print with $10\%_{wt.}$ hydroxyapatite additive under BF light and a heatmap of the same cube showing the height of individual elements taken with a DSX1000 optical microscope.

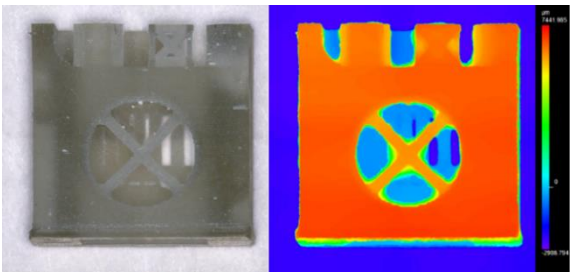

Figure 5.3.23 A photo of a UV TOUGH resin cube print with 10% wt. halloysite nanoclay additive under BF light and a heatmap of the same cube showing the height of individual elements taken with a DSX1000 optical microscope.

In the case of cubes printed from the WATER WASH-based nanocompositions (Figure 5.3.25, Figure 5.3.**26**,Figure 5.3.**27**), their resolution is similar to that of cubes printed from pure WATER WASH resin (Figure 5.3.24). In this situation, the cube with the addition of hydroxyapatite (Figure 5.3.26) is characterized by the absence of pronounced agglomerations of the nanocomposite on its surface, which distinguishes it from the other two cubes with the addition of aluminium (III) oxide (Figure 5.3.25) and halloysite nanoclay (Figure 5.3.27).

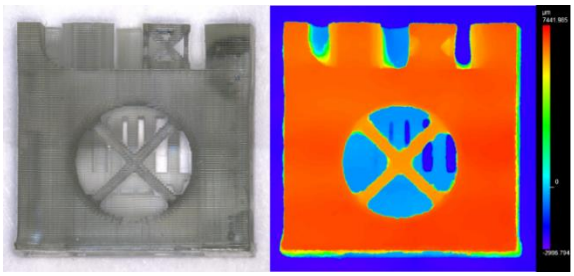

Figure 5.3.24 A photo of a printout of a WATER WASH resin cube without nano-additives under BF light and a heatmap of the same cube showing the height of individual elements taken with a DSX1000 optical microscope.

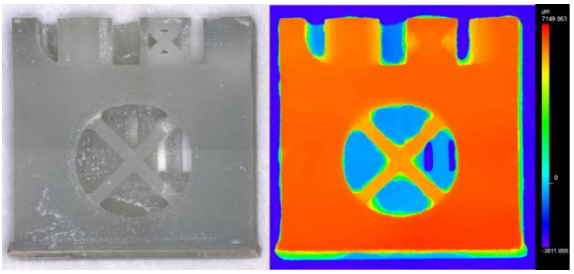

Figure 5.3.25 A photo of a printout of a WATER WASH resin cube with $10\%_{wt.}$ aluminium (III) oxide additive under BF light and a heatmap of the same cube showing the height of the individual elements taken with a DSX1000 optical microscope.

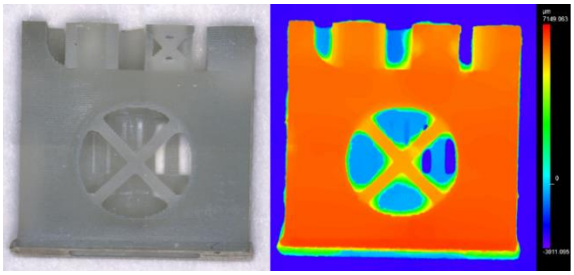

Figure 5.3.26 A photo of a printout of a WATER WASH resin cube with $10\%_{wt.}$ hydroxyapatite additive under BF light and a heatmap of the same cube showing the height of individual elements taken with a DSX1000 optical microscope.

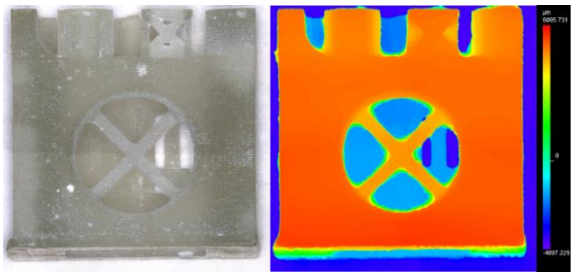

Figure 5.3.27 A photo of a printout of a WATER WASH resin cube with $10\%_{wt.}$ halloysite nanoclay additive under BF light and a heatmap of the same cube showing the height of the individual elements taken with a DSX1000 optical microscope.

Cubes with a gyroid structure printed on ABS-LIKE resin with aluminium (III) oxide, hydroxyapatite and halloysite nanoclay nanofillers (Figure 5.3.29, Figure 5.3.30, Figure 5.3.31) show a resolution at the level of cubes made from pure ABS-LIKE resin (Figure 5.3.28). No visible agglomeration of nanofillers is observed on the walls of the same cubes, which may be due to the very shape of their design. ABS-LIKE resin-based cubes with aluminium (III) oxide, hydroxyapatite and halloysite nanoclay nanofillers were used for scanning electron microscope (SEM) imaging.

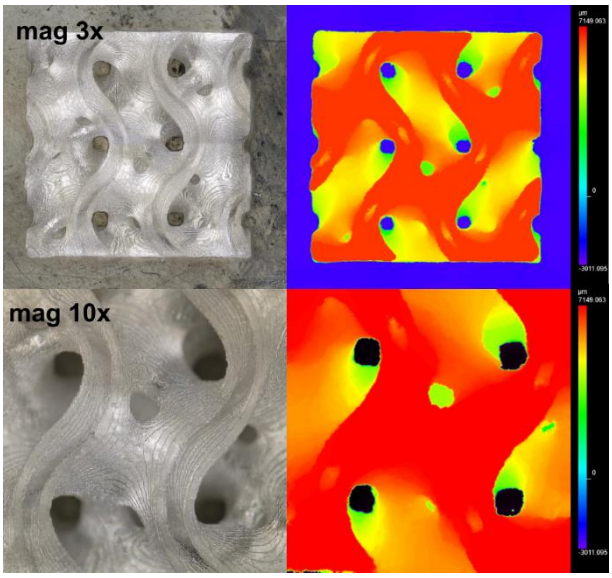

Figure 5.3.28 Images in two close-ups of a print of a gyroid struc-ture cube made of ABS-LIKE resin without nano-additives under MIX light, and a heatmap of the same cube showing the height of individual ele-ments taken with a DSX1000 optical microscope.

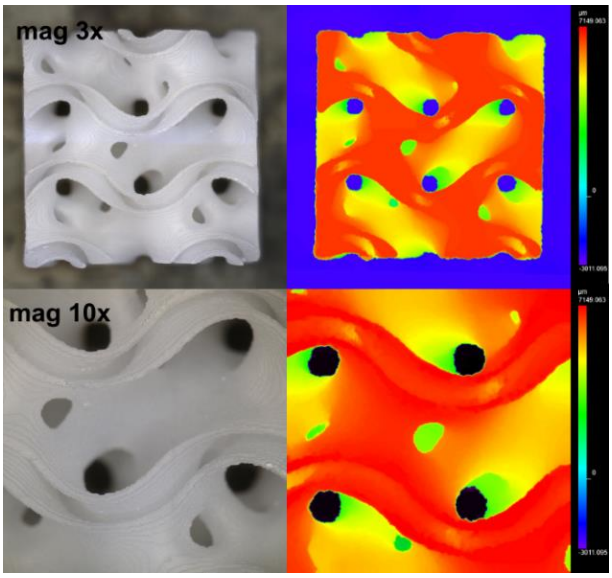

Figure 5.3.30 Images in two close-ups of a print of a gyroid structure cube made of ABS-LIKE resin with 10%$_{wt.}$ hydroxyapatite additive under MIX light, and a heatmap of the same cube showing the height of individual elements taken with a DSX1000 optical microscope.

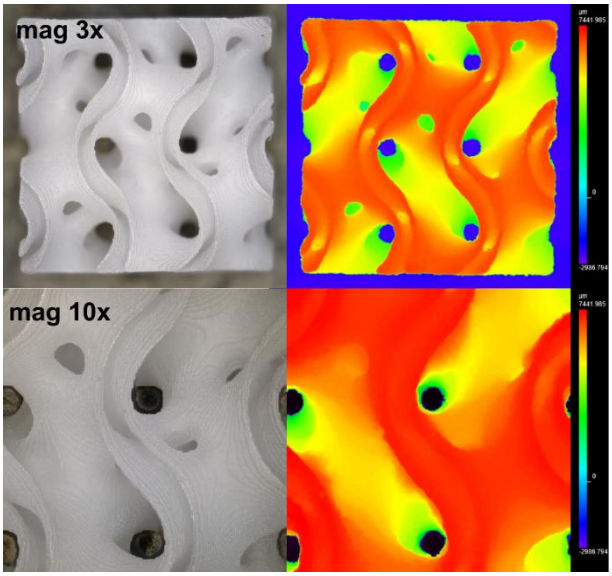

Figure 5.3.29 Images in two close-ups of a print of a gyroid struc-ture cube made of ABS-LIKE resin with 10%$_{wt.}$ aluminium (III) oxide additive under MIX light, and a heatmap of the same cube showing the height of individual elements taken with a DSX1000 optical microscope.

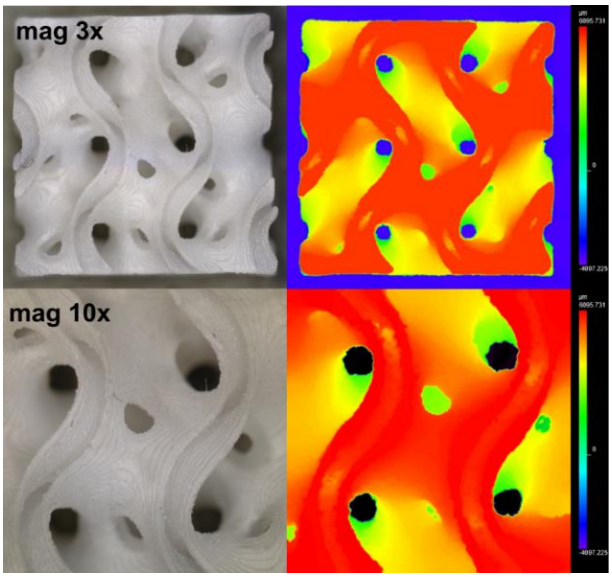

Figure 5.3.31 Images in two close-ups of a print of a gyroid struc-ture cube made of ABS-LIKE resin with 10% wt. halloysite nanoclay additive under MIX light, and a heatmap of the same cube showing the height of individual elements taken with a DSX1000 optical microscope.

SEM Images

In images, taken by scanning electron microscopy (SEM), of ABS-LIKE resin prints with the nanofillers aluminium (III) oxide (Figure 5.3.33), hydroxyapatite (Figure 5.3.35) and halloysite nanoclay (Figure 5.3.37), about 10 µm agglomerations can be observed on the outer sides of the printed layers.

However, EDS studies of each of the samples, which consisted of imaging the distribution of elements specific to a given nano-additives (Figure 5.3.34; Figure 5.3.36; Figure 5.3.38), did not show an agglomeration of the compounds used in the respective compositions, and an even dispersion of the used nano-fillers can be observed in that images.

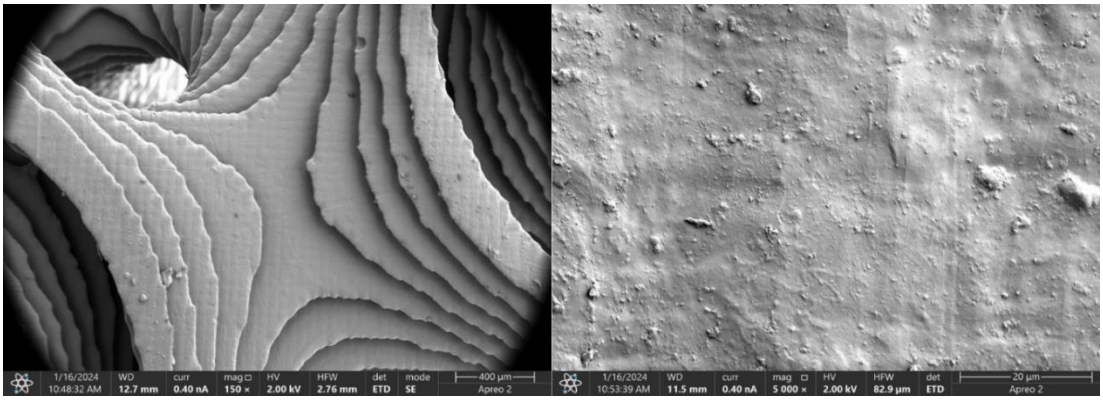

Figure 5.3.32 Images of printed gyroid cube made from ABS-LIKE resin without nano-additives taken with a scanning electron microscope in 150-magnification and 5000-magnification.

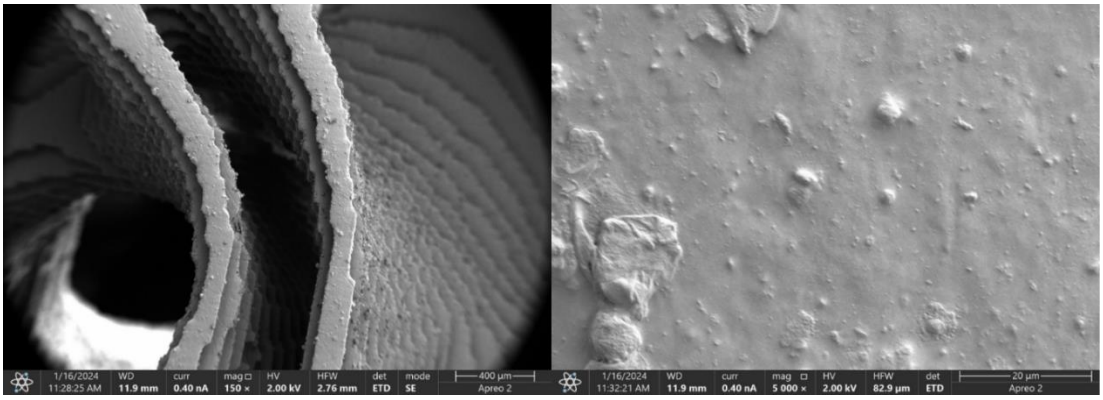

Figure 5.3.33 Images of printed gyroid cube made from ABS-LIKE resin with 10%$_{wt.}$ aluminium (III) oxide additive taken with a scanning electron microscope in 150-magnification and 5000-magnification.

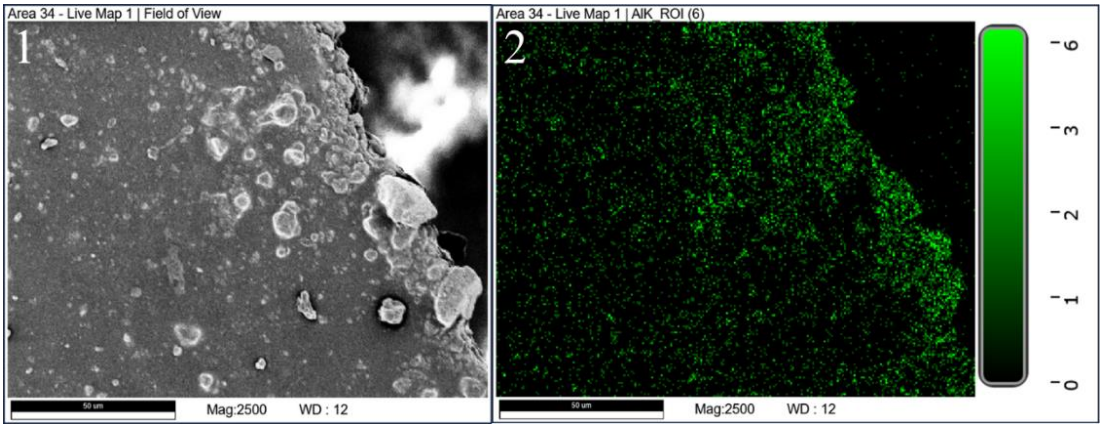

Figure 5.3.34 The EDS image of 1) tested site od gyroid cube and the element mapping image of the 2) aluminium (Al) on the print of the ABS-LIKE resin gyroid cube with 10%$_{wt.}$ aluminium (III) oxide (Al_2O_3) taken with a scanning electron microscope in 2500-magnificat

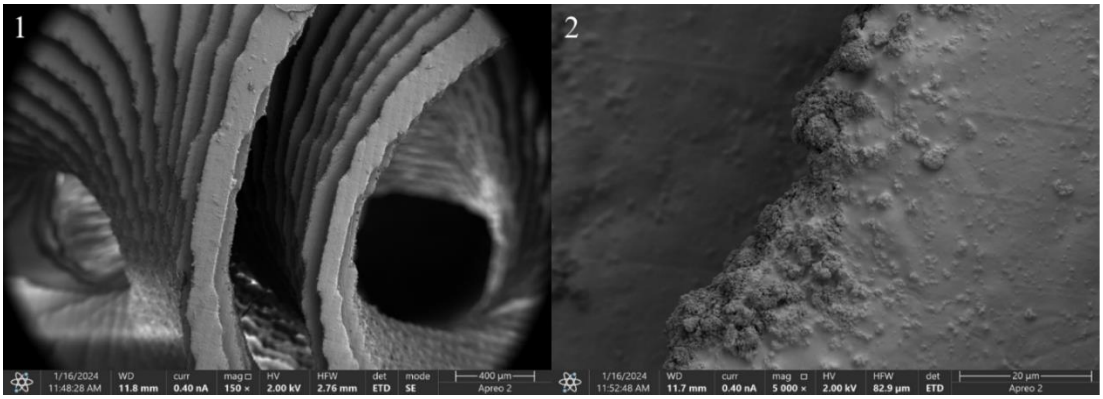

Figure 5.3.35 Images of printed gyroid cube made from ABS-LIKE resin with 10%$_{wt.}$ hydroxyapatite additive taken with a scanning electron microscope in 150-magnification and 5000-magnification.

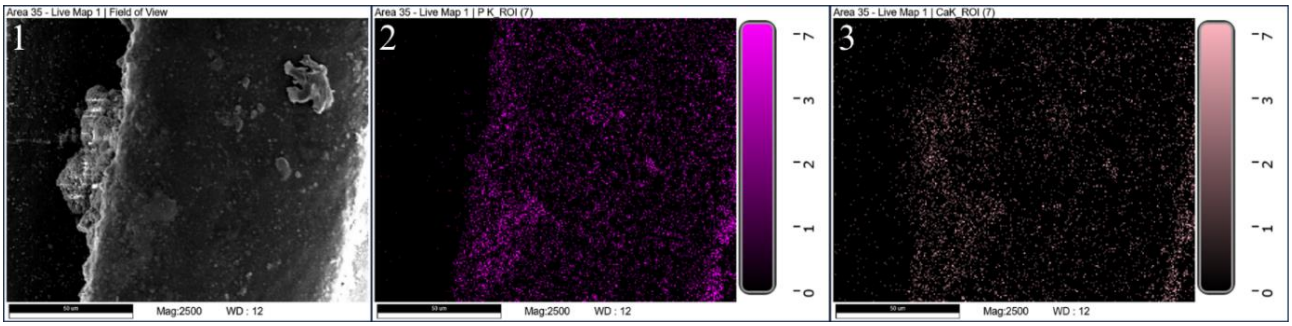

Figure 5.3.36 The EDS image of 1) tested site od gyroid and elemental mapping images of 2) phosphorus (P) and 3) calcium (Ca) on the print of the ABS-LIKE resin gyroid cube with 10%$_{wt.}$ hydroxyapatite ($Ca_{10}(PO_4)_6(OH)_2$) taken with a scanning electron microscope in 2500-magnification.

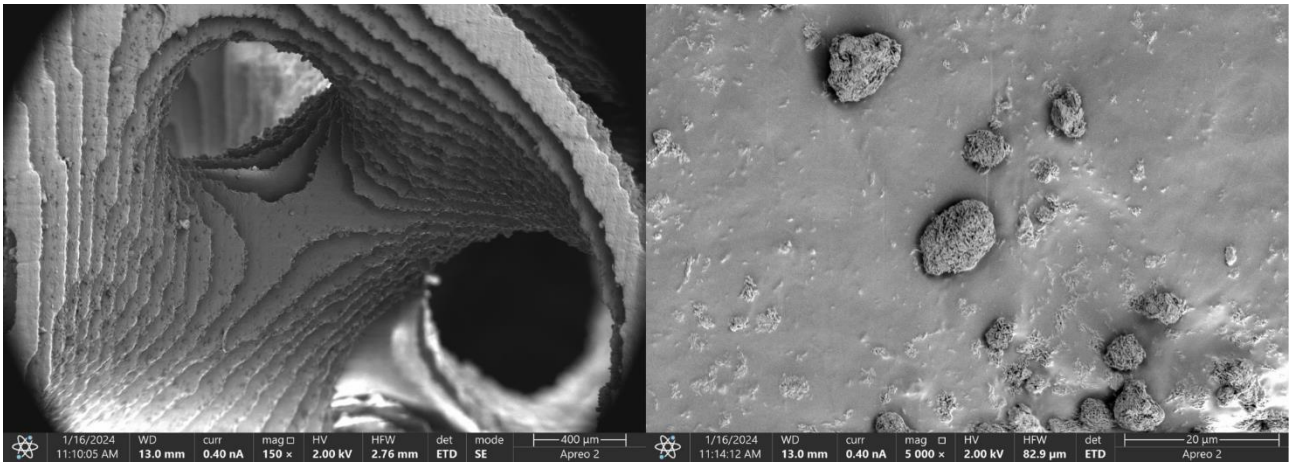

Figure 5.3.37 Images of printed gyroid cube made from ABS-LIKE resin with 10%$_{wt.}$ halloysite nanoclay additive taken with a scanning electron microscope in 150-magnification and 5000-magnification.

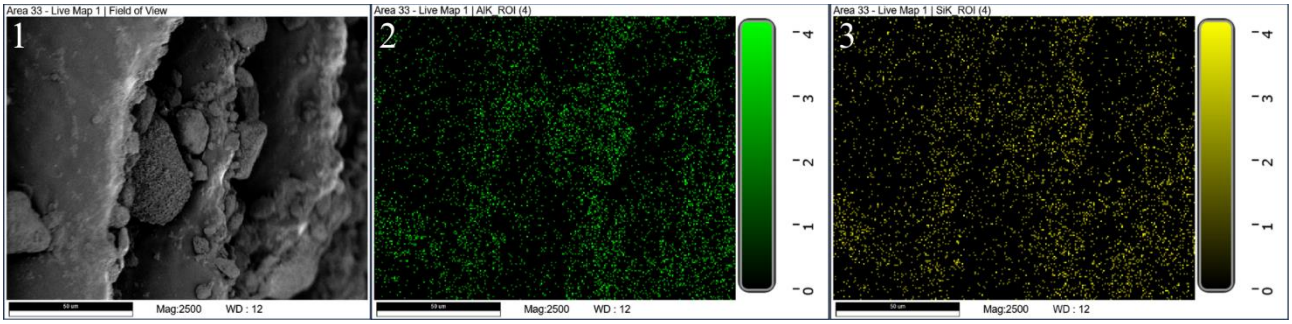

Figure 5.3.38 The EDS image of 1) tested site od gyroid and elemental mapping images of 2) aluminium (Al) and 3) silicon (Si) on the print of the ABS-LIKE resin gyroid cube with 10%$_{wt.}$ halloysite nanoclay ($Al_2Si_2O_5(OH)_4 \cdot 2\ H_2O$) taken with a scanning electron microscope in 2500-magnification

Tensile strength studies

Measurement of mechanical tensile strength was performed parallel to the layers of printed beams (Figure 5.3.4; Figure 5.3.15), placing them vertically in a Shimadzu measuring device (Figure 5.3.3).

For ABS-LIKE resin, an increase in the modulus of elasticity was observed in all tested cases after the addition of nanofillers (Figure 5.3.39). In the case of tensile stress at break, a slight increase in the value was noted when aluminium (III) oxide and hydroxyapatite were used (Figure 5.3.40).

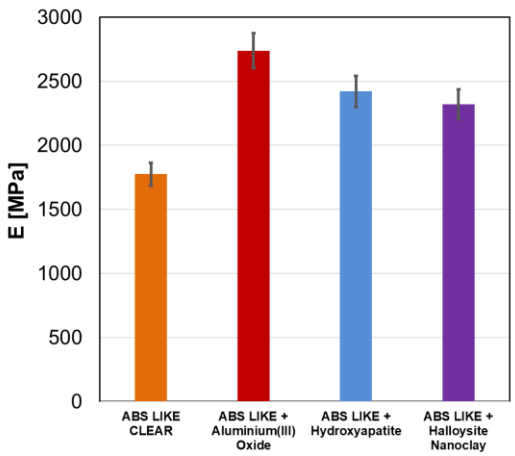

Figure 5.3.39 Graph of elastic modulus values for the tested ABS-LIKE resin compositions.

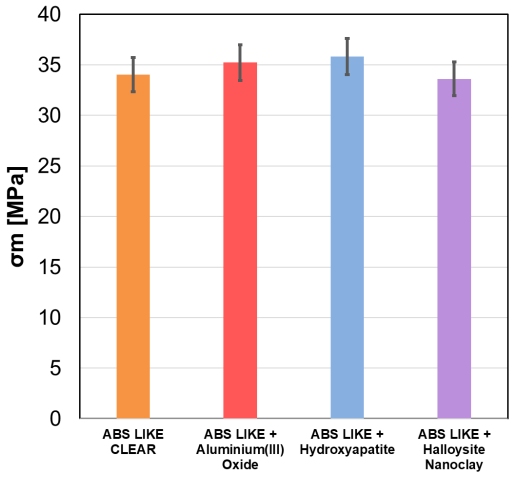

Figure 5.3.40 Graph of tensile stress at break values for the tested ABS-LIKE resin compositions.

Tensile strength measurements performed for the UV TOUGH resin and its based compositions showed a slight increase in elastic modulus (Figure 5.3.41) and tensile stress at break (Figure 5.3.42) after the addition of nanofillers, but in this case the addition of kaolin nanoclay performed best.

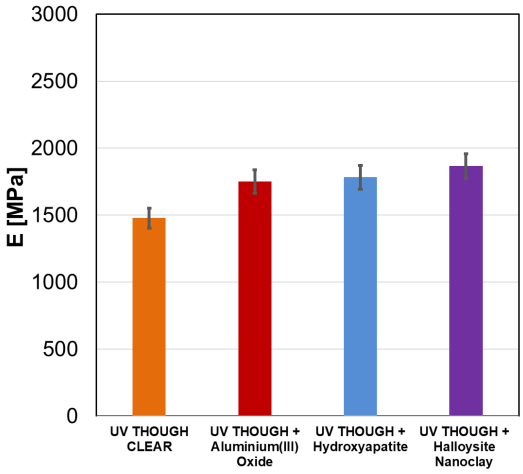

Figure 5.3.41 Graph of elastic modulus values for the tested UV TOUGH resin compositions.

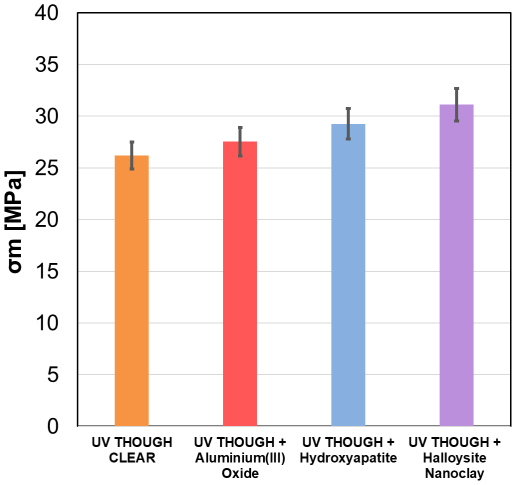

Figure 5.3.42 Graph of tensile stress at break values for the tested UV TOUGH resin compositions.

The data collected from the elastic modulus measurements for WATER WASH resin remained at 1750 MPa for the beam made from pure resin as well as for the beams made with the addition of the nanofillers aluminium (III) oxide, hydroxyapatite and kaolin nanoclay (Figure 5.3.43). The shaper made of pure WATER WASH resin showed a tensile stress at break value of 32 MPa, while the addition of nanofillers to this resin reduced this value below 30 MPa (Figure 5.3.44).

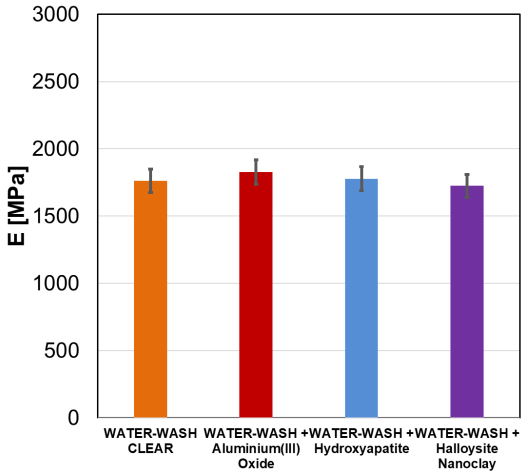

Figure 5.3.43 Graph of elastic modulus values for the tested WA-TER WASH resin compositions.

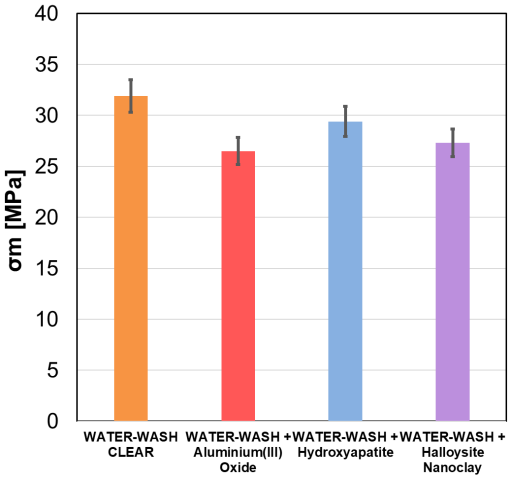

Figure 5.3.44 Graph of tensile stress at break values for the tested WATER WASH resin compositions.

Conclusions

According to the literature, even a small amount of nano-additives affects the properties of the composite, such as tensile strength and hardness, as well as polymerization kinetics. Our research results support this theory. The highest final conversion in the tested nanocompositions was obtained in systems containing titanium oxide (TiO_2), the reason for this may be that titanium (IV) oxide exhibits high photocatalytic activity and absorbs UV radiation (Kosmala et al. 2016; Pastrana-Martínez et al. 2013) indicating its beneficial effect on photopolymerization performance. In the case of ABS-LIKE resin, all tested nanofillers

improved the kinetics of the photopolymerization process and shortened the induction time, highlighting their potential as reaction modifiers. However, for the other two resins (UV TOUGH and WATER WASH), it was noted that the addition of silicon oxide (SiO_2) significantly reduced the final conversion of the composition, which may be due to its unfavourable interaction with the polymer matrix. In terms of print quality, cubes made from compositions containing hydroxyapatite, aluminium (III) oxide and halloysite nanoclay had a resolution comparable to pure resin, indicating their neutral effect on the quality of detail reproduction. Mechanical testing of the tensile strength of the printed polymer composites showed that the ABS-LIKE-based system with 10% wt. aluminium (III) oxide had the highest elastic modulus values. On the other hand, the tested nanocomposites based on WATER WASH resin showed a lower value of tensile stress at break in each case. This implies an easier rupture of each of these samples compared to the WATER WASH sample without nano-additives. The research underscore the need for careful selection of nanofillers to strike a balance between improving mechanical properties and print quality.

Acknowledgements

This research was funded by the National Science Centre under the OPUS LAP 20 Program, titled "Advanced Photopolymerized Nanocomposite Materials Processed by Additive Manufacturing," grant number 2020/39/I/ST5/03556.

References

Ahmad, N., Sultana, S., Azam, A., Sabir, S., & Khan, M. Z. (2017). Novel bio-nanocomposite materials for enhanced biodegradability and photocatalytic activity. New J. Chem., 41(18), 10198–10207. https://doi.org/10.1039/C7NJ00842B

Barton, J., Niemczyk, A., Czaja, K., Korach, Ł., & Sacher-Majewska, B. (2014). Kompozyty, biokompozyty i nanokompozyty polimerowe. Otrzymywanie, skład, właściwości i kierunki zastosowań. CHEMIK 2014, 68(4), 280-287.

Chen, X., Sun, J., Cai, P., Huang, J., Liang, H., Yuan, J., Yu, S., & Bai, J. (2024). Enhancing precision in ceramic vat photopolymerization 3D printing through dispersant optimization. Ceramics International, 50(22), 45114–45124. https://doi.org/10.1016/J.CERAMINT.2024.08.351

Fu, S., Sun, Z., Huang, P., Li, Y., & Hu, N. (2019). Some basic aspects of polymer nanocomposites: A critical review. Nano Materials Science, 1(1), 2–30. https://doi.org/10.1016/J.NANOMS.2019.02.006

He, X., Wang, R., Qi, S., Cheng, J., Ye, H., Li, H., Chen, S., Jian, B., & Ge, Q. (2023). Vat photopolymerization 3D printing of polymer-derived SiOC ceramics with high precision and high strength. Additive Manufacturing, 78, 103889. https://doi.org/10.1016/J.ADDMA.2023.103889

Jankowska, M., Lepcio, P., Chachaj-Brekiesz, A., Galek, M., Petko, F., Vozárik, A., & Ortyl, J. (2024). High-efficiency pentafluorostilbene-based photocatalysts dedicated to preparing fluorescent 3D printed polymer nanocomposites. Virtual and Physical Prototyping, 19. https://doi.org/10.1080/17452759.2023.2301030

Kalkal, A., Kumar, S., Kumar, P., Pradhan, R., Willander, M., Packirisamy, G., Kumar, S., & Malhotra, B. D. (2021). Recent advances in 3D printing technologies for wearable (bio)sensors. Additive Manufacturing, 46, 102088. https://doi.org/10.1016/J.ADDMA.2021.102088

Kosmala, K., & Szymańska, R., (2016). Nanocząstki tlenku tytanu (IV). Otrzymywanie, właściwości i zastosowanie. Kosmos. Problemy Nauk Biologicznych, 65(2), 235-245

Nichols, M. R. (2019). How does the automotive industry benefit from 3D metal printing? Metal Powder Report, 74(5), 257–258. https://doi.org/10.1016/J.MPRP.2019.07.002

Noworyta, M., Topa-Skwarczyńska, M., Jamróz, P., Oksiuta, D., Tyszka-Czochara, M., Trembecka-Wójciga, K., & Ortyl, J. (2023). Influence of the Type of Nanofillers on the Properties of Composites Used in Dentistry and 3D Printing. International Journal of Molecular Sciences, 24, 10549. https://doi.org/10.3390/ijms241310549

Pastrana-Martinez, L., Morales-Torres, S., Kontos, A., Moustakas, N., Faria, J., Dona-Rodriguez, J., Falaras, P., Silva, A. (2013). TiO2, surface modified TiO2 and graphene oxide-TiO2 photocatalysts for degradation of water pollutants under near-UV/Vis and visible light. Chemical Engineering Journal, 224(15), 17-23. https://doi.org/10.1016/j.cej.2012.11.040

Petko, F., Hola, E., Jankowska, M., Gruchała-Hałat, A., & Ortyl, J. (2023). 3D-VAT printing of nanocomposites by photopolymerization processes using amino-metaterphenyls as visible light-absorbing photoinitiators. Virtual and Physical Prototyping, 18(1). https://doi.org/10.1080/17452759.2023.2244936

Pilch, M., Topa-Skwarczyńska, M., Chachaj-Brekiesz, A., Jamróz, P., Kiesiewicz, D., Noworyta, M., & Ortyl, J. (2024). Luminescence labelled surfaces mapping system dedicated for use in quality control of 3D prints produced by stereolithography 3D printing (SLA) and laser engraving. Sensors and Actuators A: Physical, 365, 114828. https://doi.org/10.1016/J.SNA.2023.114828

Robakowska, M., Gibson, I., Akkerman, R., Wurm, F. R., & Gojzewski, H. (2023). Towards more homogeneous character in 3D printed photopolymers by the addition of nanofillers. Polymer Testing, 129, 108243.
https://doi.org/10.1016/J.POLYMERTESTING.2023.108243

Shameem, M. M., Sasikanth, S. M., Annamalai, R., & Raman, R. G. (2021). A brief review on polymer nanocomposites and its applications. Materials Today: Proceedings, 45, 2536–2539. https://doi.org/10.1016/J.MATPR.2020.11.254

Spychaj, S., Spychaj, T., Sobolewska, E., Frczak, B., Ey-Chmielewska, H. & Niegowska, I. (2007). Wpływ napełniaczy nanocząstkowych na właściwości stomatologicznych kompozytów akrylowych. Engineering of Biomaterials, 10(62), 18–25.

Stabik, J. (2004). Wybrane problemy reologii uplastycznionych polimerów napełnionych. Gliwice: Wydawnictwo Politechniki Śląskiej, 64-65

Zhu, H., Xu, R., Wan, T., Yuan, W., Shu, K., Boonprakob, N., & Zhao, C. (2024). Nanocomposites of Conducting Polymers and 2D Materials for Flexible Supercapacitors. Polymers (Vol. 16, Issue 6). https://doi.org/10.3390/polym16060756

6 Scientific articles

6.1 The effect of recycle amount on the properties of organic fertilizers

Gabija Aleksaitytė*,1, Odeta Pocienė, Rasa Šlinkšienė

1. Kaunas University of Technology, Kaunas, Lithuania

e-mail: gabija.aleksaityte@ktu.edu

KEYWORDS: *technology, organic fertilizers, buckwheat groats waste, recycle*

Abstract

Food and agriculture waste generated worldwide poses significant challenges, as decomposing waste releases substantial amounts of gas, contributing to climate change. One way to address this issue could be the use of organic waste from the food industry for fertilizer production. Granulated organic fertilizers would not only help reduce waste and emissions but also improve soil fertility. During the industrial production of such fertilizers, some granules do not meet the required size and must be returned to the process as recycle. This recycle can affect the properties of the final product, and its use requires additional technological equipment. In this study, biomass, buckwheat husks, buckwheat husk ash—which contains plant nutrients (C, N, P, K, Ca, Mg, Zn, Fe, Mn, Cu)—molasses solution, beaten eggs, and polyvinyl acetate were used for organic fertilizer granulation. The obtained results show that the highest amount of commercial granules was produced with 30% and 40% recycle; however, recycle does not significantly change other properties of fertilizers. Fertilizer granules were plastic or had a static strength between 7.03–10.05 N/granule, because the strength depends on the nature of solid raw materials and especially the liquid binder. The bulk density of fertilizers ranged from 232.2 kg·m^{-3} to 429.0kg·m^{-3}, and the pH interval was 6.9–13.6, depending on the composition of the raw material mixture.

Introduction

Agricultural industries have always been the foundation of global food production, with fertilizers playing a key role in increasing crop yields (Sutton et al., 2013). Fertilizers provide essential nutrients for plant growth and development, with the most important being nitrogen (N), phosphorus (P_2O_5), and potassium (K_2O). However, the excessive use of concentrated mineral fertilizers is linked to harmful impacts on ecosystems (Javed et al., 2022). Soil degradation, loss of organic matter, reduction in microorganisms, erosion, and declining fertility pose significant challenges to sustainable farming, underscoring the need for more efficient and sustainable fertilizer use (Roy et al., 2006; Buneviciene et. al., 2021). Farmers must strive to achieve high yields while minimizing their negative environmental impact, in line with the goals of the Green Deal.

Innovations such as nutrient recycling, biofertilizers, and improved nutrient use efficiency are becoming increasingly important. According to the World Bank, waste generation is projected to increase by 70% by 2050 (The World Bank, 2018). The Food and Agriculture Organization (FAO) reports that global food waste amounts to 1.6 billion tons, including 1.3 billion tons of edible waste (FAO, 2013). When biodegradable waste decomposes in landfills, it releases methane, a potent greenhouse gas that contributes to climate change.

One solution is to recycle organic waste from food industries, crop residues, and animal by-products into fertilizers. Organic fertilizers improve soil structure, fertility, and water retention, supporting sustainable agriculture and reducing reliance on synthetic fertilizers (IFA, 2021). Recycling waste into fertilizers represents a significant step toward reducing the environmental impact of waste and promoting a circular economy. This process includes composting and other conversion methods, transforming waste into nutrient-rich fertilizers for agricultural use.

While traditional methods such as composting, vermicomposting, and pyrolysis are common, they have limitations (Karps et al., 2017; Greinert et al., 2019). Composting, for example, releases greenhouse gases, and the inconsistent composition of compost makes direct application less effective. Therefore, producing granulated fertilizers with consistent composition and added value is a better option. These granules can be applied evenly using standard spreading equipment (Le Capitaine, 2023).

Granulation combines various raw materials containing essential plant nutrients to create a balanced and effective fertilizer. This process converts powdered materials into 2–5 mm granules, making them easier to handle. However, the process is complex, and obtaining high-quality granules often requires process improvements, including the reuse of granules that do not meet size specifications. These granules, known as "recycle," can improve product properties when used properly.

Materials

In this study, the waste materials used were sourced from the Lithuanian company “Ekofrisa”, a buckwheat groats producer. The main materials included uncleaned biomass (BM), buckwheat husk (BH), and buckwheat husk ash (BHA). These materials contain essential nutrients such as carbon (C), nitrogen (N), phosphorus (P), potassium (K), calcium (Ca), magnesium (Mg), zinc (Zn), iron (Fe), manganese (Mn), and copper (Cu). They were combined with binders such

as molasses solution (MS), beaten eggs (BE), and polyvinyl acetate (PVA) to produce organic fertilizers.

The properties of the granulated fertilizers, including particle size distribution, granule strength, bulk density (loose and compacted), moisture content, and pH, were analysed using standardized laboratory methods.

Methodology

Granulation was performed using a laboratory drum granulator-dryer (Figure 1.). Depending on the mixture's thermal stability, the temperature was maintained at 50–60 °C or 70–80 °C. The drum was inclined at a 5° angle and rotated at 20 rpm.

Moisture content was measured using a KERN MLS 50-3HA160N electronic moisture analyser (Germany).

Particle Size Distribution of raw materials and granulated products was determined using a set of sieves with different mesh sizes. Different fractions were weighed to an accuracy of ±0.001 g using KERN EW/EG-(N) electronic scales (Germany).

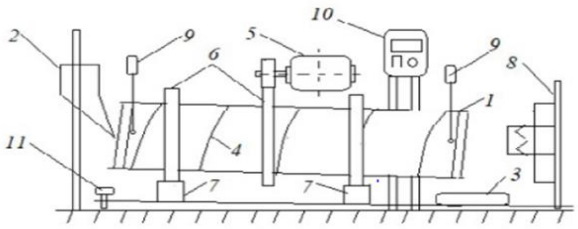

Figure 6.1.1 Laboratory drum granulator-dryer. 1 – granulator drum; 2 – raw material vent; 3 – product discharge opening; 4 – blades; 5 – electric motor; 6 – gearwheel; 7 – support roller; 8 – hot air supply; 9 – thermocouples; 10 – control panel; 11 – tilt angle lock.

pH values of 10% fertilizers aqueous solutions were determined by dissolving samples in distilled water and filtering the suspension through a 2–3 μm filter. Measurements were made using a HANNA Instruments pH 211 microprocessor pH–meter (USA).

Static Granule Strength was measured using the IPG-2 device (Russia) on 2–3 mm and 3–4 mm granules. At least 20 granules of similar size and shape were tested for each fraction.

Bulk density was determined by weighing an empty cylinder, then filling it with granules and measuring the weight difference. For the tapped density, the cylinder is subject to vibrations and compaction occurs until constant volume. The calculated mass difference between the empty cylinder and the cylinder with material is equal to the mass of tapped material per volume unit.

Scanning electron microscopy (SEM) whit electron microscope model S-3400N, (Japan) was used to determined surface morphology of organic fertilisers analysis.

Results

Even though fertilizers are produced industrially in large quantities and granulation processes are usually well known, the development of new fertilizers requires additional research and equipment improvements. To produce high-quality, stable fertilizers, many different factors (raw materials properties, moisture content, granulator parameters, process conditions) play an important role (Muranda, 2018; Woodroof, 2021). Therefore, this work attempted to evaluate the numerous factors mentioned and determine their influence on the organic fertilizers. Since organic materials are not inherently plastic or polar, their particles exhibit weak adhesion and cohesion forces. As a result, agglomeration is poor, making the use of binders essential for granulation. Organic fertilizers were produced from biodegradable raw materials (BHA, BH, BM), combined in different ratios with binders (PVA, BE, MS) and 20%, 30%, 40% recycle (R). For the granulation of bulk organic fertilizers, mixtures of raw materials with four different compositions were prepared, using the mentioned solid materials, liquid binders, and recycle. These fertilizers were dried, fractionated, and their physical properties evaluated.

The dependence of the amount of the commercial fraction (granule size 2–4 mm) of the granular product on the amount of recycle used in the raw material mixture and the moisture content of this mixture is presented in Figure 6.1.2. Other properties characterizing the quality of the fertilizer are presented in Table 6.1.1.

Table 6.1.1 Properties of the bulk organic fertilizer

Sample No.	Conditions of granulation process		The main properties of fertilizers				
	Amount of recycle (%)	Amount of binder (%)	Crushing strength of granules, (N/granule)	Density of granules ($kg \cdot m^{-3}$)		Humidity of granules (%)	pH of 10% fertilizer solution
				Bulk	Tapped		
I. 40% BHA : 60% BM + PVA (Binder)							
1	20	50.0	Plastic	375.9	396.9	13.40	13.2
2		48.7		312.4	333.7	12.58	13.1
3		47.4		310.8	321.8	11.72	13.3
4	30	50.0		370.9	393.0	15.08	13.6
5		48.7		364.1	351.1	13.30	13.2
6		47.4		308.7	328.8	12.38	13.2
7	40	48.7		350.8	373.2	13.38	13.1
8		47.4		348.3	372.7	12.95	13.3
9		46.0		335.9	365.7	11.15	13.3
II. 20% BHA : 80% BM + PVA (Binder)							
10	20	51.2	Plastic	323.6	336.6	20.84	8.0
11		50.0		298.3	314.2	17.77	8.5
12		48.7		289.7	310.4	16.65	9.2
13	30	51.2		417.2	429.0	21.27	9.1
14		50.0		376.9	397.8	18.48	9.2
15		48.7		336.5	361.1	16.90	9.8
16	40	51.2		405.2	415.2	21.46	9.8
17		50.0		372.6	383.8	18.19	10.1
18		48.7		364.2	381.7	17.18	10.5
III. 20% BHA : 40% BH : 40% BM R + BE (Binder)							
19	20	47.4	7.64	353.4	372.7	11.43	6.9
20		46.0	7.03	306.8	321.6	10.22	7.4
21		44.4	7.23	276.8	288.0	9.51	7.5
22	30	48.7	9.44	346.4	368.4	11.17	7.2
23		47.4	8.42	345.4	363.3	9.54	6.9
24		46.0	7.29	310.5	330.1	8.16	7.5
25	40	47.4	7.81	398.4	364.5	9.69	7.5
26		46.0	8.60	342.8	350.7	9.55	7.5
27		44.4	10.05	311.1	327.1	8.58	7.5
IV. 20% BHA : 40% BH : 40% BM + MS (Binder)							
28	20	50.0	Plastic	326.4	342.7	10.55	7.4
29		48.7		309.2	332.5	9.81	7.3
30		47.4		306.3	334.4	9.64	7.4
31	30	50.0		339.3	354.2	11.63	7.0
32		48.7		336.4	351.5	11.00	7.2
33		47.4		326.7	342.9	9.52	7.2
34	40	50.0		359.2	381.4	13.71	7.4
35		48.7		337.9	358.1	10.23	7.1
36		47.4		232.2	239.0	9.41	7.0

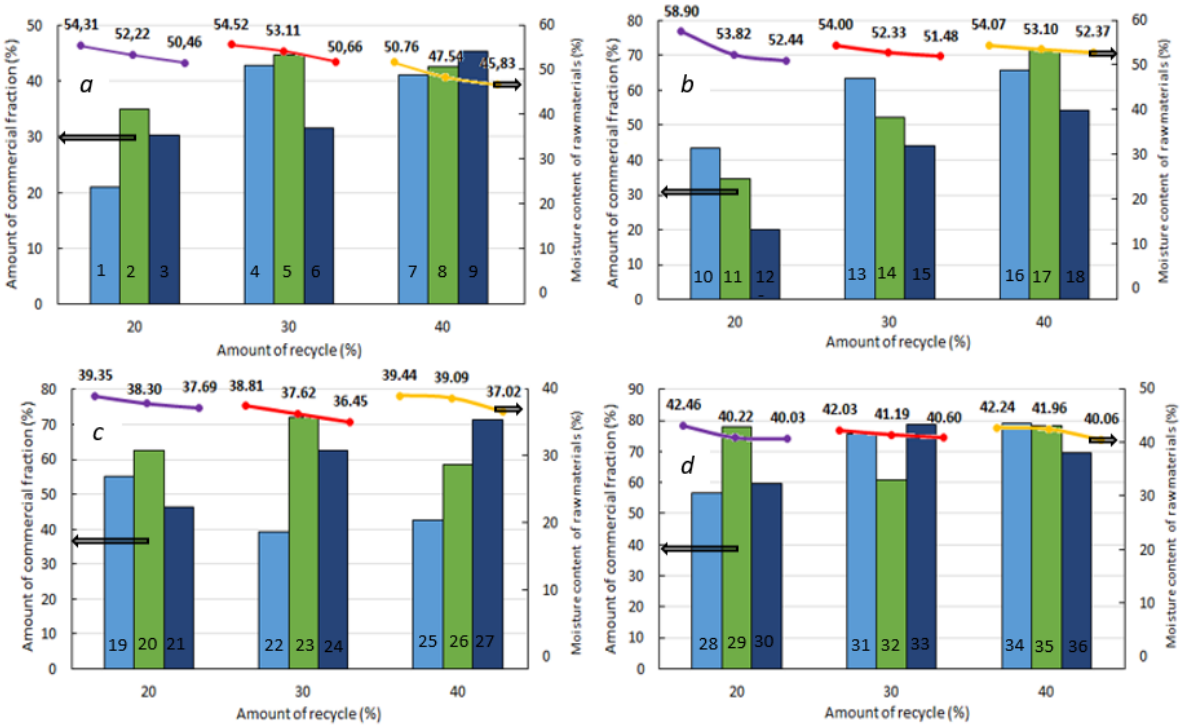

Figure 6.1.2 The influence of the humidity and the amount of recycle in the raw material mixture on the amount of the commercial fraction: a – composition IV.

In composition I (solid materials BHA, BM, R, and PVA solution as the liquid binder), the highest commercial fraction (35.07%) with 20% recycle and moisture content of 52.22% was obtained in sample 2. With 30% recycle, the highest commercial fraction (44.78%) was obtained in sample 5 where the moisture content was 53.11%. Using 40% recycle resulted in the highest commercial fraction (45.36%) in sample 9, despite the moisture being lower than that of the other samples. Other properties were influenced by moisture level and changed consistently.

In composition II, using the same raw materials but in a different ratio, a similar trend was observed. A higher commercial fraction correlated with an increase in the amount of recycle used: 43.21% (20% recycle, 58.90% moisture), 63.44% (30% recycle, 54.00% moisture), and 71.75% (40% recycle, 53.10% moisture). However, when 40% recycle was used, the binder's effect became inconsistent, and increasing the binder quantity did not necessarily improve granulation.

In composition III, where BH was added to BHA, BM, and R, and BE was used as a binder, the highest commercial fraction was obtained in samples 23 and 27. Sample 23 (30% recycle) had 37.62% moisture and yielded 72.18%, while sample 27 (40% recycle) had 37.02% moisture and yielded 71.45%. When 20% recycle was used (sample 20), the marketable fraction was lower (62.69%) with 38.30% moisture. In accordance with the conclusions of other scientists (Walker, 2003; Szluc, 2024), it can be stated that the amount of commercial fraction of fertilizers and the strength of granules depend on both the nature of the binder and the amount of liquid phase used. BE, a strong binder, was used here, making this composition's granules the only ones with measurable static strength (7.03–10.05 N/granule).

In composition IV, BHA, BM, BH, and R were used, moistened with MS. A consistently high commercial fraction (~78–79%) was achieved regardless of the recycle percentage. Sample 34, with 40% recycle and 42.24% moisture, yielded the highest fraction (79.03%). The pH of these compositions was neutral due to the high biomass content and the properties of the molasses solution binder.

It can be said that the granules obtained in all compositions except III are plastic. This means that they would not break up into smaller particles during transportation, which is an undesirable process (Woodroof, 2021). However, on the other hand, they may stick together because they are very humid. Also, due to their chemical composition, the granules are heterogeneous and porous (Figure 3), so they may start to mould when stored in a humid environment. More research is needed to solve these problems, but we assume that the quality of the granules could be improved by changing the drying conditions and coating them with conditioning agents.

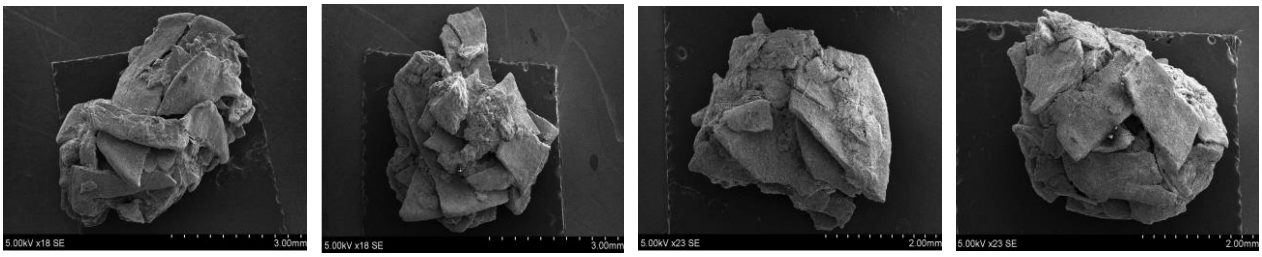

Figure 6.1.3 SEM image of granules: a – composition I; b – composition II; c – composition III;

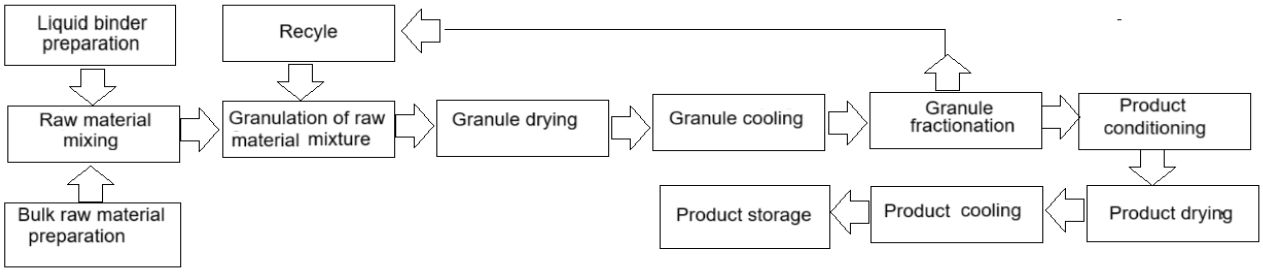

Figure 6.1.4 Scheme of organic fertilizer production with recycle

After evaluating the obtained results and the parameters of the granulation process, an organic fertilizer production scheme was created, which is presented in Figure 6.1.4

In conclusion, the use of recycle and binders significantly affects the granulation process and the quality of the final product, with 30-40% recycle often providing the optimal balance for high commercial fractions and consistent properties.

Conclusions

The results showed that using recycle especially 30 and 40%, resulted in a high amount of commercial fraction in all compositions. The highest commercial fraction yield, approximately 80%, was obtained in composition IV (20% buckwheat husk ash, 40% buckwheat husk, 40% biomass, and molasses solution as a binder), regardless of the amount of recycle used. However, other properties, such as pH, density of granules, and static strength, were more influenced by the composition and type of raw materials, as well as the binder's amount and type, than by the recycle. The pH of the first composition was highly alkaline (13.1–13.6) due to the high ash content, whereas the second composition had a lower pH (8.0–10.5). The third and fourth compositions had nearly neutral pH values (6.9–7.5). Granules in the first, second, and fourth compositions were plastic, while those in the third composition exhibited static strength (7.03–10.05 N/granule), influenced by the beaten egg binder. The loose bulk density of granules across all compositions ranged from 232.2 to 417.2 kg·m^{-3} and their tapped density, ranging from 239.0 to 429.0 kg·m^{-3}, indicated that the granules were lightweight.

Acknowledgements

The research was financed by the Lithuanian Research Council of Lithuania project no. S-SV-24-378.

References

Buneviciene, K., Drapanauskaite, D., Mazeika, R., Baltrusaitis, J. A. 2021. Mixture of Green Waste Compost and Biomass Combustion Ash for Recycled Nutrient Delivery to Soil. Agronomy. 11, 641. https://doi.org/10.3390/agronomy11040641.

Sutton, M.A, Bleeker, A., Howars, C.M. et al. 2013. Our Nutrient World Centre for Ecology and Hydrology (CEH), Edinburgh UK. P. 128. ISBN: 978-1-906698-40-9.

FAO. Food wastage footprint. Impacts on natural resources. Summary report 2013. https://www.fao.org/3/i3347e/i3347e.pdf

Greinert, A., Mrówczyńska, M., Szefner, W. 2019. Study on the Possibilities of Natural Use of Ash Granulate Obtained from the Combustion of Pellets from Plant Biomass. Energies. 12, 2569. https://doi.org/10.3390/en12132569.

IFA. 2021. Re-thinking the Role of Plant Nutrients. Food System Summit. https://www.scribd.com/document/521183161/2021-IFA-Re-thinking-the-Role-of-Plant-Nutrients.

Javed, A., Ali, E., Afzal, K.B., Osman, A., Riaz, S. 2022. Soil Fertility: Factors Affecting Soil Fertility, and Biodiversity. Responsible for Soil Fertility. Int J Plant Anim Environ Sci. 12 (1): 021-033. DOI: 10.26502/ijpaes.202129.

Karps, O., Aboltins, A., Palabinskis, J. 2017. Biomass ash utilization opportunities in agriculture Proceedings of the 8th International Scientific Conference Rural Development. 193-198. DOI: 10.15544/RD.2017.083.

Le Capitaine, S. Systems for Granular Fertilizer and Soil Amendment Production. Feeco International. 2023. https://feeco.com/systems-for-granular-fertilizer-and-soil-amendment-production/.

Muranda, F. Effect of fertilizer formulation on dust formation. 2018.

Senhaji, M.L, Hafnaoui, A., Khouloud, M., Agri A.E., Boulahna, A., Asri M.E., Formulation of anti-dust coating agent for monoammonium phosphate fertilizer using experimental design. Chemometrics and Intelligent Laboratory Systems. 2021, 216. https://www.sciencedirect.com/science/article/pii/S016974392100143X

Szulc, A., Skotnicka, E., Gupta, M., Krolczyk, J. Powder agglomeration processes of bulk materials – A state of the art review on different granulation methods and applications. Powder Technology. 2024. No. 413. https://www.sciencedirect.com/science/article/pii/S0032591023008756?via%3Dihub

Roy, R.N., Finck, A., Blair, G.J., Tandon, H.L.S. 2006. Plant nutrition for food security. FAO Fertilizer and Plant Nutrition Bulletin 16. https://www.fao.org/3/a0443e/a0443e.pdf.

The World Bank. 2018. Press release. https://www.worldbank.org/en/news/press-release/2018/09/20/global-waste-to-grow-by-70-percent-by-2050-unless-urgent-action-is-taken-world-bank-report.

Walker, G.M., Moursy, H.E.M.N., Holland, C.R., Ahmad, M.N. Effect of process parameters on the crush strength of granular fertiliser. Powder Technology. 2003, No.132. https://www.sciencedirect.com/science/article/pii/S0032591003000391

Woodroof, N. Size Matters. Word Fertilizers. 2021. https://www.worldfertilizer.com/special-reports/05042021/size-matters/?utm_source=chatgpt.com

7 Abstracts: Materials engineering

7.1 Impact of selected process parameters on the characteristics of calcium carbonate-rich powder produced during the direct mineral carbonation of gypsum

Temesgen Abeto Amibo*[,1,2], Donata Konopacka-Łyskawa

1. Gdansk University of Technology, Faculty of Chemistry, Department of Process Engineering and Chemical Technology, Poland
2. School of Chemical Engineering, Jimma Institute of Technology, Jimma University, Jimma, Ethiopia

e-mail: temesgen.amibo@pg.edu.pl

KEYWORDS: *gypsum, mineral carbonation, calcium carbonate, polymorphs*

The main reasons for the global warming is the high concentration of carbon dioxide in the atmosphere. Various carbon dioxide reduction strategies are proposed to mitigate the effects of high atmospheric carbon dioxide concentrations. Mineral carbonation (MC), which is used in these studies to produced calcium carbonate, is one of the industrial carbon capture technologies. This work aimed to present the influence of selected process parameters on the quality of $CaCO_3$ powder produced during MC of gypsum in ammonia solution. In the current investigation, the following variables Ca:NH_3 ratio, 1,4-butanediol (BUD) concentration, and the stirring speed were optimized to produce the powder with the high $CaCO_3$ concentration. The solid-to-liquid ratio of the reaction mixture was 1:0.015 $g \cdot dm^{-3}$, the volume flow rate of gas introduced into the batch reactor was $0.5 dm^3 \cdot min^{-1}$, and the CO_2 volume fraction in gas was 15% by volume. The determined p-values for the influence of all tested factors on the dependent variables characterizing synthesized $CaCO_3$ were less than 0.05, which indicates their significance on MC products. An increase in the Ca:NH_3 molar ratio and BUD concentration resulted in significantly higher gypsum conversion. The highest concentration of $CaCO_3$ in the obtained powder was 88.48%, and the dominant polymorphic form of calcium carbonate in the products was vaterite. The effect of the Ca:NH_3 molar ratio and BUD concentration on the polymorphic composition of the tested samples was significant, and the vaterite concentration's dependence on both of these parameters showed a minimum. On the other hand, with the increase in the stirring speed, the vaterite concentration decreased. The highest vaterite content in $CaCO_3$ powder was 86.97%. The presence of BUD in the solution significantly affected the specific surface area, and an increase in BUD concentration resulted in an increase of this parameter. However, an increase in the Ca:NH_3 molar ratio and stirring speed slightly increased the surface area of $CaCO_3$ powder. The highest surface area of the obtained powder was 5.18 $m^2 \cdot g^{-1}$. The pore volume of the obtained powders was small and reached a maximum of 0.000346 $m^3 \cdot g^{-1}$.

7.2 Investigation of the heavy metals sorption properties of porous materials based on coffee grounds and agar

Jan Ciołkowski[1,*], Jagoda Dyderska, Adrian Malinowski, Andrzej Krasiński

1. Scientific Club of Chemical and Process Engineering "Venturi", Faculty of Chemical and Process Engineering, Warsaw University of Technology, Warsaw, Poland

e-mail: jan.ciolkowski.stud@pw.edu.pl

KEYWORDS: *coffee grounds, heavy metals removal, sustainable sorbent, water purification, zero waste*

Heavy metals represent a significant class of pollutants in surface waters, posing serious threat to the public health. Accordingly, the elimination of these contaminants from drinking water is of utmost importance. A variety of processes, such as ion exchange, membrane technologies, and adsorption are routinely employed in water treatment to achieve this goal. At the same time, regulatory standards for drinking water quality have become increasingly stringent, resulting in lower allowable concentrations of specific contaminants, including heavy metals ions. In the context of adsorption, various sorbents can be utilized. In line with the principles of sustainable development and the closed-loop economy, there is a growing emphasis on repurposing waste materials for various applications. Spent coffee grounds, for instance, serve as one such material that can be successfully applied as a sorbent of various contaminants dissolved in the water. The "Venturi" Scientific Club of Chemical and Process Engineering has confirmed the sorption capabilities of spent coffee grounds and works on development of a macroporous composite material derived from this residue and agar. Future research will focus on optimization of the structure for operation in flow and determination of performance parameters. Finally, prototype system that utilizes the material will be designed to demonstrate the efficiency of heavy metal removal from water.

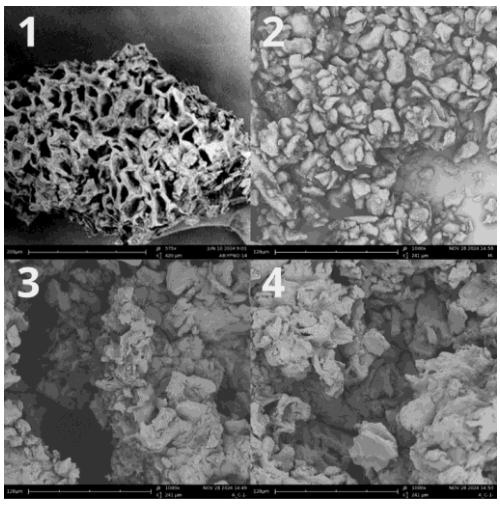

Figure 7.2.1 SEM images of 1) used coffee ground 575x, 2) ultra fine milled coffee grounds 1000x, 3),4) integrated coffee-agar porous structures 1000x

Acknowledgements

The project was funded by Rector's grant for scientific clubs within the Excellence Initiative: Research University (IDUB) programme.

7.3 Research on the synthesis of rhenium oxides on different catalytic supports and their use as catalysts in a DBD cold plasma reactor

Krzysztof Czyżewski[1], Agata Dorosz, Arkadiusz Moskal, Katarzyna Jabłczyńska*

1. Faculty of Chemical and Process Engineering, Warsaw University of Technology, Warsaw, Poland

e-mail: katarzyna.jablczynska@pw.edu.pl

KEYWORDS: *rhenium trioxide, plasma reactor, CO_2 conversion, O_2 conversion*

Rhenium is a rare and valuable element with catalytic properties that remain partially unexplored, offering promising opportunities for further investigation. The main goal of this study was to investigate methods for depositing nanoparticles of rhenium oxides onto different types of reactor fillings forming a packed bed and to evaluate their catalytic activity in a dielectric barrier discharge (DBD) plasma reactor.

The supports used included 3 mm glass beads, small copper springs and glass beads pre-coated with titanium dioxide. The supports were coated with a layer of rhenium oxide using the physical vapor deposition (PVD) method with hopes of obtaining nanoparticles. Characterization of the rhenium oxide coating on the supports was conducted using scanning electron microscopy (SEM) and an X-ray diffraction (XRD). A cylindrical, coaxial DBD plasma reactor made of glass (16 mm inner diameter, 0.5 m length) was used for the catalytic tests. The reactor utilized a 5 mm diameter steel rod as the central collecting electrode, while a copper foil acted as the discharge electrode. The study examined the ability to convert oxygen from atmospheric air into ozone and carbon dioxide in an argon atmosphere into carbon monoxide, which can be further utilized in the production of synthetic fuels. The influence of process variables, including gas flow rate (ranging from 5 to 25 $l \cdot min^{-1}$) and energy input (up to 150 W), was also investigated.

We demonstrated better catalytic activity for catalysts where rhenium oxides were deposited on titanium dioxide-precoated glass beads or copper springs compared to chemically neutral support.

Figure 7.3.1 Scanning electron microscopy (SEM) image of rhenium trioxide crystals deposited onto a glass substrate through physical vapor deposition (PVD).

7.4 Synthesis and Stability Assessment of Rhenium Oxide for Catalytic Applications

Jagoda Dyderska[1], Katarzyna Jabłczyńska*

1. Faculty of Chemical and Process Engineering, Warsaw University of Technology, Warsaw, Poland

e-mail: katarzyna.jablczynska@pw.edu.pl

KEYWORDS: *rhenium oxides, pH-dependent stability, physical vapor deposition*

The stability of particle suspensions is critical for the effective application of nanomaterials in catalysis, electronics, and environmental remediation. Rhenium oxides (ReO_x) are promising materials due to their unique properties; however, their suspension stability has not been extensively studied. This research aimed to investigate the short-term and long-term stability of ReO_x particle synthesized via physical vapor deposition (PVD) in aquous suspensions.

Rhenium oxide particles were produced by heating ammonium perrhenate (NH_4ReO_4) in a beaker placed on a hot plate set to 400°C. The low sublimation temperature of ReO_x (~250 °C) allowed the oxides to vaporize and deposit as a thin film on the cooler surface of 3 mm diameter glass beads layered above the precursor. The resulting blue ReO_x particles were then washed off the glass beads using an ultrasonic cleaner for 10 minutes.

The stability of the suspensions was assessed across a range of pH levels (from 4 to 11) to identify optimal conditions for maintaining dispersion. Stability was evaluated through absorbance measurements with a spectrophotometer and particle size distribution analysis via dynamic light scattering (DLS).

Results indicated a significant influence of pH on the absorbance of the suspensions. After redispersing the particles in pure water, the absorbance remained stable for 30-40 minutes, showing only slight decreases during this period, regardless of the day. However, in alkaline conditions, absorbance dropped dramatically by 60-80% within the first 10 minutes, indicating colloidal instability primarily due to particle agglomeration and sedimentation. Over the subsequent days, higher pH levels correlated with increased discoloration, evidenced by a gradual decrease in absorbance. The suspension's color, immediately following ultrasound redispersion, lightened significantly each day, suggesting a loss of stability and the occurrence of chemical transformations that likely led to the formation of soluble rhenium compounds. The average size of ReO_x particles redispersed in pure water increased significantly over the three days, starting at approximately 200 nm on the first day and growing to between 500 and 700 nm by the third day. In contrast, the smallest particle sizes were observed in acetic acid, where the size distribution remained stable for at least an hour.

In conclusion, these findings highlight the importance of pH in maintaining the stability of ReO_x suspensions, with acidic conditions notably enhancing colloidal stability. This insight may improve the performance of rhenium-based nanomaterials in various practical applications.

7.5 Hydration mechanism of polyimide aerogels

Bertold Ecsédi[1], Attila Forgács, József Kalmár*

1. HUN-REN Mechanisms of Complex Homogeneous and Heterogeneous Chemical Reactions Research Group, Department of Inorganic and Analitical Chemistry, University of Debrecen, Debrecen, Hungary

e-mail: kalmar.jozsef@science.unideb.hu

KEYWORDS: *aerogel, NMR, polyimide, hydration*

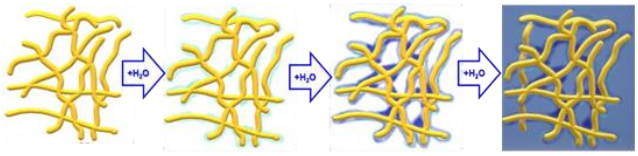

Figure 7.5.1 Schematic picture of hydration of polyimide aerogels

Aerogels are highly mesoporous materials characterized by a large surface area and low envelope density. These materials are excellent thermal and electrical insulators. Due to their frequent application in wet environments, investigating their hydration mechanisms is essential, which can be studied using nonconventional liquid-phase NMR techniques. This presentation focuses on the hydration of two cross-linked 3D-structured polyimide aerogels with slightly different chemical structures, but similar mechanical properties.

Scanning electron microscopy images have shown that both aerogels are composed of polymer nanofibrils. N_2 sorption measurements have demonstrated that these aerogels are predominantly mesoporous (with pore diameters ranging from 2 to 50 nm), but macropores are also present.

For the partially hydrated aerogels, NMR relaxometry have identified three types of water-structures with different chemical environments (relaxation domains) in the pores. At low water content, two domains were detected with short transverse relaxation times (T_2). Adding more water to the system caused the appearance of a third domain with much higher T_2 values. The domains with lower T_2 values correspond to water absorbed into and adsorbed onto the fibrils. The third domain, with the highest relaxation times, represents small water droplets in the pores.

NMR cryoporometry, solid-phase NMR, and NMR diffusometry measurements have confirmed that the morphology of these materials does not change significantly during hydration.

Acknowledgements

„Supported by the EKÖP-24-2 University Research Scholarship Program of the Ministry for Culture and Innovation from the source of the National Research, Development and Innovation Fund.”

7.6 Advanced magnetic membranes as the key for CO_2 recovery from the CO_2/N_2 mixtures

Paweł Grzybek*[1,2], Janusz Pryciuk, Gabriela Dudek

1. Department of Physical Chemistry and Technology of Polymers, Silesian University of Technology, Gliwice, Poland
2. PhD School, Silesian University of Technology, Gliwice, Poland

e-mail: pgrzybek@polsl.pl

KEYWORDS: *CO_2 recovery, gas separation, membrane*

The aim of the presentation is demonstration of novel polyimide nanocomposite membranes (PI_NMs), including the preparation method and its application for separation of the carbon dioxide/nitrogen (CO_2/N_2) mixture.

The PI_NMs were prepared from the solution using solvent casting. As the fillers, the hematite (Fe_2O_3) and magnetite (Fe_3O_4) nanoparticles were used. The scheme of the preparation method was showed in Figure 7.6.1.

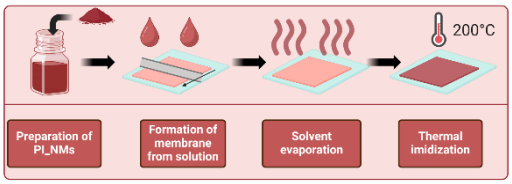

Figure 7.6.1 The preparation method of the PI_NMs membranes.

Both the Fe_2O_3 and Fe_3O_4 possess high sorption capacity of the CO_2 due to their basic nature and great specific surface area. Moreover, the Fe_3O_4 particles are strong magnets, while the Fe_2O_3 particles have antiferromagnetic properties. Therefore, in presented study, we studied the relation between sorption (IGA), structure (SEM, AFM) and magnetic nature (magnetometer) of the PI_NMs applied for the separation of CO_2/N_2 mixture.

PI_NMs indicated high selectivity for CO_2/N_2 mixture, while the permeance of the CO_2 was very low. The investigation of the structural, sorption and magnetic properties of PI_NMs enabled the precise explanation, which of these played the crucial role in view of gas separation performance.

Acknowledgements

This research was funded in whole or in part by the National Centre of Science, Poland 22/47/O/ST8/01853. For the purpose of Open Access, the author has applied a CC-BY public copyright licence to any Author Accepted Manuscript (AAM) version arising from this submission.

7.7 The influence of hydrothermal synthesis conditions on zinc oxide morphology and photocatalytic properties

Zuzanna Kupniewska*[,1], Łukasz Werner

1. Faculty of Chemical and Process Engineering, Warsaw University of Technology, Warsaw, Poland

e-mail: zuzanna.kupniewska.stud@pw.edu.pl

KEYWORDS: *zinc oxide, morphology, synthesis, photocatalysis, kinetics*

Nanostructured zinc oxide (ZnO) is a material of great potential for its applications in numerous fields such as photocatalysis, solar cells or sensors. The chemical bath deposition (CBD) synthesis method with ethanolamine as a chelating agent has been chosen due to its ability to easily control the morphology of the synthesised ZnO particles.

By adjusting reaction conditions such as the concentration of the reagent in the mixture, the molar ratio between $Zn(OAc)_2$ and NH_4OH, the volume ratio of the ethanolamine/water, the star-like particles ZnO with different morphology were obtained, all exhibiting a hexagonal (wurtzite) structure. Various analytical techniques (eg. SEM, XRD, TGA, FTIR) were used to investigate the morphology and physicochemical properties of the particles. The influence of synthesis conditions on the ZnO growth kinetics has also been shown.

The study shows that the concentration of the precursor dramatically influences the axial and radial growth of ZnO particles.

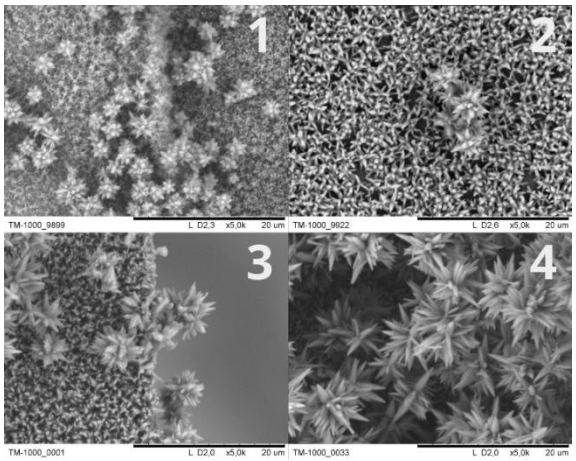

Figure 7.7.1 SEM images of ZnO star-like particles synthesised in reaction mixtures differing in the molar ratios of the substrates.

Acknowledgements

The research was funded by POB Materials Technologies of Warsaw University of Technology within the Excellence Initiative: Research University (IDUB) program.

7.8 Properties of antibacterial surfaces

Dominik Műller[1], Agata Krakowska*, Joanna Zontek-Wilkowska, Żaneta Binert-Kusztal, Beata Paczosa-Bator

1. Department of Analytical Chemistry and Biochemistry, Faculty of Materials Science and Ceramics, AGH University of Krakow, Krakow, Poland

e-mail: agata.krakowska@uj.edu.pl

KEYWORDS: *surface, etchnig process, properties*

Appropriate modification of the surface of materials significantly affects the change and improvement of barrier properties. This is of great importance, for example, in obtaining antiseptic and antibacterial surfaces. And appropriate design of the surface modification process translates into obtaining surfaces of a biomimetic nature, with clearly differentiated hierarchical structures.

Hence, it is justified to search for new solutions that will significantly improve surface parameters while reducing the risk of its contamination. Techniques that have so far only been used in electrical, optoelectronic and special materials are increasingly used. One of them is the reactive ion etching technique (REA), which allows for controlled etching of selected areas of the material surface with argon ions. It uses a combination of chemical and physical reactions, and the reaction products produced on the surface permanently change the surface properties.

In the conducted studies, model glass samples from the SLS system were subjected to the ion etching process. In order to determine the optimal conditions of the material surface etching process using argon ions, the range of argon ion concentrations and exposure time were determined. As a result, a surface was obtained characterized by increased light transmittance parameters, increased surface roughness and the formation of an oxide layer. The obtained material was characterized by a repeatable layer structure (honeycomb), which has confirmed antibacterial properties.

Acknowledgements

Research project supported by program "Excellence initiative-research university" for the AGH University of Krakow.

7.9 Kinetic Studies of New Photoinitiating Systems to Obtain High-Performance Resins Dedicated to 3D Printing

Jakub Pietraszewski[1], Monika Topa-Skwarczyńska, Karolina Kozanecka, Filip Petko, Mariusz Galek, Joanna Ortyl[*]

1. Faculty of Chemical Engineering and Technology, Cracow University of Technology, Cracow, Poland

e-mail: jortyl@pk.edu.pl

KEYWORDS: *radical photopolymerization, kinetics, photoinitiators, polymer materials, 3D printing*

Radical photopolymerization is a fast chemical reaction with low energy requirements that solidifies resins by forming polymer networks when exposed to light, typically at room temperature, which saves energy. In 3D printing, this process enables the precise layer-by-layer construction, essential in fields like dentistry and medical device manufacturing. Yet, many photoinitiators on the market rely on UV light, which can be limiting for manufacturing techniques that use visible light sources. This study addresses the need for more versatile photoinitiators that can work effectively with safer, cost-effective light sources, such as those at a 405 nm wavelength, commonly found in modern 3D printers,

The aim of this study was to develop and test new two-component photoinitiating systems capable of initiating radical photopolymerization under visible light. This research sought to create versatile, high-performance resin formulations for 3D printing applications where UV exposure poses limitations, particularly in fields requiring safer and more energy-efficient solutions.

To evaluate the performance of these new systems, a range of spectroscopic methods was used, including absorbance, photolysis, and emission studies, to closely examine their behaviour. Real-time FT-IR spectroscopy provided key insights into the polymerization kinetics of methacrylate-based compositions, allowing to monitor bond conversion rates and induction times accurately. This detailed analysis provided insights into the efficiency and control offered by these two-component systems.

This work demonstrates that these new systems significantly improve reactivity, delivering high conversion rates and low induction times, which are critical for achieving consistent and high-quality prints. The adaptability and compatibility with visible light sources offer high print quality, stability, and durability, making these systems a viable alternative to traditional UV-based initiators. Overall, this study contributes to advancing the use of radical photopolymerization in 3D printing.

Acknowledgements

This research was funded by National Centre for Research and Development in Poland under the Lider Program, grant number LIDER13/0156/2022.

7.10 Investigations into the influence of the type of 3D printers available on the market and their parameters on the resolution and shrinkage of the obtained printouts

Jakub Pietraszewski[1], Monika Topa-Skwarczyńska, Joanna Ortyl[*]

1. Faculty of Chemical Engineering and Technology, Cracow University of Technology, Cracow, Poland

e-mail: jortyl@pk.edu.pl

KEYWORDS: *polymer materials , 3D printing , photopolymerization , polymerization shrinkage*

3D printing is an incremental material manufacturing method that is widely used in many industries, such as dentistry, medical device manufacturing, due to its ability to produce parts with extremely high resolution and detail. One variation of 3D printing is VAT photopolymerization, in which parts are produced during the selective curing of light-cured resin compositions layer by layer. Among 3D printers operating according to VAT photopolymerization technology, one can mention DLP printers – in which case the light source is a projector - and LCD printers – which use a flat-panel LCD screen as a mask to selectively block or allow UV or visible light from an LED array, curing resin layer by layer with precise control over light exposure.

Accuracy, resolution and stability of 3D printed structures are critical factors in 3d-VAT printing applications, where high precision is often required for detailed parts and functional prototypes. However, these factors can vary with different printing parameters and the type of 3D printer used. The discrepancy between them can be a challenge for consistent 3D printing with high detail and structural integrity. Therefore, it is important to optimize printing parameters (layer exposure time and power) so that the resulting product has excellent resolution and low polymerization shrinkage, which directly affects the quality and dimensions of the resulting product.

This study analysed how different types of 3D printers and printing parameters such as layer cure exposure time, layer height and varying incident light intensity on the layer affect the resolution, dimensional fidelity and shrinkage of 3D printed objects from light-curing resins. Standard resins dedicated to 3D-VAT printing were used in the study.

The results obtained allowed to conclude that the type of 3D printer used, and the printing parameters set for it significantly affect the resolution and polymerization shrinkage of the final product. By exploring the various 3D printer models and the various parameters used in the process, this work provides valuable insight into optimizing 3D VAT printing.

Acknowledgements

This research was funded by National Centre for Research and Development in Poland under the Lider Program, grant number LIDER13/0156/2022.

7.11 Investigation of surfactant effect on the properties of solvent-free synthesized silica aerogels

Aleksandra M. Pisarek*,1, Bartosz Nowak, Emilia Sumińska, Jakub M. Gac

1. Faculty of Chemical and Process Engineering, Warsaw University of Technology, Warsaw, Poland

e-mail: aleksandra.pisarek2.dokt@pw.edu.pl

KEYWORDS: o*rganosilica aerogel, solvent-free synthesis, surfactant, nucleation & growth, spinodal decomposition*

Traditional aerogel synthesis procedure requires the use of alcohol (which serves as solvent) or surfactant. Their role is to increase the miscibility of the reactants and control the gelation process to achieve the desired morphologies. However, the presence of alcohols can complicate the synthesis by introducing additional variables—such as differences in reactivity, or evaporation rates —that may lead to inhomogeneity in the gelation. Moreover, many alcohols are toxic and highly flammable, raising safety concerns and environmental impact issues. In contrast, surfactants offer several advantages over alcohols - they not only facilitate the formation of stable emulsions and control the growth of the silica gel structure but also enhance the homogeneity of the resulting materials. Moreover, using surfactants can also improve the safety profile of the synthesis.

This study investigated the influence of surfactant type and its concentration on the final structural parameters of silica aerogels, including density, porosity, and volume shrinkage during drying. Additionally, the morphology of the obtained structures was characterized by analyzing the secondary particle size distribution and polydispersity. The structural analysis was also aimed at enabling the tracing of the phase separation mechanisms during the condensation process. The research involved two-step acid-base sol-gel synthesis in which vinyltrimethoxysilane (VTMS) was used as a precursor.

The results provided a comprehensive framework that correlates the type and concentration of surfactant used with the properties of the resulting aerogels in a solvent-free synthesis. We observed how surfactants influenced the structure formation, identifying both of the phase separation mechanisms - nucleation and growth and spinodal decomposition - through morphological observations. These results demonstrate the potential of solvent-free synthesis as a more efficient approach to producing aerogels. This work also expands the knowledge about the selection of optimal conditions and can lead to the development of aerogels with tailored properties for specific applications, such as thermal insulation, lightweight materials, and advanced filtration systems.

Acknowledgements

This work was supported by The National Science Centre, Poland - project "Super-flexible double-crosslinked organosilica aerogels dried via cheap and scalable ambient pressure method" PRELUDIUM BIS.

7.12 Research on cytotoxicity of photosensitisers used as components of photoinitiating systems dedicated to photopolymerization processes

Kacper Piskorz[1], Katarzyna Starzak, Patrycja Środa, Filip Petko, Andrzej Świeży, Małgorzata Tyszka-Czochara, Joanna Ortyl*

1. Faculty of Chemical Engineering and Technology, Cracow University of Technology, Cracow, Poland

e-mail: joanna.ortyl@pk.edu.pl

KEYWORDS: *cytotoxicity, photopolymerization, photosensitisers*

In this study, the cytotoxicity of various photosensitisers used in photoinitiating systems required for free-radical and cationic photopolymerization processes was investigated, with a particular focus on their safety and efficacy in biomedical applications of 3D printing materials. The evaluation was carried out using the MTT assay to measure cell viability in both normal human fibroblasts and cancer cell lines, providing important insights into the biocompatibility of these compounds. By comparing the effects on normal and cancerous cells, the study aims to identify photosensitisers that offer minimal cytotoxicity while maintaining effective polymerisation capabilities.

Additionally, the study investigates the integration of these photosensitisers into 3D printed polymeric materials, assessing the structural and functional integrity of the resulting constructs. With this dual approach, the research addresses not only the potential biological impact of photosensitisers, but also their practical application in creating high-resolution, biocompatible 3D printed materials for advanced medical and industrial applications.

The findings from this study are expected to significantly contribute to advancing the field of photopolymerization technologies, paving the way for safer and more efficient methods of producing medical devices and other applications in the biomedical sector. In light of the growing demand for innovative solutions in health care, understanding the interplay between the chemical properties of photosensitizers and their biological effects stands to enhance the quality of 3D printed materials used in critical environments, ultimately improving patient outcomes and expanding the horizons of medical technology.

Acknowledgements

Research financed by the project funded by the Ministry of Science and Higher Education entitled: 'Students' scientific associations create innovations' contract number SKN/SP/602770/2024.

7.13 Multicomponent photoinitiating systems containing polycyclic aromatic hydrocarbons (PAHs) for photopolymerization processes, and their application in 3D printing

Kacper Piskorz[1], Katarzyna Starzak, Patryk Szymaszek, Marcin Lindner, Joanna Ortyl*

1. Faculty of Chemical Engineering and Technology, Cracow University of Technology, Cracow, Poland

e-mail: joanna.ortyl@pk.edu.pl

KEYWORDS: *3D printing, photopolymerization, photosensitisers*

Photopolymerization, driven by light to initiate polymer formation, is crucial across industries like coatings, adhesives, dental composites, inks, and printing plates, as well as in fields such as microelectronics and materials engineering. A key component in this process is the photoinitiator, which must align with the light source's wavelength. With advances in materials science and 3D printing—often using light in the 405–450 nm range—there's a growing demand for photoinitiators that absorb visible light.

Photoinitiators often face limitations in wavelength absorption and low initial quantum yields. To address this, photoinitiating systems use photosensitizers to broaden their absorption range. Research now focuses on developing efficient photoinitiators using organic dyes (photosensitizers) and co-initiators.

The present study investigates photoinitiator systems that absorb visible light up to almost 600 nm. The study includes comprehensive spectroscopic analyses to examine the optical properties of these systems, providing insight into their light absorption capabilities. Additionally, FT-IR analyses were conducted to investigate the kinetics of the photopolymerization process, allowing for a detailed understanding of how these systems perform under various conditions. Furthermore, the research involved the assessment of the photorheological properties of the materials, which are crucial for determining flow behavior during the printing process. Photo DSC (Differential Scanning Calorimetry) analyses were also performed on the tested photopolymer compositions, enabling evaluation of thermal properties and curing behavior. The potential use of these systems in 3D printing was assessed, highlighting their applicability in advanced manufacturing techniques.

Acknowledgements

The research was funded by the National Science Centre (NCN) from the OPUS project, contract number 2021/41/B/ST5/04533.

7.14 Flame synthesis of composite metal oxide nanoparticles with bacteriostatic properties

Kamil Pruchniak*[,1], Katarzyna Jabłczyńska

1. Faculty of Chemical and Process Engineering, Warsaw University of Technology, Warsaw, Poland

e-mail: Kamil.pruchniak01@gmail.com

KEYWORDS: *flame spray pyrolysis, antibacterial, antifungal, antiviral*

In today's world, microorganisms are a growing problem. New viruses and antibiotic-resistant bacteria are appearing more and more frequently. Filtration systems, both conventional and membrane-based, are highly susceptible to degradation caused by microorganisms, which raises the cost of maintaining these systems. Eliminating biofilm formation on the surface of filters and membranes can contribute to enhancing the reliability of these systems.

This study will present the synthesis of titanium oxide (TiO_2) nanoparticles using the flame spray pyrolysis method on the LS-FSR Version 2.20 reactor. Titanium oxide will be additionally doped with other metal oxides exhibiting biostatic properties. Three metals were selected—silver, copper, and zinc—with varying doping levels. The addition of these metals may influence the photocatalytic properties of titanium, potentially leading to enhanced biostatic properties or, to a small extent, biocidal properties. The oxide precursors will be dissolved in acetonitrile and acetohexonic acid in a volume ratio of 1:1 at various concentrations. Other key process parameters include oxygen flow (O_2) at 5 $L \cdot min^{-1}$ and 2 bar pressure, and the flow of the oxygen and methane stoichiometric mixture (CH_4 + O_2) at 3,75 $L \cdot min^{-1}$.

The properties of the synthesized oxides will be examined using the following methods: (i) Laser diffraction, (ii) X-ray diffraction (XRD), (iii) Diffuse Reflectance Spectroscopy (DRS), (iv) Thermogravimetric Analysis (TGA), (v) Zeta Potential Measurement

The next stage will involve quantitative analysis of the biostatic and biocidal properties of the synthesized metal oxides. To determine whether a photocatalytic effect occurs, half of the samples will be exposed to sunlight.

The final stage will involve modifying the surface of the adsorbent, aluminum oxide (Al_2O_3), using the nanoparticles synthesized in the previous step. This oxide is commonly used in water and wastewater treatment processes, primarily for the removal of fluoride, phosphates, and heavy metals.

Subsequently, studies will be conducted to assess how the modification affects the adsorption properties of the base material and whether the designed filtration media contaminate water with metal oxide nanoparticles. Additionally, the filters will be evaluated for their resistance to biofouling.

7.15 Impact of nanofillers on the kinetics of the photopolymerization process and the printing resolution of 3D photopolymerizable polymer resins with the study of the properties of nanocomposites produced using 3D-VAT printing technology

Kamil Pulit[1], Małgorzata Noworyta, Magdalena Jankowska, Paweł Niezgoda, Joanna Ortyl*

1. Faculty of Chemical Engineering and Technology, Cracow University of Technology, Cracow, Poland

e-mail: joanna.ortyl@pk.edu.pl

KEYWORDS: *photopolymerization, 3D printing, nanofillers, nanocomposites, polymer materials*

Photopolymerization is a critical process in the 3D printing of polymer resins, particularly in applications that demand high precision and intricate structures. Recently, the incorporation of nanofillers into photopolymerizable resins has garnered significant attention for their potential to enhance both material properties and printing performance. The addition of nanoparticles can influence polymerization kinetics, allowing for better control over the curing process and improving the mechanical, thermal, and optical properties of the final printed structures.

This study explores how nanofillers impact the speed and efficiency of the photopolymerization process and their effect on achievable printing resolution, which is essential in fields such as microelectronics, biomedical devices, and high-precision manufacturing. To assess the effects of nanofillers, a series of experiments were conducted using real-time FT-IR spectroscopy to monitor the photopolymerization process, in conjunction with 3D-VAT printing technology, known for its high-resolution output and compatibility with photopolymerizable resins. Various nanofillers were integrated into the polymer resin matrix to investigate their effects on the properties of the resulting nanocomposites. Moreover, the impact of nanofillers on printing resolution was evaluated by analysing the fidelity of printed structures in relation to the original digital model. The tensile mechanical properties of the cured nanocomposites were also examined to gain insights into the final performance of the printed objects.

The results indicate that the incorporation of nanofillers significantly influences photopolymerization kinetics. Enhanced printing resolution and improved mechanical properties were observed with specific types of nanofillers. This study provides valuable insights into the role of nanofillers in optimizing both the photopolymerization process and the quality of 3D-printed structures, showcasing the promising potential of nanocomposites in industries requiring high-performance, precisely engineered materials.

Acknowledgements

This research was funded by the National Science Centre under the OPUS LAP 20 Program, titled "Advanced Photopolymerized Nanocomposite Materials Processed by Additive Manufacturing," grant number 2020/39/I/ST5/03556.

7.16 Spectroscopic and kinetic studies of new photoinitiating systems for application in photo-curable 3D printing polymer materials with low polymerisation shrinkage

Kamil Pulit[1], Monika Topa-Skwarczyńska, Patryk Szymaszek, Joanna Ortyl*

1. Faculty of Chemical Engineering and Technology, Cracow University of Technology, Cracow, Poland

e-mail: joanna.ortyl@pk.edu.pl

KEYWORDS: *photopolymerization, photoinitiators, polymer materials, 3D printing*

The increasing demand for high-performance materials in 3D printing has highlighted the need for photoinitiating systems that not only enable efficient curing but also minimize polymerization shrinkage. Polymerization shrinkage can lead to dimensional inaccuracies and reduced mechanical properties in the final printed objects, which are critical factors in applications such as dentistry and precision engineering.

Therefore, the primary goal of this study was to investigate the spectroscopic and kinetic properties of novel photoinitiating systems, utilizing techniques such as UV-Vis spectroscopy and real-time FT-IR to monitor the curing process. This research focuses on the development and characterization of new photoinitiating systems designed specifically for photocurable polymer materials that exhibit low polymerization shrinkage, aiming to improve the overall performance and reliability of 3D-printed components. A series of experiments were conducted to evaluate the efficiency of various photoinitiators in promoting polymerization and to analyse the corresponding shrinkage behaviour during the curing process. The study also included rheological measurements to understand the flow properties of the resin before and after curing. Furthermore, the performance of 3D printing using the newly developed photoinitiating systems was evaluated, highlighting the potential for producing high-resolution parts with reduced defects.

The results indicate that the newly developed photoinitiating systems contribute to a reduction in polymerization shrinkage while maintaining efficient photocuring. Observations suggest that certain formulations may enhance dimensional accuracy in printed parts compared to traditional photoinitiators. Additionally, spectroscopic analyses reveal effective initiation and conversion rates associated with these novel systems. This research provides valuable insights into the design of photoinitiating systems aimed at minimizing shrinkage in 3D printing applications, paving the way for advancements in high-quality photopolymer materials suitable for a range of industrial applications.

Acknowledgements

The spectroscopic and kinetic studies were funded by the National Science Centre (NCN) from the OPUS 21 project, contract number 2021/41/B/ST5/04533.

The 3D printing experiments were funded by the National Centre for Research and Development in Poland under the Lider Program, grant number LIDER13/0156/2022.

7.17 Spectroscopic, kinetic and applicational analysis of novel photoinitiating systems dedicated to obtaining safe and non-toxic dental materials manufactured using 3D printing methods

Katarzyna Starzak[1], Monika Topa-Skwarczyńska, Patryk Szymaszek, Magdalena Jankowska, Andrzej Świeży, Joanna Ortyl[*]

1. Laboratory of Photochemistry and Optical Spectroscopy, Faculty of Chemical Engineering and Technology, Cracow University of Technology, Cracow, Poland

e-mail: joanna.ortyl@pk.edu.pl

KEYWORDS: s*pectroscopy, photopolymerization kinetics, photoinitiators, dental materials*

The emergence and ongoing growth of photopolymerizable dental materials, notably dental composite restoratives, represents a significant, practical advancement in dentistry. This new method had considerable advantages, including a single-paste system that required no mixing, and total operator control over working time, with a quick cure starting on command. Additive manufacturing (AM) solutions are not new to the dentistry sector. These technologies, often known as '3D printing', have received a lot of interest in modern dentistry. Researchers are thrilled and hopeful about the potential that this technology has still to provide in the dentistry profession, taking the dental practice to a higher level.

Camphorquinone and tertiary amine initiators have been widely used in dental composite restoratives, prompting research into the initiation process and photopolymerization parameters. However, the use of such a photoinitiating system is not an ideal solution if only because of the yellow color of the composition resulting in an unwanted colour of the final dental material. In addition, the most common monomers used to produce materials dedicated to stomatology are mertacrylates or acrylates, whose toxicity and oxygen inhibition leave much to be desired in terms of patient safety and dentist's work comfort. The development of novel monomer systems with lower polymerization shrinkage and stress has been a primary focus of dental biomaterials research. One technique is to employ cationically polymerizable matrix resin systems made up of dioxiranes and comonomers that can expand during polymerization.

In view of current trends in the development of new dental materials, this paper presents spectroscopic, kinetic and application studies of new iodonium salts for the role of one-component initiating systems thanks to which it is possible to obtain dental materials with low toxicity using both radical and cationic polymerization.

Acknowledgements

This research was funded by National Centre for Research and Development in Poland under the Lider Program, grant number LIDER13/0156/2022.

7.18 Nature as a source of raw materials for the synthesis of new chromophores for use as photosensitizers in photoinitiating systems dedicated to 3D bioprinting applications

Katarzyna Starzak[1], Alicja Wysocka, Patryk Szymaszek, Łukasz Waluda, Wiktor Kasprzyk, Joanna Ortyl[*]

1. Laboratory of Photochemistry and Optical Spectroscopy, Faculty of Chemical Engineering and Technology, Cracow University of Technology, Cracow, Poland

e-mail: joanna.ortyl@pk.edu.pl

KEYWORDS: s*pectroscopy, photopolymerization kinetics, bio-based compounds, 3D bioprinting*

Photopolymerization is changing the way we produce polymer materials, providing novel solutions in a variety of sectors. This dynamic process converts monomers and oligomers into solid polymers when exposed to light, which is triggered by photoinitiators. This approach uses photoinitiators, which absorb light and produce reactive molecules or free radicals that initiate the polymerization process. Radical photopolymerization is the process that occurs when photoinitiators produce radicals, which then activate polymerization processes. When exposed to light, the photoinitiator photodegrades and moves from the ground to excited states. 3D printing and photopolymerization-based 3D bioprinting are fast expanding technologies with significant applications in medicine, engineering, and industry. Researchers are continuously exploring for novel materials to increase print accuracy and biocompatibility while also allowing for more complex shapes.

The production of fluorescent compounds from natural sources, such as citric acid, has lately sparked widespread attention, owing to their low cost and high photoluminescence (PL) quantum yields. Fluorophores derived from citric acid and other natural substances have been widely used in a variety of applications. They are utilized in a variety of applications, including pH sensors, biomarkers, fluorescent inks, solar cell materials, fluorescent probes for detecting various ions and compounds, and fluorescent tracers.

This study examined the use of four fluorophores derived from citric acid and particular β-amines for free-radical photopolymerization. The effectiveness of the tested starting systems was validated using real-time Fourier-Transform Infrared Spectroscopy (FTIR). Photorheological investigations were employed as an additional tool to investigate the kinetics of photopolymerization processes and the appropriateness of the produced compositions for 3D bioprinting applications.

Acknowledgements

This research was funded by the NCN project OPUS ("Emerging strategy approaches for the design and functionalization of carbon dots as multifunctional, dynamic, green systems photoinitiators and photocatalysts involved in photopolymerisation processes"), Grant No. UMO-2021/41/B/ST5/04533.

7.19 PHA biocomposites: advancing circular economy through waste natural fillers

Abhishek Thakur*,1, Marta Musioł, Marek Kowalczuk

1. Center of Polymer and Carbon Materials, Polish Academy of sciences, Zabrze, Poland

e-mail: Abhishek.Thakur@polsl.pl

KEYWORDS: *polyhydroxyalkanoates (PHAs), biodegradable composites, natural fillers, biodegradation, sustainable materials*

Polyhydroxyalkanoates (PHAs) have emerged as a sustainable and versatile class of biodegradable polymers, offering a great alternative to conventional plastics. Derived from renewable feedstocks via microbial fermentation, PHAs are known for their biodegradability, biocompatibility, and customizability, making them ideal for a wide range of applications. As the globe fights against plastic pollution, PHAs provide a compelling answer that combines material innovation with environmental responsibility.

One of the key advantages of PHAs lies in their adaptability. They can be tailored to exhibit diverse physical and mechanical properties, such as flexibility, thermal stability, and tensile strength, through advances in biotechnology and blending techniques. PHAs find extensive applications in biomedical fields, including surgical sutures, drug delivery systems, and tissue engineering, owing to their controlled biodegradability and biocompatibility. In packaging, PHAs serve as eco-friendly alternatives for single-use plastics, with the added advantage of compostability. Additionally, their potential extends to agriculture, where they are used in mulch films and controlled-release systems, and textiles, as sustainable fibers.

Innovations in composite development have further expanded the scope of PHAs. Reinforcing PHAs with natural fillers, such as cellulose, lignin, or agricultural by-products, enhances their mechanical performance while reducing production costs. These composites open new possibilities in the fields of automotive parts, electronics, and high-performance materials, offering a blend of durability and sustainability.

PHAs also align with circular economy principles, as they degrade naturally in environments when come in contact with likes of soil and marine ecosystems, mitigating long-term pollution. However, challenges remain in reducing production costs, improving scalability, and optimizing properties for specific uses. This research explores the unique properties, current applications, and future potential of PHAs with the addition of waste natural fillers, highlighting their role in transforming material science and addressing global sustainability challenges.

7.20 Enhancing antimicrobial properties in biodegradable films: a comparative study for sustainable food packaging

Sonia Wardejn*,1, Gabriela Dudek

1. Silesian University of Technology, Department of Physical Chemistry and Technology of Polymers, Gliwice, Poland

e-mail: sw300312@student.polsl.pl

KEYWORDS: *biofilms, food packaging, antimicrobial, environmentally friendly*

Increasing environmental concerns regarding synthetic packaging have led to a growing demand for eco-friendly alternatives in the food packaging sector. Biopolymer films derived from polysaccharides have emerged as a promising solution due to their biodegradable nature. The purpose of the study was to improve the antimicrobial properties of biopolymer films based on starch, chitosan, alginate, and their blends (starch/chitosan, starch/alginate); and to evaluate the effects of biopolymer matrix as well as modifiers i.e., plant extracts, plasticizers, cross-linking agents, and nanofillers.

Films were prepared through the Solution Casting Method. Various modifiers were applied to polysaccharide films, including different plasticizers, calcium chloride, oxidized sucrose, and nanofiber cellulose (NC). Chestnut, nettle, grape, and graviola extracts were tested for antimicrobial activity against *S. epidermidis*, *E. coli*, and *C. albicans* by using Inhibition Zone Assay. Films' mechanical and hydrophilic properties were studied as well.

The results showed that chestnut extract demonstrated the strongest antimicrobial activity compared to other investigated plant extracts, leading to its incorporation in all films. Chitosan films displayed better antibacterial activity against Gram-positive than Gram-negative bacteria but were ineffective against *C. albicans*. NC significantly enhanced the mechanical and antibacterial properties of chitosan films. Alginate films, modified with various plasticizers, cross-linked with calcium chloride, demonstrated the highest antimicrobial efficacy against *E. coli*. Starch films crosslinked with oxidized sucrose exhibited slightly lower antimicrobial resistance than alginate films due to the more compact structure. Films with optimal hydrophilicity and mechanical properties, such as ALG6 and ALG5, including plasticizers EPGOS and PGOS, respectively; achieved the highest antimicrobial activity against *S. epidermidis*, *E. coli*, and *C. albicans* by maintaining a balance between swelling, structural integrity, and antimicrobial agent release.

Acknowledgements

This research was funded by the project "Student Scientific Circles Create Innovations" (SKN/SP/569054/2023) from the Ministry of Education and Science and the PBL project (31/010/SDU20/0006-10) from the Silesian University of Technology.

7.21 Emerging photosensitizers for iodonium salt as high-performance component for photoinitiating systems in photopolymerization processes for 3d printing

Weronika Wielgus[1], Andrzej Świeży, Filip Petko, Monika Topa-Skwarczyńska, Mariusz Galek, Joanna Ortyl*

1. Faculty of Chemical Engineering and Technology, Cracow University of Technology, Cracow, Poland

e-mail: joanna.ortyl@pk.edu.pl

KEYWORDS: *photopolymerization, spectroscopy, 3D printing, coinitiator, Real-Time FT-IR*

Today, 3D printing is a growing field. A key component of this technology is the development and use of new photosensitizers for diaryliodonium salts, which are essential for cationic and free-radical photopolymerization processes. These advanced components increase the efficiency and precision of light-induced polymerization, facilitating the creation of high-resolution 3D printed materials under visible light (405 nm).

An effective photosensitizer should have several important properties, including strong light absorption in the appropriate wavelength range, chemical and photochemical stability, good solubility in compatible solvents or polymer matrices, safety and non-toxicity, compatibility with the polymer matrix, and specificity of action. The research conducted investigated the suitability of new photosensitizers for photoinitiating systems, focusing on their application in 3D printing.

To this end, new potential photosensitizers were investigated, namely benzoxazolone derivatives, a group of 16 compounds differing in their substituents (a methoxy group, a cyano group, and an additional phenolic ring). The experiments carried out included spectroscopic analysis, such as measurements of absorbance, photolysis, and evaluation of photopolymerization parameters using the real-time FT-IR technique, which allows for real-time analysis of this process. After the above experiments, the most promising compounds were selected to proceed to the phase of initial 3D printing tests. The conducted tests showed that the efficiency of the given compounds in the photopolymerization process depends on the type of substituent.

Acknowledgements

The research was funded by the National Science Centre (NCN) from the OPUS project, contract number 2021/41/B/ST5/04533.

7.22 Design and printing of potentiometric sensor platform using a 3D printer

Aleksandra Zalewska*[,1], Jakub Marchewka, Beata Paczosa-Bator

1. AGH University of Science and Technology, Kraków, Poland

e-mail: azalewska@agh.edu.pl

KEYWORDS: *3D printing, FDM, potentiometry, analytical chemistry, ion-selective electrodes, solid-contact electrodes, conductive polymers*

In the modern world, chemical analysis is present in numerous fields, including industry, medicine, and environmental protection. Rapid development demands that scientists continue to develop new quantitative and qualitative analysis methods and improve parameters such as sensitivity and accuracy in existing methods. Sciences focused on chemical sensors are developing intensively. Chemical sensors have gained popularity due to several features, including the capability for point-of-use (POU) measurements. Modern designs enable the in situ measurement of analyte concen-trations, eliminating the need for sampling. This is especially important for environ-mental monitoring, including water and soil pollution control. The quick availability of measurement results is crucial for analyses in diagnostics and patient health monitor-ing, facilitated by point-of-care (POC) devices.

In chemical sensors, electrochemical methods are most commonly used due to the relatively easy miniaturization of the measurement system. This presentation will be focused on potentiometric sensors which are used to determine the quantitative amount of an analyte in test samples. Its advantages include high selectivity, high sensitivity, and a low detection limit. Such sensors are based on ion-selective electrodes, where the membrane is responsible for the sensor's selectivity.

The experimental part involved designing and manufacturing prototypes of single- and double- electrode platforms using additive prototyping techniques – 3D printing. The project utilized environments such as AutoCAD Inventor and FlashPrint5. The printing was done on a FlashForge printer with two separate extruders, allowing simultaneous printing with two filaments. The sensors were made from two materials: non-conductive PLA and conductive PLA filament with carbon black from ProtoPasta. Their potentiometric response to ions was then examined using a ion-selective membrane.

The research demonstrated that a 3D printer with two extruders enables rapid sensor production. The analyzed sensors exhibited high linearity in tests and enabled ion measurements in liquid samples. The study highlights the potential for future optimization of printing technology and sensor design for more durable and multi-ion field measurements.

Acknowledgements

This research project was supported by the program titled "Excellence initiative–research university" at the AGH University of Krakow.

7.23 Electrochemical properties of 3D printed potenctiometric sensor platforms

Aleksandra Zalewska*,1, Beata Paczosa-Bator

1. AGH University of Science and Technology, Kraków, Poland

e-mail: azalewska@agh.edu.pl

KEYWORDS: *3D printing, potentiometry, ion-selective electrodes, electrochemical impedance spectroscopy, chronopotentiometry*

In today's world, chemical analysis plays a critical role across sectors like industry, medicine, and environmental protection. Rapid advancements demand continuous improvements in analytical methods, particularly in sensitivity and accuracy. Chemical sensors, popular for enabling on-site measurements, allow real-time analysis without sampling, making them invaluable for environmental monitoring (e.g., water and soil testing) and health diagnostics.

Among these, electrochemical methods, especially potentiometry, are favored for their ease of miniaturization and high selectivity. Potentiometric sensors, which use ion-selective electrodes, are known for their sensitivity and low detection limits, making them effective for precise analyte quantification.

This study presents the development and comprehensive characterization of various prototypes for a 3D sensor platform aimed at precise analyte quantification. Multiple sensor configurations were designed and fabricated using distinct materials, including polylactic acid (PLA), PETG, and commercially available conductive filaments. Both single- and multi-electrode sensor models were printed and subsequently evaluated through voltammetric, chronopotentiometric, and electrochemical impedance spectroscopy (EIS) techniques. These methods enabled a detailed analysis of the electrical properties of each platform configuration. The results provide valuable insights into the electrochemical performance of different materials and electrode architectures, offering a foundation for optimizing 3D-printed sensor platforms for enhanced analyte quantification in various applications.

Acknowledgements

This research project was supported by the program titled "Excellence initiative–research university" at the AGH University of Krakow.

8 Abstracts: Bioengineering, biotechnology, biomedical engineering

8.1 The effect of recycle amount on the properties of organic fertilizers

Gabija Aleksaitytė*,1, Odeta Pocienė, Rasa Šlinkšienė

1. Kaunas University of Technology, Kaunas, Lithuania

e-mail: gabija.aleksaityte@ktu.edu

KEYWORDS: *technology, organic fertilizers, buckwheat, recycle*

Introduction

Food and agriculture waste generated worldwide pose significant challenges, as decomposing waste releases substantial amounts of gas, contributing to climate change. One way to address this issue could be the use of organic waste from the food industry for fertilizer production. Granulated organic fertilizers would not only help reduce waste and emissions but also improve soil fertility. During industrial production of such fertilizers, some granules do not meet the required size and must be returned to the process as recycle. This recycle can affect the properties of the final product, and its use requires additional technological equipment. A significant amount of waste accumulates at the Lithuanian company "Ekofrisa," which produces buckwheat groats. This waste includes biomass, buckwheat husks, and buckwheat husks ash, and contains plants nutrients (C, N, P, K, Ca, Mg, Zn, Fe, Mn, Cu). Therefore, are suitable as a raw material for organic fertilizer production. In this study, molasses solution, beat eggs, and polyvinyl acetate were used as binder.

Methods

The main properties of the produced granular fertilizers, such as granulometric composition, granule strength, bulk density, moisture content, and fertilizers pH, were determined following standardized fertilizer analysis methods and using specialized laboratory equipment.

Results

The results show that the highest number of commercial granules is achieved with 30% and 40% recycle content, however, recycle does not significantly change other properties. The strength of the granules depends on the solid raw materials, and especially the binder. Fertilizers granules are soft or have a static strength between 7.03–20.05 N/granule. The bulk density ranges from 232.2 $kg \cdot m^{-3}$ to 598.4 $kg \cdot m^{-3}$, indicating that the granules of organic bio-fertilizers are very lightweight. The pH of organic fertilizers ranges from 6.9 to 13.6 depending on the composition of raw materials mixture.

Conclusions

The pH values, bulk density, and static strength of the organic fertilizers depend more on the raw materials, especially the binder, than on the recycle. However, it is evident that the higher amount of recycle in the raw material mixture, the higher amount of commercial granules obtained.

Acknowledgements

The research was financed by the Lithuanian Research Council of Lithuania project no. S-SV-24-378.

8.2 The intensification of taxanes production in *Taxus x media* transgenic roots using biomaterials made of TEOS and TMCS aerogels and chitosan

Szymon Bober [1], Kamil Wierzchowski*,[1], Bartosz Nowak[1], Mateusz Kawka, Katarzyna Sykłowska–Baranek, Maciej Pilarek[1]

1. Faculty of Chemical and Process Engineering, Warsaw University of Technology, Warsaw, Poland

e-mail: kamil.wierzchowski@pw.edu.pl

KEYWORDS: *transgenic (hairy) roots, plant secondary metabolites, biomaterials, chitosan, aerogel*

Paclitaxel belongs to the group of taxanes and is considered as one of the most powerful natural anticancer agents. Primarily, it was isolated from the *Taxus brevifolia* yew. Paclitaxel is successfully used against breast and ovarian cancer under the Taxol® trade name. Unluckily, the slow growth of the yews and the yielding of paclitaxel obtained naturally from plants is too low to satisfy medical needs. Another problem is that the semi-synthetic method of producing the paclitaxel is very ineffective economically. Also, natural origin drugs are characterized by less toxicity and higher activity than their chemically synthesized substitutes, so the application of *in vitro* biomass cultures and bioengineering methods can be used for the intensification of taxane production. These methods are well known for increasing the growth and productivity of plant biomass. The simultaneous use of aerogels for immobilization of the transgenic roots biomass and elicitors, such as chitosan, could be a useful tool in overcoming problems with obtaining the plant-origin paclitaxel.

The scope of the study was to examine the influence of the tetraethylorthosilicate (TEOS) and trimethylchlorosilane (TMCS) aerogels and both of them in combination with chitosan on *Taxus x media* transgenic roots biomass proliferation and taxanes, especially paclitaxel, production. The *in vitro* cultures were carried out on TEOS and TMCS aerogels and on both aerogels with the content of 0.05 g, 0.1 g, 0.2 g, 0.4 g, and 0.6g chitosan. As a reference system, transgenic roots were cultured without aerogels and chitosan. The increase in the amount of plant biomass and produced taxanes were determined quantitatively.

The application of TEOS and TMCS aerogels has a slight effect on Taxus x media transgenic root biomass growth and shows a noticeable influence on the production of paclitaxel. Further addition of chitosan to the *in vitro* culture systems with aerogel shows greater impact on plant biomass growth and the secretion of secondary metabolites than the application of only TEOS and TMCS aerogels and in the reference system.

Acknowledgments

This work has been funded by (POB Biotechnology and Biomedical Engineering) Warsaw University of Technology within the Excellence Initiative: Research University (IDUB) program (YOUNG PW II).

8.3 Benzylidene fluorescent probes: a novel approach for albumin detection with applications in health and industry

Małgorzata Kowalewska[1], Patryk Szymaszek, Filip Petko, Mariusz Galek, Joanna Ortyl*

1. Faculty of Chemical Engineering and Technology, Cracow University of Technology, Cracow, Poland

e-mail: joanna.ortyl@pk.edu.pl

KEYWORDS: *bovine serum albumin (BSA), biosensor, fluorescence, benzylidene derivatives*

Albumin is an important protein present in the body, predominantly found in blood plasma. Serum albumin transports endogenous and exogenous substances, such as amino acids, fatty acids, drugs, and toxins. It is used in medical diagnoses as a biomarker for various diseases, as the concentration of albumin in plasma is closely related to health. Detecting and quantifying albumin is therefore crucial, as it significantly impacts multiple industries, including medicine, biochemistry, and food production. Consequently, there is a demand for selective and sensitive detectors of serum albumin. Bovine serum albumin (BSA) is a well-studied globular protein with a structure similar to that of human serum albumin (HSA), making it widely used as a model protein. The fluorescence of BSA is attributed to tryptophan residues, which can be quenched by various fluorophores. The detection of spectral changes is rapid, selective, and sensitive compared to classical protein detection methods. As a result, fluorescence methods are gaining more attention in the field of biosensor development. The studies were conducted on the quenching of tryptophan fluorescence of BSA in relation to the concentration of the fluorophore (benzylidene derivatives) and the emission of fluorophore fluorescence based on BSA concentration. Selected benzylidene derivatives diluted in DMSO-PBS and BSA dissolved in PBS buffer were examined. Fluorescence changes were investigated at different dilutions of both the protein and the fluorophore, at wavelengths corresponding to or close to the maximum fluorescence of both the protein and the fluorophores. The tested benzylidene derivatives exhibited quenching of the tryptophan fluorescence of BSA while enhancing their own fluorescence, suggesting their potential use as fluorescent BSA probes; however, further research is needed for more detailed analysis.

Acknowledgements

Research financed by the project funded by the Ministry of Science and Higher Education entitled: 'Students scientific associations create innovations' contract number SKN/SP/602770/2024.

8.4 Evaluating the mutagenic risk of benzylidene derivatives through Ames test: ensuring safe integration in biosensor development

Małgorzata Kowalewska[1], Patryk Szymaszek, Filip Petko, Mariusz Galek, Joanna Ortyl*

1. Faculty of Chemical Engineering and Technology, Cracow University of Technology, Cracow, Poland

e-mail: joanna.ortyl@pk.edu.pl

KEYWORDS: *Ames test, mutagenic, benzylidene derivatives*

The Ames test is a bacterial reverse-mutation assay designed to identify potential mutagenic chemicals. The test uses modified strains of *Salmonella typhimurium*, which are unable to synthesize histidine and cannot grow on a medium lacking this amino acid. Exposure to a mutagen causes a reversal of mutation, allowing newly mutated bacteria to synthesize histidine and grow on medium lacking it. Substances that can cause mutations have the potential to induce cancer; thus, identifying mutagenic potential is an important step in the safety assessment of chemical compounds. The Ames test is relatively easy and quick to perform and does not require advanced laboratory equipment or high financial outlays, making it a valuable tool for assessing mutagenicity. Benzylidene derivatives show potential as fluorescent sensors for biological applications. Therefore, the studies on the potential mutagenicity of selected benzylidene derivatives were conducted using the Ames test. A series of dilutions of benzylidene derivatives in DMSO was prepared. *S. typhimurium* bacteria were incubated with these dilutions and the controls on an indicator medium containing a pH-sensitive indicator in 384-well plates. If a tested substance exhibited mutagenic properties, the mutation of the bacteria would be reversed, allowing them to grow in the medium, changing its pH and the color of the indicator. After 48 to 72 hours, colony counts were recorded for each well. It is important that potential biosensors are not mutagenic due to their use in detecting biomolecules or visualizing cellular structures. Hence, studies on the mutagenicity of such compounds are essential to ensure their safety for use. The results of the Ames test indicate that the tested benzylidene derivatives are not potentially mutagenic, suggesting that they can initially be considered safe for use as biosensors; however, further and more detailed research on their cytotoxicity is needed.

Acknowledgements

The project is financed with funds from the state budget granted by the Minister of Science within the framework of the program "Student Scientific Circles Create Innovations" contract number SKN/SP/602770/2024. In addition, the spectroscopic research was funded by the National Science Centre (NCN) from the OPUS project contract number 2021/41/B/ST5/04533.

8.5 Fertilizers with organic additives

Karina Kuzborskaja*,1, Kristina Jančaitienė

1. Department of Physical and Inorganic Chemistry, Kaunas University of Technology, Kaunas, Lithuania

e-mail: karina.kuzborskaja@ktu.edu

KEYWORDS: *fertilizers, banana peels, bio-additives*

The goal of this work is to address soil degradation by developing fertilizers enriched with organic bio-additives. Intensive agricultural practices contribute to the decline in soil organic matter, which is essential for maintaining soil health. Soil organic matter (SOM) influences key soil properties, including moisture retention, pH balance, nutrient availability, structure, and resistance to erosion. Additionally, SOM serves as an indicator of soil quality and is critical for the ecological stability of the biosphere. As SOM levels decline, soil properties deteriorate: aeration, water absorption, and structural stability decrease, while soil density and surface runoff increase, leading to erosion. Over time, when farming in this way for a longer period of time, the soil seems to die, and in order to maintain crop productivity, the use of mineral fertilizers and pesticides has to be increased.

The chemical composition of banana peels was analyzed by employing methods of chemical analysis: the concentration of phosphorus (P_2O_5) was determined by using the photocolorimetrical method (T70/T80 UV–VIS); the concentration of potassium (K_2O) was discovered by employing the marginal solutions method using the flame photometer "PFP–7."

The increasing emphasis on sustainable agriculture has driven interest in fertilizers with bio-additives sourced from natural materials such as animal manure, plant residues, insect biomass, biogas by-products, and other agricultural waste. For example, banana peels contain beneficial elements, including potassium (K_2O at 9.12%) and phosphorus (P_2O_5 at 0.02%), which are valuable for soil nutrient enrichment. Bio-additives in fertilizers enhance soil microbial activity, promoting crop growth and plant health while reducing soil acidification, ultimately leading to higher yields. Both solid and liquid bio-fertilizers can be effectively used in agricultural applications to support soil health and productivity.

8.6 Itaconate-based polymers with diols as promising bio-inks for 3D printing in tissue engineering

Magdalena Miętus[1], Maria Marecka, Agnieszka Gadomska-Gajadhur*

1. Faculty of Chemistry, Warsaw University of Technology, Warsaw, Poland

e-mail: Agnieszka.gajadhur@pw.edu.pl

KEYWORDS: *itaconic polyesters, UV-crosslinking, bio-printing, tissue engineering, post-polymerization reactions*

Itaconic acid is a biocompatible dicarboxylic acid industrially produced in the fermentation processes of sugars. The synthesis is performed by the fungus *Aspergillus itaconicus*, which is in line with the principles of Green Chemistry. A C=C double bond in the side chain of itaconic compounds is present. It enables post-polymerization reactions (PPM) to obtain products with different properties. The presented work draws attention to the possibility of UV-crosslinking of itaconic compounds for 3D printing applications using the Direct Ink Writing (DIW) method.

Currently, acrylic compounds and their derivatives are the most commonly used materials for conducting 3D printing processes. Those are toxic, which can have a negative impact on the environment and the biocompatibility of the potential final product. Furthermore, acrylic compounds can be obtained through petrochemical processes, leading to greenhouse gas emissions. However, because of its structure, those can crosslink very quickly. It is a significant advantage, which explains the use of acrylic compounds in 3D printing of photocurable materials. Nonetheless, itaconic compounds structurally resemble acrylic compounds, which makes them suitable replacements for acrylic ones.

This work reports the synthesis of potential itaconic ink for UV 3D printing. The polyester structure was characterized by FTIR and NMR methods. The product was checked for its rheological properties. Then, the resin was crosslinked with the addition of seven photoinitiators of the first and second types. The obtained products were characterized mainly by their gel content, water uptake, mechanical (primarily tensile strength, flexural strength, Young modulus, hardness), and thermal (DSC, TG, DTG) properties. The most suitable photoinitiator was selected to perform a rapid, radical polymerization reaction of the synthesized itaconic polymer.

Performed studies allow for considering possible applications of the obtained itaconic polyester as ink in biomaterials and tissue engineering.

Acknowledgments

This research was financed from the budgetary funds of the YOUNG PW II program - "Photo-crosslinked polyesters of itaconic acid and selected dihydroxyl diols enriched with magnetic microparticles for medical applications (MagnetItac)".

8.7 Application of the optical method to quantify the mixing process in a single-use wave-assisted bioreactor

Mateusz Sączek[1], Mateusz Bartczak, Kamil Wierzchowski, Maciej Pilarek*

1. Faculty of Chemical and Process Engineering, Warsaw University of Technology, Warsaw, Poland

e-mail: maciej.pilarek@pw.edu.pl

KEYWORDS: *mixing time, single-use bioreactor, wave mixing, Design of Experiments*

Single-use bioreactors are devices used to conduct mammalian and plant cell cultures in single-use tanks made of plastic. These kinds of bioreactors are currently trending as an alternative to conventional tank bioreactors due to their numerous advantages over their counterparts. The flow of liquid culture medium inside the culture vessel of the wave-type agitated bioreactor is induced by the oscillatory movement of the platform on which the disposable bag is positioned. This mixing mechanism is characterized by low shear stresses, which are less harmful to sensitive cells that could be otherwise damaged in bioreactors equipped with mechanical stirrers. The subject of this experimental study was the application of an optical method to quantify the mixing process in a single-use wave-assisted bioreactor.

The ReadyToProcess WAVE™25 bioreactor equipped with a Cellbag™ polymer culture vessel with a total volume of 10 dm^3 was used in this study. A series of experiments were conducted on the WAVE 25 bioreactor to determine the effect of three selected operational parameters on the mixing time. The chosen parameters were (i) the angle and (ii) the frequency of oscillations of the bioreactor platform, and (iii) the volume of the liquid phase in the culture vessel. The mixing time was determined using an optical method assisted by computer image analysis, and the results obtained were analyzed and compared with the results obtained from the literature using the sensor method. The experiments were planned according to the methodology of statistical experiment planning, with the application of the Box-Behnken plan.

The results of the experiments were analyzed using Statistica software. The frequency of platform oscillations had the biggest impact on the obtained values of mixing time, the angle of platform oscillations had a smaller effect, and the volume of the liquid phase in the culture vessel had the smallest impact among the three tested parameters. It was also found that the optical method exhibited a clear advantage over the sensor method in terms of precision.

Acknowledgments

This work has been funded by (POB Biotechnology and Biomedical Engineering) Warsaw University of Technology within the Excellence Initiative: Research University (IDUB) program (YOUNG PW I).

8.8 The influence of cell disruption technique on the efficiency of GFP isolation from BY-2 cells

Karolina Tomczuk[1], Kamil Wierzchowski*[,1], Mateusz Kawka, Maciej Pilarek[1], Katarzyna Sykłowska–Baranek

1. Faculty of Chemical and Process Engineering, Warsaw University of Technology, Warsaw, Poland

e-mail: kamil.wierzchowski@pw.edu.pl

KEYWORDS: *protein isolation, GFP, cell disruption, BY-2 cells, plant biomass*

Proteins are among the most important macromolecules found in cells. They play key roles in numerous biological processes and are significant in pharmacy, diagnostics, and biotechnology. The study of intracellular proteins requires their isolation, which involves releasing cellular components through cells by using cell disruption methods. The cell disruption process consists of breaking down the cell wall, causing a loss or weakening of cell integrity, and releasing cellular contents into solution. The cell disruption approach has a notable influence on the protein isolation yield and the activity of the desired macromolecule.

The aim of this study is to select a suitable method for the isolation of GFP (Green Fluorescent Protein) from *Nicotiana tabacum* BY-2 cells. The scope of the study includes a literature selection of available protein isolation techniques dedicated to plant biomass, batch cultivation of *Nicotiana tabacum* BY-2 cell suspension, disruption of the BY-2 cells, and quantitative analysis of the GFP and overall protein concentrations.

The following cell disruption methods have been selected based on the literature studies: (i) three cycles of freezing at -20 °C and thawing, (ii) sonication using ultrasonic homogenizer probes, (iii) grinding in the ball mill, and (iv) disruption using a Dounce homogenizer. The isolation of GPF was carried out under different process conditions to identify the optimal parameters of each technique. The overall protein concentration was determined using the spectrophotometric Bradford assay. The concentration of GFP was estimated based on the measurement of GFP fluorescence at 510 nm detection wavelength (488 nm excitation wavelength) using an INFINITE multiwell plate reader (TECAN).

All of the proposed cell disruption technique allows to obtain the proteins with satisfactory efficiency. However, depending on the cell disruption method used, the concentration of GFP was different. Perhaps the cell disruption technique used influences the activity of GFP.

Acknowledgments

This work has been funded by (POB Biotechnology and Biomedical Engineering) Warsaw University of Technology within the Excellence Initiative: Research University (IDUB) program (YOUNG PW I).

8.9 Experimental modeling of mechanical deformation of human arteries

Krzysztof Truchel[1,*], Krzysztof Wojtas, Julia Bilska, Beata Butruk-Raszeja, Iwona Łopianiak, Łukasz Makowski, Krystian Jędrzejczak, Wojciech Orciuch, Paweł Gierycz, Radosław Rzepliński, Mikołaj Sługocki, Bogdan Ciszek

1. Faculty of Chemical and Process Engineering, Warsaw University of Technology, Warsaw, Poland

e-mail: Krzysztof.Truchel.dokt@pw.edu.pl

KEYWORDS: *mechanical properties; tensile test; rupture; intracranial arteries; neurovascular diseases*

Endovascular procedures in the cerebral and coronary circulation are becoming increasingly common. Although these procedures are effective, they are not without risk of complications. These can include stent migration, restenosis, and arterial rupture or dissection. The intervention requires the insertion of appropriate catheters, guidewires, balloons, etc., into the vascular system. This inevitably results in local mechanical stress. While critical rupture pressure in major human cerebral arteries has been investigated, data on tensile strength are lacking in the available literature.

Many tissue engineering studies also focus on identifying the most effective materials or techniques for producing phantoms or arterial scaffolds. However, a major limitation is the lack of comprehensive data sets, making it difficult to assess these structures' mechanical properties accurately. Currently, the strength parameters of these structures are often only compared to those of animal arteries or not at all. The availability of more extensive data would facilitate the selection of suitable elastic materials for 3D printing through laser measurements or enable the extension of computational fluid dynamics simulations to include simulations with dynamic wall deformation.

This study presents the strength parameters of the major intracranial and coronary arteries obtained by performing single-cycle tensile tests on human biological specimens. The measured parameters included Young's modulus, ultimate strength, rupture strength, and rupture strain allowed the determination of mean values for each artery type and were the basis for a multiple comparison analysis between groups. The study also showed that the measured strength parameters are directly dependent on the thickness of the arterial wall. In addition, a safe value of 10% is suggested for the maximum relative strain during arterial procedures.

Based on the results of the strength parameters, a suitable 3D printing method (SLA) and resin (Formlabs BioMed Elastic 50A V1) were selected. Fracture tests were conducted on the printed artery phantoms due to increasing fluid pressure. Based on this, critical rupture spots such as stenosis, presence of aneurysms, branching, or attachment sites were located.

Acknowledgments

Research was funded by the Warsaw University of Technology within the Excellence Initiative: Research University (IDUB) programme.

8.10 Increasing the packing of bimodal zirconium oxide nanoparticles in a photocurable resin for precise 3D printing of bio-inspired ceramic bone scaffolds

Weronika Wałczyk[*,1], Magdalena Jankowska, Klaudia Trembecka-Wójciga, Joanna Ortyl

1. Department of Biotechnology and Physical Chemistry, Faculty of Chemical Engineering and Technology, Cracow University of Technology, Cracow, Poland

e-mail: weronikawalczyk24@gmail.com

KEYWORDS: *bimodal nanoparticles, zirconium oxide, bio-inspired ceramic bone scaffolds, 3D printing*

Photochemistry and polymerization processed initiated by light are essential in materials science, with photopolymerization being widely utilized in industries such as biomedical engineering, automotive manufacturing, and dentistry. These processes are evolving quickly, particularly with advancements in light-activated 3D printing technologies.

The additive manufacturing of polymers incorporating nanopowders using Digital Light Processing (DLP) is a rapidly growing research area. This method is known for its high resolution, speed, and accuracy, making it suitable for numerous applications, especially in biomedical engineering. It allows to effectively mix liquid resin with various nanofillers to create functional nanocomposites that improve the mechanical and thermal properties of the material.

Using 3D-printed polymer scaffolds with zirconium dioxide (ZrO_2) nanopowder offers a promising method for bone defect repair. Nano-zirconia enhances polymer hydrophilicity and biocompatibility, and its elastic modulus, high strength, and osseointegration make it suitable for bone integration. These properties improve the mechanical performance of composite materials, enabling them to meet bone scaffold requirements.

The proposed bio-inspired ceramic bone scaffolds show great promise for tissue engineering and regenerative medicine. Combining 3D printing with zirconia nanopowders enables the production of patient-specific scaffolds with enhanced biological functionality and superior mechanical properties. The 3D scaffolds were produced using DLP technology (Lumen X, Cellink), and various research techniques, including scanning electron microscopy (SEM) and mechanical testing, were employed to evaluate the microstructure, phase composition, and mechanical properties of the printed scaffolds.

Acknowledgements

The present research work was funded by the LIDER NCBiR project contract number LIDER13/0081/2022 "Innovative porous ceramic materials printed in the DLP technique with the use of high-performance photochemical initiators dedicated to integration with bone tissue".

8.11 The influence of various dispersants in photocurable resin formulations with bimodal nanoparticles on 3D printing performance and precision

Weronika Wałczyk*[,1], Magdalena Jankowska, Klaudia Trembecka-Wójciga, Joanna Ortyl

1. Department of Biotechnology and Physical Chemistry, Faculty of Chemical Engineering and Technology, Cracow University of Technology, Cracow, Poland

e-mail: weronikawalczyk24@gmail.com

KEYWORDS: *dispersants, resins, bimodal nanoparticles, zirconium oxide, 3D printing*

Photochemically initiated polymerization processes are fundamental in materials science and have a wide range of industrial applications, including in biomedical engineering, automotive manufacturing, and dentistry. These processes are advancing rapidly, especially with developments in light-activated 3D printing, which has expanded the possibilities for creating complex structures with precise mechanical and thermal properties. Digital Light Processing (DLP) is particularly effective for additive manufacturing with polymers and nanopowders, offering high resolution and accuracy. By incorporating zirconium dioxide (ZrO_2) nanopowder into 3D-printed polymer scaffolds, it is possible to enhance hydrophilicity, biocompatibility, and mechanical properties—qualities essential for applications in bone defect repair.

This study explores the impact of different dispersants in photocurable resin formulations containing bimodal nanoparticles on the performance and precision of 3D printing. Dispersants play a crucial role in stabilizing nanoparticles within resin matrices, directly affecting print resolution, material homogeneity, and mechanical properties. Several dispersants were examined to determine their effectiveness in evenly distributing bimodal nanoparticles, which consist of two distinct particle size ranges, within the resin. The study evaluated each formulation's impact on print accuracy, surface finish, and structural integrity. Findings indicate that optimal dispersant choice not only improves nanoparticle distribution but also enhances the overall performance and fidelity of printed structures. This work provides valuable insights for developing advanced resin formulations for high-precision 3D printing applications, particularly in fields requiring fine detail and reliable material performance.

Acknowledgements

The present research work was funded by the LIDER NCBiR project contract number LIDER13/0081/2022 "Innovative porous ceramic materials printed in the DLP technique with the use of high-performance photochemical initiators dedicated to integration with bone tissue".

8.12 Study of *Nicotiana tabacum* BY-2 cell suspension rheology cultured in a rocking bioreactor

Dariusz Węsek[1], Kamil Wierzchowski*[,1], Radosław Krzosa[1], Łukasz Makowski[1], Maciej Pilarek[1]

1. Faculty of Chemical and Process Engineering, Warsaw University of Technology, Warsaw, Poland

e-mail: kamil.wierzchowski@pw.edu.pl

KEYWORDS: *rheology, single-use bioreactor, wave-induced mixing, BY-2 cells, plant biomass*

Disposable (i.e., single-use) rocking bioreactors are suitable for in vitro bioprocessing of fragile animal or plant cells, aggregates of such cells, tissues, and organs. The bubble-free surface aeration of the culture medium, which occurs in rocking bioreactors, provides sufficient oxygen transfer for cultured biomass. Furthermore, oscillatory movements of the disposable culture vessel ensure gentle conditions for cultures of shear-sensitive cells, tissues, and organs. Plant biomass is used as a renewable feedstock and a source of bioactive and medically valuable compounds by the pharmaceutical industry. The cultures of plant cells in the suspended form are characterized by high growth rates, and due to that, the physicochemical properties of the culture medium change significantly during cultivation. In order to conduct the cultivation process at optimal conditions, it is essential to know the changes in rheology during cultures. The changes in viscosity have a significant impact on oxygen transfer rate (oxygen accessibility), mixing efficiency (nutrient accessibility), and shear stresses (cell shearing). All of these factors can be enhanced or limited by appropriate choice of bioreactor working parameters.

The aim of this study was to determine the changes in the rheology of *Nicotiana tabacum* BY-2 cell suspension during the cultivation process in a rocking bioreactor. The BY-2 cell suspension was cultured using the Ready-ToProcess WAVE 25 bioreactor system (Cytiva) for 10 days at 25 °C. The oxygen level was measured using the DO sensors built into the bottom of the culture vessel. A modular rotational rheometer model MCR 302e (Anton Paar) was used to determine the rheology of the samples harvested daily from the bioreactor system.

The results show a strong decrease in oxygen concentration during the cultivation process. The reduction of oxygen accessibility was correlated with a high increment of the culture medium viscosity and cell density during culturing. The results of the study allow us to develop and optimize the working parameters program, which provides the most suitable conditions for cultures of BY-2 cells in suspended form.

Acknowledgments

This work has been funded by (POB Biotechnology and Biomedical Engineering) Warsaw University of Technology within the Excellence Initiative: Research University (IDUB) program (YOUNG PW I).

8.13 Emerging photosensitizers for iodonium salt as high-performance component for photoinitiating systems in photopolymerization processes for 3D printing

Weronika Wielgus[1], Andrzej Świeży, Filip Petko, Monika Topa-Skwarczyńska, Mariusz Galek, Joanna Ortyl*

1. Faculty of Chemical Engineering and Technology, Cracow University of Technology, Cracow, Poland

e-mail: joanna.ortyl@pk.edu.pl

KEYWORDS: *photopolymerization, spectroscopy, 3D printing, coinitiator, Real-Time FT-IR*

Today, 3D printing is a growing field. A key component of this technology is the development and use of new photosensitizers for diaryliodonium salts, which are essential for cationic and free-radical photopolymerization processes. These advanced components increase the efficiency and precision of light-induced polymerization, facilitating the creation of high-resolution 3D printed materials under visible light (405 nm).

An effective photosensitizer should have several important properties, including strong light absorption in the appropriate wavelength range, chemical and photochemical stability, good solubility in compatible solvents or polymer matrices, safety and nontoxicity, compatibility with the polymer matrix, and specificity of action. The research conducted investigated the suitability of new photosensitizers for photoinitiating systems, focusing on their application in 3D printing.

To this end, new potential photosensitizers were investigated, namely benzoxazolone derivatives, a group of 16 compounds differing in their substituents (a methoxy group, a cyano group, and an additional phenolic ring). The experiments carried out included spectroscopic analysis, such as measurements of absorbance, photolysis, and evaluation of photopolymerization parameters using the real-time FT-IR technique, which allows for real-time analysis of this process. After the above experiments, the most promising compounds were selected to proceed to the phase of initial 3D printing tests. The conducted tests showed that the efficiency of the given compounds in the photopolymerization process depends on the type of substituent.

Acknowledgements

The research was funded by the National Science Centre (NCN) from the OPUS project, contract number 2021/41/B/ST5/04533.

8.14 The new iridium(III) complexes as an innovative theranostic photosensitizers for photodynamic therapy (PDT) and sensors for precise imaging at a single cell level

Weronika Wielgus[1], Patryk Szymaszek, Anna Chachaj-Brekiesz, Małgorzata Tyszka-Czochara, Joanna Ortyl*

1. Faculty of Chemical Engineering and Technology, Cracow University of Technology, Cracow, Poland

e-mail: joanna.ortyl@pk.edu.pl

KEYWORDS: *iridium (III) complexes, cytotoxicity, cancer cell, photodynamic therapy*

These days, there is a dramatic increase in cancer incidence and mortality. Consequently, there is a constant need to improve cancer diagnostics and therapeutic approaches. Iridium (III) complexes are proving to be promising compounds in the context of developing advanced photosensitizers for photodynamic therapy (PDT) and as sensors for precise imaging at the single cell level. Thanks to their unique photophysical and photochemical properties, these complexes can significantly contribute to advances in the field of theranostics, an interdisciplinary field combining therapy and diagnostics.

Photodynamic therapy (PDT) is one of the treatments used primarily to treat cancer and certain skin diseases. It involves three basic components: a photosensitizer, light of a certain wavelength and oxygen. Iridium(III) complexes can be activated with light of the appropriate wavelength leading to the production of reactive oxygen species (ROS), which successively cause damage to cell structures and cancer cell death. As iridium (III) complexes represent a novel and versatile class of compounds that can find applications in both photodynamic therapy and advanced cellular imaging techniques, a study of new iridium (III) complexes was conducted.

The main objective of this study was to determine their cytotoxicity. The study was conducted in an in vitro model using cancer cell lines. A colorimetric MTT assay of compound cytotoxicity was used to determine the cytotoxicity of the compounds by assessing the enzymatic activity of mitochondrial dehydrogenases. Basic spectrophotometric studies were also performed to characterize iridium (III) complexes.

Acknowledgements

Research financed by the project funded by the Ministry of Science and Higher Education entitled: 'Students scientific associations create innovations' contract number SKN/SP/602770/2024.

8.15 Impact of Carbon Dioxide Nanobubbles on the Growth and Metabolic Activity of Murine Fibroblasts

Aleksandra Zambrzycka[1], Aleksandra Wojciechowska, Karol Ulatowski*

1. Department of Biotechnology and Bioprocess Engineering, Faculty of Chemical and Process Engineering, Warsaw University of Technology, Warsaw, Poland

e-mail: Karol.Ulatowski@pw.edu.pl

KEYWORDS: *nanobubbles, carbon dioxide, L929, diabetic foot*

Nanobubbles have gained attention for enhancing the metabolic activity and promoting cell growth of microorganisms, plants and even mammalian cells. Additionally, they have shown potential in therapeutic applications, particularly in the treatment of diabetic foot ulcers, where their unique properties promote wound healing, significantly improving the patients' life and comfort.

This work is the preliminary investigation for the study focusing on the impact of carbon dioxide nanobubbles on blood vascular cells. Its purpose was to determine whether exposure to carbon dioxide nanobubbles has a positive effect on L929 cells (murine fibroblasts) and successfully develop the analytical methods that could be implemented in further research. The cells were cultured for a period of 96 hours in the suitable medium. Every 24 hours the cells were incubated for a period of 30 minutes with a fresh medium dispersed with CO_2 nanobubbles, then a series of tests was conducted to monitor the cells' metabolic activity and viability. Metabolic activity was assessed using Presto Blue and LDH assays while the viability was evaluated microscopically using the LIFE/DEAD assay. A hemocytometer was used to measure the cell density. Simultaneously, a reference culture was carried out, where the cells were incubated with a traditionally CO_2-infused medium instead of a nanobubble dispersion.

Comparing the obtained results, we can conclude that the exposure to CO_2 nanobubbles positively affects L929 cultures, promoting cell growth. Furthermore, the methods used in this study have proven to be successful and can be implemented in further stages of the research.

Acknowledgements

This work was supported by the Scientific Council of Chemical Engineering Discipline at Warsaw University of Technology (grant number I.Chem-4.3.3.) and National Science Centre, Poland (grant number 2020/39/I/ST5/01131).

9 Abstracts: Process equipment & environmental protection

9.1 Carbon dioxide bubbles removal in direct formic acid fuel cell

Maciej Gruberski*,1, Monika Jałowiecka, Łukasz Makowski

1. Faculty of Chemical and Process Engineering, Warsaw University of Technology, Poland

e-mail: maciej.gruberski.stud@pw.edu.pl

KEYWORDS: *direct-formic acid fuel cell, two-phase flow, degassing layer, SLA*

Direct formic acid fuel cells (DFAFCs) are a type of Proton Exchange Membrane (PEM) fuel cells supplied with liquid formic acid and air. They are known to be a promising candidate as low-emission power supplies that can substitute combustion engines. However ongoing electrochemical reaction, on their anodic side, produces CO_2. This phenomenon results in forming two-phase flow that negatively affects the performance of fuel cell decreasing its effeciency.

Therefore the way of in situ CO_2 bubbles removal via hydrophobic porous structure enhanced by geometrical design is proposed in this work. The usage of material containing macropores (70-80 µm) instead of a sub-micron for bubble-trap layer is known to be a novel approach that might create the possibility of a wide variety of new materials to be used for this purpose. Using the advantage of rapid prototyping with SLA 3D printing multiple channels geometrical designs are tested and compared. Prototypes are evaluated in the field of effective bubble removal as well as leakage prevention using optical observation. This analysis results in geometrical guidelines for designing such structures. Finally, the working transparent DFAFC incorporating gas removal system is constructed to justify the appropriateness of the proposed material as a bubble-trap layer in working fuel cell conditions. For this purpose, optical observation and electrochemical performance analysis is used.

This work underlines the importance of gas removal in liquid supplied fuel cells and rapid prototyping as swift and tremendously effective workflow for R&D tasks.

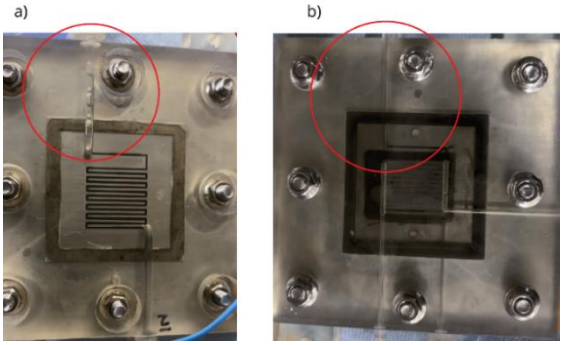

Figure 9.1.1 a) reference fuel cell for I = 0.2 [A] - visible gas in outlet channel b) fuel cell with gas-removing structure for I = 0.2 [A] no visible gas in outlet channel.

9.2 Intensification of process in PEM electrolyzes

Maria Jarząbek-Karnas[1], Zuzanna Bojarska, Łukasz Makowski

2. Faculty of Chemical and Process Engineering, Warsaw University of Technology, Poland

e-mail: maria.jarzabek.dokt@pw.edu.pl

KEYWORDS: *hydrogen, green energy, electrolysis*

The European Union (EU) focus on reducing greenhouse gas emissions and replacing conventional energy sources with alternative ones in response to climate change. As part of its plan to achieve climate neutrality by 2050, the EU invests in renewable energy sources (RES), improves energy efficiency, and develops other clean, low-emission technologies. Among these RES technologies, hydrogen has been identified as a promising fuel of the future.

Current PEM electrolyzers are expensive due to components such as titanium bipolar plates and electrodes made from rare metals like platinum and iridium. My research focuses on reducing the production costs of electrolyzers by utilizing cheaper catalytic materials such molybdenum disulfide (MoS_2), rhenium disulfide (ReS_2), and carbon nanomaterials.

To assess the suitability of the studied catalysts for use in electrolyzers, samples of transition metal dichalcogenides, such as MoS_2 and ReS_2, were prepared and deposited on carbon nanomaterials. Various mass ratios of materials were used in the sample preparation, including 5:1, 10:1, 30:1, and 50:1. These samples underwent electrochemical tests to investigate their efficiency and stability in the water electrolysis thoroughly. Linear sweep voltammetry (LSV), cyclic voltammetry (CV), and electrochemical impedance spectroscopy (EIS) were conducted. The results of this study will make it possible to determine which proportions of MoS_2 and ReS_2 on the carbon nanomaterial show the best catalytic activity, the lowest energy loss and the highest stability.

As part of the research, a detailed analysis of the internal structure of the catalyst was performed using various techniques, including X-ray diffraction (XRD), Fourier-transform infrared spectroscopy (FTIR), X-ray fluorescence spectroscopy (XRF), thermogravimetric analysis (TGA), and scanning electron microscopy (SEM). Each of these methods provided valuable information about the material's crystalline, chemical, and morphological structure. These studies made it possible to investigate how different aspects of the internal structure of the catalyst affect its electrochemical efficiency.

This research will contribute to developing more efficient and cost-effective electrolyzers, supporting the transition to a sustainable hydrogen economy.

9.3 Generation of budesonide aerosol in three commercial vibrating mesh nebulizers

Izabela Kazimierczak[1], Aleksandra Sawczuk, Tomasz Sosnowski*

1. Faculty of Chemical and Process Engineering, Warsaw University of Technology, Poland

e-mail: tomasz.sosnowski@pw.edu.pl

KEYWORDS: *nebulization, vibrating mesh nebulizer, aerosol, generic drugs*

Vibrating mesh nebulizers (VMNs) are relatively new medical devices dedicated to atomizing liquid medicines to aerosols for inhalations to treat lower respiratory system disorders. Inhaled corticosteroid (ICS) aerosols, including budesonide (BUD), are commonly applied in pulmonary infections. Several generic BUD products for nebulization are available on the market however their atomization efficiency in different VMNs has not been systematically studied. It was shown that aerosol generation with generic BUD products in a single VMN was different due to variations in the physicochemical properties of BUD suspensions.

This study aimed to evaluate the mass output of seven commercial BUD nebulization products during their atomization in three VMNs. The results are essential for the future optimization of drug delivery from VMNs using the engineering-based approach.

Three VMNs: Sanity Silent Mesh (SSM), Sanity Fast Mesh (SFM), and Ca-Mi One Pro (OP), were used to atomize seven commercial BUD (products 0.25 $mg \cdot ml^{-1}$). The airflow through the nebulizer (the mouthpiece) was generated by the breathing flow simulator ASL 5000 XL (Ingmar Medical, USA) applying the breathing pattern of a healthy adult. The mass of emitted aerosol of each drug was determined gravimetrically by weighing the VMN at two-minute intervals. Each drug in each nebulizer was studied in triplicate.

The aerosol emission of each drug after atomization in each inhaler was reproducible. SSM nebulizer emissions ranged from 0.19-0.23 $g \cdot min^{-1}$, SFM: 0.18-0.24 $g \cdot min^{-1}$, and OP: 0.25-0.29 $g \cdot min^{-1}$. The differences between the drug emission rates were probably caused by slight differences in their physicochemical properties. Despite these variations, all tested devices are capable of atomizing the whole volume of each BUD product in less than 10 minutes, although not all emitted aerosols will be delivered to a patient due to the periodic nature of flow during breathing.

Acknowledgements

Nebulizers and drug products were donated by Albert Polska. Work co-supported by project Infrastart CePT.

9.4 Parametric comparison of different manufacturing methods for production of bipolar plates in fuel cells

Jakub Lewandowski*[,1], Monika Jałowiecka[1], Zuzanna Bojarska[1], Paweł Gierycz[1], Łukasz Makowski[1]

1. Faculty of Chemical and Process Engineering, Warsaw University of Technology, Poland

e-mail: jakub.lewandowski9.dokt@pw.edu.pl

KEYWORDS: *fuel cell, bipolar plate, parametric comparison*

Scientists are preparing for an energy transformation that would provide cheap, safe and clean electricity to the world. Direct formic acid fuel cells abbreviated as DFAFC are an innovative solution to this problem. Together with technologies that allow for production of green hydrogen they are an indispensable part of a diversified energy network.

This study is focused on the element of DFAFC called a bipolar plate. This is a key element whose task is to deliver fuel to the area of the reaction, remove products of the reaction and collect an electric charge. Currently, bipolar plates are manufactured out of graphite or stainless steel. Literature suggests that such bipolar plates constitute about 55% of the mass and 20-30% of the price of the fuel cell stack. Usage of novel materials and manufacturing methods could provide a lighter and cheaper fuel cell stack with similar performance parameters.

In the first stage of the research bipolar plates were manufactured using CNC (computerized numerical control) machining. The first set of bipolar plates was made of stainless steel, and the second one form graphite. In the next stage a set of bipolar plates was manufactured from conductive filament using FDM (fused deposition modeling) 3D printing. The last set of bipolar plates was produced using SLA (stereolithography) 3D printing. Conductive 3d printing resin suspension was prepared by mixing Clear v4 resin from Formlabs with graphite powder GraphNSEK1 Bio from 3D Resyns. All of the sets of bipolar plates share the same geometry. Range of experiments have been conducted to compere the performance of each set of bipolar plates. Before each test the stability of open circuit voltage was checked to ensure correct assembly of the fuel cell and uninterrupted flow of fuel. The resistance of a fuel cell was determined by conducting electrochemical impedance spectroscopy. Activity and power density as well as stability over time of the fuel cell have been determined. The outcome of the research is parametric comparison of four sets of bipolar plates focusing on the performance of the fuel cell, complexity of the manufacturing process, cost and weight of bipolar plates.

Acknowledgements

Research was founded by Warsaw University of Technology within The Labtech of Excellence program.

9.5 Investigation of FeC catalyst regeneration by coke gasification with CO_2

Stanisław Murgrabia*,1, Robert Cherbański, Tomasz Kotkowski, Eugeniusz Molga, Andrzej Stankiewicz

1. Faculty of Chemical and Process Engineering, Warsaw University of Technology, Warsaw, Poland

e-mail: stanislaw.murgrabia.dokt@pw.edu.pl

KEYWORDS: *catalyst coking, methane pyrolysis, reaction kinetics, coke gasification, TGA*

Steam methane reforming (SMR, Eq. 9.5.1) is the industry-leading hydrogen production process, accounting for approx. 48% of global H_2 production. However, the associated direct CO_2 emissions from the non-CCS process are approximately 9 kg CO_2 equivalent per kg hydrogen.

$$CH_4 + H_2O_{(liq)} \rightarrow 4H_2 + CO_2, \ \Delta H = 63.2 \left(kJ/mol_{H_2}\right) \quad (9.5.1)$$

Carbon dioxide is one of the major greenhouse gases (GHGs) that contribute significantly to global warming, while reducing the carbon footprint remains a key challenge for industry.

Methane pyrolysis (MP) is frequently considered a bridge technology in transitioning from fossil to renewable fuels. The most important benefit of MP is that it produces hydrogen without emitting CO_2. Instead, solid carbon is generated (Eq. 9.5.2) in large quantities (3 kg of C per 1 kg of H_2), which can be utilized or safely deposited.

$$CH_4 \rightarrow 2H_2 + C, \ \Delta H = 37.5 \ (kJ/mol_{H2}) \quad (9.5.2)$$

Although MP can be performed through pure thermal decomposition, the use of different catalysts enhances the process and reduces energy consumption. One of the critical issues associated with MP is catalyst coking, which leads to catalyst deactivation.

This study investigates the regeneration of a selected catalyst via CO_2 gasification. Thermogravimetric analysis (TGA) coupled with gas chromatography was used to monitor mass loss and gas composition. The results confirm that coke gasification proceeds efficiently at elevated temperatures, enablig effective carbon removal and catalyst regeneration. Additionally, increasing CO_2 concentration further enhances this process. These findings demonstrate that CO_2 gasification is a viable strategy for sustaining catalyst performance, ensuring continuous MP operation.

Acknowledgements

Funded by the European Union. Views and opinions expressed are, however, those of the authors only and do not necessarily reflect those of the European Union or the European Climate, Infrastructure and Environment Executive Agency (CINEA). Neither the European Union nor the granting authority can be held responsible for them.

9.6 Separation of oil and water aerosols using plasma modified fiberglass coalescing filters

Małgorzata Purta1*, Andrzej Krasiński, Joanna Kacprzyńska-Gołacka

1. Faculty of Chemical and Process Engineering, Warsaw University of Technology, Warsaw, Poland

e-mail: malgorzata.purta.stud@pw.edu.pl

KEYWORDS: *gas filtration, aerosol separation, coalescing filters, oil and water aerosols, modification of filter media*

This work focuses on the process of separating oil or water mist from an air stream by filtration using flan fiberglass panels operating as coalescing media. Oil and water mist separation is of key importance in several industrial processes where technological or environmental requirements require a specific level of purity of gases.

The research was carried out to assess the efficiency and flow resistance of two modifications of a polymer filter obtained by the physical vapor deposition (PVD) method with AlSiON and ZnSnON coatings (the unmodified commercial grade of fiberglass material was considered as a reference). The external surfaces of the native structure made of glass fiber were covered in the PVD (physical vapour deposition) process coating using magnetron sputtering, thanks to cooperation with the Institute of Sustainable Technologies (Łukasiewicz Research Network in Radom). The influence of the applied layer on the efficiency of the oil aerosol separation process was studied. For the oil-saturated material, also the separation of water aerosol was tested. For the given flow conditions, droplet size distribution and inlet concentration, the pressure drop was recorded and at specific times the separation efficiency (total and fractional) was measured. In order to determine the surface properties important for the operation of coalescing filters, capillary rise and static wetting angles with both liquids used in the experimental separation tests were determined. The analysis of the results focused on two negative parameters of the native structures, which were tried to be eliminated using a plasma-based modification: 1) a sudden increase in the pressure drop during measurements in the saturation state, when the filter was removed from the system several times, and 2) low efficiency of water mist removal by the filter previously saturated with oil.

The experimental results confirmed that by proper modification of surface properties, the capillary conduction, which is responsible for oil "surge" leading to filter blocking, can be significantly reduced. However, reaching a high efficiency of water separation is a much more difficult task. A heterogeneous surface obtained by magnetron sputtering from two targets operated in N_2 and O_2 ambient gases led to a noticeable improvement in removal of water droplets from the air.

Acknowledgements

This work was supported by the Polish National Centre for Research and Development, grant no. TECHMATSTRATEG-III/0005/2019-00.

9.7 Impact of the valved holding chamber (VHC) on the inhalation efficiency of a steroid drug atomized in vibrating mesh nebulizers

Aleksandra Sawczuk*,1, Izabela Kazimierczak, Tomasz Sosnowski

1. Faculty of Chemical and Process Engineering, Warsaw University of Technology

e-mail: aleksandra.sawczuk.stud@pw.edu.pl

KEYWORDS: *nebulization, drug delivery*

Budesonide (BUD) is one of the most widely used glucocorticosteroids, delivered via nebulization (atomization) and inhalation to the respiratory system for treating asthma and other pulmonary diseases. Various types of nebulizing devices are employed to generate aerosol with the required droplet size distribution, including pneumatic, ultrasonic, and vibrating mesh nebulizers (VMNs). The efficiency of drug delivery through nebulization is limited by the cyclical airflow of breathing, as the aerosol continuously released by the nebulizer can only reach the lungs during inhalation. During other parts of breathing, the aerosol is emitted into the environment and wasted, so methods to enhance the availability of nebulizer-generated aerosol for the patient are essential. One potential solution is to use a valved holding chamber (VHC), which accumulates aerosol during exhalation and makes it available for delivery to the lungs during the subsequent inhalation.

The study aimed to evaluate the change in the mass output of five BUD drugs after using the VHC attached to two VMNs: Sanity Silent Mesh and Sanity Fast Mesh. The nebulizers were connected to the breathing cycle simulator ASL 5000 XL (Ingmar Medical, USA), and the aerosol mass was determined gravimetrically.

For all drugs and both VMNs, the amount of aerosol available to the patient increased, even though some aerosol was always deposited within the VHC. The increase in aerosol availability varied depending on the nebulizer design and the specific drug used. The amount of aerosol available to the patient increased by 60–270% compared to nebulization without the VHC.

The study confirmed that a valved holding chamber increases the aerosol dose available for inhalation during therapy using VMNs. However, due to differences in nebulizer design and aerosol characteristics, the quantitative effect is specific to each setup and cannot be generalized. An engineering approach for dispersed systems can help explain the observed phenomena and optimize the use of each nebulizer-chamber combination.

Acknowledgments

Nebulizers and drug products were donated by Albert Polska. The authors thank Prof. Andrzej Emeryk from the Medical University of Lublin for valuable discussions. Work co-supported by project Infrastart CePT.

9.8 Investigation of mixing intensity in plant tank using jet flow mixer

Julia Wilewska[1], Wojciech Orciuch, Łukasz Makowski, Adam Dudała

1. Faculty of Chemical and Process Engineering, Warsaw University of Technology, Poland

e-mail: julia.wilewska.dokt@pw.edu.pl

KEYWORDS: *jet flow mixer, mixing, computational fluids dynamics*

Despite their widespread use in the industry, scientific research on jet flow mixers has yet to be conducted. This type of mixer allows efficient fluid mixing without the risk of injecting gas into the system or using multiple devices such as a pump, traditional jet mixer or rotor-stator. Therefore, determining the optimal positioning of the jet flow mixer in the plant tank is crucial to conducting the cost- and energy-efficient process. Reduced operating costs will allow financing investments in the modernisation of the factory, resulting in further reduction in energy consumption. Lower energy consumption by manufacturers is key to restraining pollution, minimising the production of greenhouse gasses, and making more efficient use of energy from renewable sources, consequently maintaining our planet in a condition not worse than today.

In this study, fluid flow inside the jet flow mixer and the plant tank was considered. The aim of the research was to determine the optimal placement for the jet flow mixer inside the tank. The numerical analysis, performed using computational fluid dynamics software (ANSYS Fluent), consisted of two stages. Initial simulations were performed for the jet flow mixer and allowed the determination of flow rate and power number generated by three types of impellers: propeller impeller and Pitched Blade Turbine with three and four blades. Calculations were performed for impeller rotational speed equal to 1500 rpm. The obtained results were used to simulate fluid flow, mixing intensity, and power consumption inside the plant tank for different positions of the agitator. The simulation was performed in a real-size system – a 30 m^3 cylindrical tank with an ellipsoidal bottom equipped with a mixer with a diameter of 0.4 m. Calculations were performed for six industrially significant fluids with diverse rheological properties (Newtonian, Non-Newtonian and high viscosity fluids).

The modelling approach used in this study allowed the selection of jet flow mixer type and its position in a plant tank, maximising mixing intensity while minimising power consumption for all types of fluids.

10 Abstracts: Mathematical modelling, simulations & optimalization

10.1 Numerical investigation of a ball mill operation during solid suspension fragmentation

Julia Chaładej*[,1], Radosław Krzosa[1], Łukasz Makowski[1], Wojciech Orciuch[1], Radosław Adamek

1. Faculty of Chemical and Process Engineering, Warsaw University of Technology, Poland

e-mail: julia.chaladej.stud@pw.edu.pl

KEYWORDS: *CFD, population balance equation, stirred ball mill*

The population balance equation (PBE) is a measure to describe and understand the time course of processes involving a dispersed phase. However, to account for transport phenomena underlying interactions between a continuous and a dispersed phase and the time evolution of chosen particles' properties the solution of PBE must be coupled with computational fluid dynamics (CFD).

This study represents a numerical investigation of grinding of solid particles in a horizontally stirred ball mill. The milled material was a water suspension of titanium dioxide comprised of agglomerates and aggregates. An empirical method of estimating the coefficient of milling balls' impacts efficiency on deagglomeration was presented. This method is based on measured size distributions of solid particles. Then the obtained values were implemented into a simplified PBE model assuming that the milling chamber interior consists of three zones with different density of balls' impacts energy available for fragmentation. These zones were characterized by an averaged value of granular temperature and residence time of solid dispersion both determined from a flow field calculated using CFD. The averaged model was validated with experimentally measured evolution of the mean size of the solid particles. However, this approach was proven insensitive to changes in the geometry of the milling balls agitator that in fact affect the spatial distribution of the available kinetic energy of balls and the residence time distribution of suspension. Therefore, a detailed approach was formulated in this study. The moments of size distribution of the particles were modeled as scalars transported throughout the milling chamber. The obtained values were coupled with Quadrature Method of Moments to solve population balance equation. This resulted in a more accurate prediction of the mean size of milled particles.

The developed model can be implemented in investigations for process intensification. It enables the evaluation of modifications of the mills' impeller geometry based on the change of mean solid particle size, energy demand for mixing affected by the changes in suspension viscosity during comminution and distributions of the residence time of suspension and of the granular temperature in the chamber space.

10.2 Chemical engineering approach for improving fuel cell efficiency

Monika Jałowiecka*[,1], Łukasz Makowski

1. Faculty of Chemical and Process Engineering, Warsaw University of Technology, Warsaw, Poland

e-mail: monika.jalowiecka.dokt@pw.edu.pl

KEYWORDS: f*uel cell, flow pattern, mass transport, two-phase flow, mesh design*

Fuel cells represent promising electrochemical reactors for high-efficiency electricity generation, aligned with the 2050 carbon neutrality goals. Their fuel flexibility enables operation with both gaseous and liquid fuels. These fuels, when obtained sustainably through renewable energy and atmospheric carbon dioxide capture, render these devices emission-neutral. The deployment of fuel cell technology is being accelerated through extensive research on liquid fuels for instance environmentally benign formic acid. The integration of sustainable fuel production with efficient fuel cell operation presents a viable pathway toward clean energy systems, addressing both environmental concerns and energy demand.

To address the primary challenges in mass transport efficiency in fuel cells, novel flow patterns have been proposed to enhance mixing, ensure uniform distribution of reagents, and facilitate CO_2 bubble removal. This study presents a comprehensive chemical engineering approach from conceptualization to validation in developing a new *mesh* distribution system that demonstrates superior performance compared to conventional serpentine systems in terms of mixing efficiency and pressure drop. The innovative design methodology incorporates advanced computational techniques and experimental validation to optimize the flow field geometry, resulting in enhanced mass transport characteristics and reduced parasitic energy losses.

The research methodology encompasses multiple stages, beginning with the proposal and computational fluid dynamics (CFD) analysis of new flow patterns, followed by optimization for uniform distribution, and culminating in the selection of designs for graphite interconnector milling. Chemical engineering principles provide the framework for mathematical modeling of electrochemical reaction kinetics coupled with transport phenomena. The developed systems underwent experimental validation in a direct formic acid fuel cell, corroborating the computational evaluations. The proposed mesh distribution system, characterized by an 85% contact area between flow channels and electrode, significantly enhances mass transfer and catalyst layer utilization. These advancements in flow field architecture demonstrate the crucial role of chemical engineering in developing more efficient and commercially viable fuel cell systems.

Acknowledgements

Research was funded by the Warsaw University of Technology within the Excellence Initiative: Research University (IDUB) programme.

11 Abstracts: Kinetics & thermodynamics

11.1 Low-temperature Electrolyzers for Simultaneous Hydrogen Generation and Organic Oxidation

Patryk Klemczak*,1, Maria Jarząbek-Karnas, Zuzanna Bojarska, Łukasz Makowski

1. Faculty of Chemical and Process Engineering, Warsaw University of Technology, Warsaw, Poland

e-mail: patryk.klemczak.stud@pw.edu.pl

KEYWORDS: h*ydrogen, electrolysis, green energy*

Since global warming is getting worse due to many factors such as gas emissions, the EU strive for reaching climate neutrality by 2050 through investing in green technologies and using renewable energy sources. Adopting green hydrogen as fuel is one of many solutions that can help in reviving our climate. The colour green indicates that obtained hydrogen was produced through water electrolysis using renewable energy sources. This technology is an ideal cure for the environment, since there are zero greenhouse gas emissions in the process.

However using water in electrolysis is sustainable, its efficiency is poor. In the research we use organic biomass components such as methanol and ethanol instead of water, since it requires less energy and the hydrogen production is higher.

As a result of using biomass components, there is a CO_2 emission through organic oxidation. Although the amount of gas obtained in this process is not large and capturable, to make the whole procedure more safe for the environment, the gas can be utilised or exploited in a different process.

In the study we use commercial PEM electrolyzer with various catalysts dedicated to water and organic fluids. That way it was possible to avoid poisoning the catalysts during the research.

Using organic fuels seems like a promising solution for lowering the costs of hydrogen production.

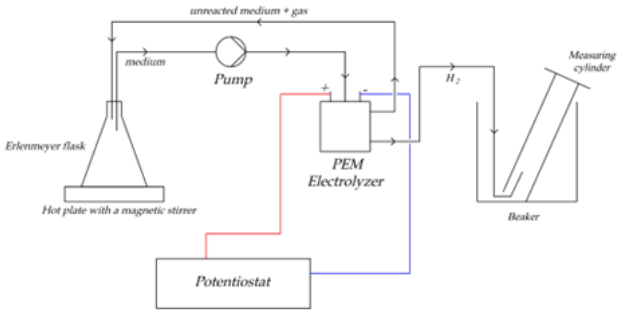

Figure 11.1.1 The diagram of the experimental setup

11.2 Influence of pH and acid catalyst used on the kinetics of methyltrimetoxysilane (MTMS) hydrolysis – *in situ* FT-IR and Raman spectroscopy investigation

Monika K. Klimek*,1, Anna Gibas, Bartosz Nowak, Bartosz Babiarczuk, Jakub M. Gac

1. Faculty of Chemical and Process Engineering, Warsaw University of Technology, Warsaw, Poland

e-mail: monika.klimek3.dokt@pw.edu.pl

KEYWORDS: *aerogel, hydrolysis kinetics, methyltrimetoxysilane (MTMS), Raman, FT-IR*

Organosilica aerogels are materials getting more and more interest due to their unique properties. In order to fully control the parameters of the final materials, it is necessary to fully understand their synthesis process. The two-step sol-gel method is the most widely used one due to the possibility of final product features control through parameters adjustment on both synthesis stages. The first step consists of a precursor hydrolysis reaction, which is preferred under acidic conditions and leads to the formation of sol. This step is controlled by many parameters, such as the precursor type, the ratio of solvent-alcohol to antisolvent-water, as well as the concentration (which affects the pH), and the type of acid (hydrolysis catalyst). The progress and final state of hydrolysis determines the entering state for the second synthesis stage - condensation.

This research investigates the effect of the acid catalyst used and the pH of the reaction mixture on the methyltrimetoxysilane (MTMS) hydrolysis kinetics. The molar ratio of water to precursor was constant, which resulted in a constant ratio of solvent (methanol) to antisolvent. As hydrolysis catalysts, three acids were used: acetic acid, oxalic acid, and sulfuric acid, and four different solution pHs were selected. The Fourier-Transform Infrared (FT-IR) and Raman Spectroscopy were utilised to study the chemical bond reorganisation in time.

The use of two measurement techniques made it possible to formulate a description of the kinetics of MTMS hydrolysis and to observe the formation of the first oligomers at the acid stage. Thus, the influence of hydrolysis parameters on sol stability was determined. The research showed that the progress of the hydrolysis step depends not only on the acid used but also on the pH of the reaction mixture. This research provides a better understanding of the first step in the sol-gel synthesis of organosilica aerogels and provides a basis to establish a correlation between sol-gel synthesis kinetics and the final product morphological parameters.

Acknowledgements

This work was founded by the Polish National Science Center (NCN) under the OPUS-LAP programme grant No. 2022/47/I/ST8/02979, "Multi-scale numerical modelling of condensation and mechanical properties of organosilica-based aerogels".

11.3 Investigation of microwave dehydration of hydrated salt ($MgSO_4 \cdot 7\ H_2O$) for its possible use as an energy carrier

Bartosz Sobolewski*[,1], Tomasz Kotkowski[1]

1. Faculty of Chemical and Process Engineering, Warsaw University of Technology, Warsaw, Poland

e-mail: bartosz.sobolewski.stud@pw.edu.pl

KEYWORDS: *microwave dehydration, energy carrier, microwave efficiency, magnesium sulfate*

In the times of climate and ecological crises, it is crucial to improve techniques for using renewable energy sources. The ability to effectively manage them is a part of the implementation of sustainable development principles. Storing renewable energy during periods of excess energy production is an important issue. One promising approach is to store energy in a product of a reversible chemical reaction.

In this work, energy storage by microwave dehydration of a hydrated salt ($MgSO_4 \cdot 7H_2O$) was investigated. RM800pc microwave reactor (Plazmatronika, Poland) with a multimode cavity and a microwave choked outlet was employed for the experiments. The power of generated microwaves at a frequency of 2.45 GHz was in the range of 0 – 72 W. The reaction was carried out in a quartz glass column. The temperature was measured at three points throughout the column's height using a TMI4 multi-channel temperature recorder from FISO Technologies Inc. (Canada) with four FOT-L-SD fiber-optic temperature sensors. The fourth sensor was used to measure the ambient temperature. During the dehydration reaction an atmosphere of an inert gas (nitrogen) was maintained, where the volumetric flow rate of the gas was kept constant for each experiment and was from the range of 200 – 1000 Nml/min. The nitrogen flow rate was stabilized by the mass flow rate regulator β-ERG-1MPSb (BetaErg, Poland). During the hydration reaction a flow of nitrogen – water vapour mixture (saturated at 25°C) was used instead of the dry N_2.

On the basis of the calorimetric measurements it was possible to determine the effectiveness of the energy storage in $MgSO_4 \cdot 7H_2O$ as well as microwave – thermal energy conversion effectiveness. It should be noted that certain issues were encountered as far as the energy recovery from the salt bed is concerned. Taking SEM photos allowed us to examine changes in the structure of salt crystals after dehydration, which was helpful to assess the reasons for the low efficiency of the salt hydration. Nonetheless, if the concept of thermochemical energy storage is to be of practical significance, further research is needed to study causes of the mentioned problem and propose plausible solutions.

12 Abstracts: Other

12.1 Nitrate-selective potentiometric sensor based on carbon nanomaterials – characteristics

Martyna Drużyńska*,1, Nikola Lenar, Beata Paczosa-Bator

1. Faculty of Material Science and Ceramics, AGH University of Krakow, Kraków, Poland

e-mail: druzynska@agh.edu.pl

KEYWORDS: *potentiometry, carbon nanomaterials, single-piece electrode, ion-selective electrode*

The search for new materials and design solutions enables ion-selective electrodes to detect a wide range of analytes while demonstrating improved performance parameters. In this research graphene, carbon black and carbon nanotubes are introduced as modifiers for a PVC-membrane.

The construction of the potentiometric sensor relies on introducing carbon nanomaterials directly into the polymeric membrane. Membranes were casted on the glassy carbon (GC) disc electrodes using the drop casting technique. The measurements of electrical parameters were performed with chronopotentiometry and Electrochemical Impedance Spectroscopy to determine electrical parameters of the electrode such as electrical capacity and resistance. The potentiometric measurements were performed to determine analytical parameters of the electrode such as sensitivity, repeatability, limit of detection, redox sensitivity.

The addition of carbon materials improved the analytical parameters of the sensor. The use of graphene, carbon black and carbon nanotubes results in a near-Nernstian response (54 mV/pNO_3^-) towards nitrate ions over a wide linear range (from 10^{-1} to 10^{-6} M NO_3^-). Despite the addition of carbon nanomaterials to the polymeric membrane, designed electrodes do not exhibit redox sensitivity. The high electrical capacity (up to 900 µF) of electrodes results in good stability of the potentiometric response. The presented design solution allows for the simplification of sensors' preparation.

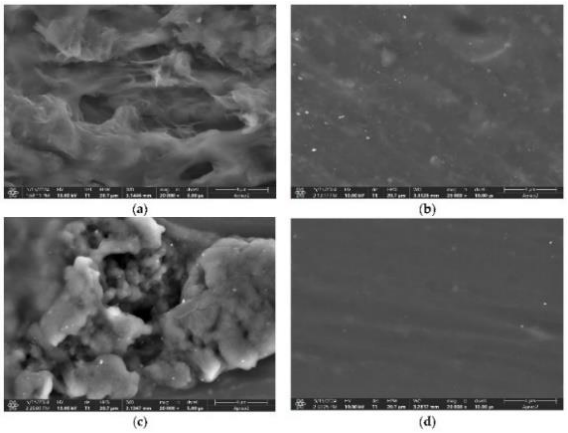

Figure 12.1.1 SEM scans of cross-sections of PVC membranes; (a) membrane modified with graphene, (b) membrane modified with carbon black, (c) membrane modified with carbon nanotubes, (d) non-modified membrane

Acknowledgements

This research project was supported by the program titled "Excellence initiative–research university" at the AGH University of Krakow.

12.2 Application of nitrate-selective potentiometric sensor based on black PVC membrane

Martyna Drużyńska*,1, Nikola Lenar, Beata Paczosa-Bator

1. Faculty of Material Science and Ceramics, AGH University of Krakow, Kraków, Poland

e-mail: druzynska@agh.edu.pl

KEYWORDS: *potentiometry, single-piece electrode, ion-selective electrode, nitrates*

In the beginning of 20th century M. Cremer demonstrated opportunities of the glass electrode for the first time thus constructed the first ion-selective electrode (ISE). The search for new materials and design solutions enables ion-selective electrodes to detect a wide range of analytes. Desirable analytical parameters of ion–selective electrodes are low limit of detection, high selectivity and sensitivity.

The main goal of the research was to construct a new type of a potentiometric sensor with enhanced analytical parameters for nitrates detection. Carbon nanomaterials were introduced as modifiers for PVC membranes for single-piece electrode. Constructed sensor allows to detect nitrate ions over a wide linear range from 10^{-1} to 10^{-6} M NO_3^-. This nitrate-selective potentiometric sensor can be used in environmental sample research such as water river. The measurements were performed in order to examine the analytical and electrical properties of designed electrodes. The potentiometric measurements were performed on the 16–channel potentiometer by Lawson Labs.

Using a newly designed ion-selective electrode, research on environmental samples can be conducted quickly, easily, and economically. The carbon–based electrodes are characterized by stable potential, repeatability and high-selectivity. The designed ion-selective electrodes find theirs use in water quality monitoring. This research has created new opportunities to design efficient potentiometric sensors with improved performance parameters for environmental monitoring.

Acknowledgements

This research project was supported by the program titled "Excellence initiative–research university" at the AGH University of Krakow.

12.3 Optimization of a photocatalytic C-alkylation reaction in a 3D printed photoreactor

Gergő Gémes[1], Dóra Richter[1], Péter Kisszékelyi, József Kupai[1]*

1. Budapest University of Technology and Economics, Department of Organic Chemistry and Technology, Budapest, Hungary

e-mail: kupai.jozsef@vbk.bme.hu

KEYWORDS: *photocatalysis, visible light, optimization, Design of Experiments*

Photocatalysis is having its renaissance. Its main advantage is that it enables us to carry out reactions in especially mild conditions, which can be useful in the late-stage functionalization of pharmaceuticals.

During our previous work we executed an open-source 3D printed photoreactor plan, which can provide fine control over the reaction parameters. We expanded the substrate scope of a known photocatalytic C–alkylation reaction, catalyzed by 4CzIPN. (Figure 12.3.1 a, b) We found eight new substrates, (Figure 12.3.1 c) one of which is methyl cyanoacetate. It is pharmaceutically relevant as an amino acid precursor. Its alkylation reaction reached 43% yield in 5 hours. We set out to optimize this reaction in the 3D printed reactor using Design of Experiments. First, we tested 15 solvents and 8 bases, then we optimized the reaction according to the relevant parameters.

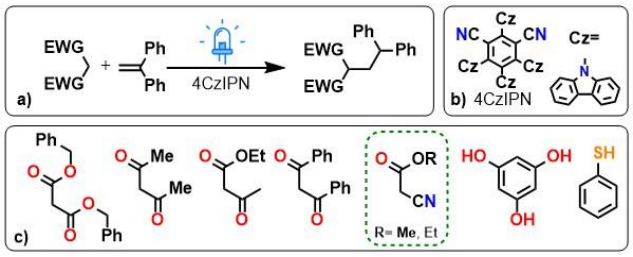

Figure 12.3.1 a) The alkylation of CH-acidic compounds b) 4CzIPN= 2,4,5,6-Tetrakis(9H-carbazol-9-yl) isophthalonitrile c) The expanded substrate scope

Acknowledgements

This research was funded by the National Research, Development, and Innovation Office (FK138037), the Excellence PhD Scholarship of the Richter Gedeon Talentum Foundation. National Research, Development and Innovation Fund (RRF-2.3.1-21-2022-00015) has been implemented with the support provided by the EU.

12.4 Synthesis of a metal-free photocatalyst and its applications in C-C bond formation reactions

Kinga Imola Hangya[1], Gergő Gémes, Dóra Richter, Péter Kisszékelyi, József Kupai*

1. Budapest University of Technology and Economics, Department of Organic Chemistry and Technology, Budapest, Hungary

e-mail: kupai.jozsef@vbk.bme.hu

KEYWORDS: *photocatalysis, C–C bond formation, Design of Experiments*

Nowadays photocatalysis is having a renaissance as it is an excellent tool for environmentally friendly chemical reactions. It allows us to carry out reactions under mild conditions, which is especially useful in the late-stage functionalization of pharmaceuticals.

Our aim was to produce 4CzIPN by a mechanochemical method. **(**Figure 12.4.1a**)** With this photocatalyst, we successfully carried out C-C bond formation reactions of 1,1- diphenylethylene with 8 different CH-acidic substrates.

Initially in the coupling reaction between methyl cianoacetate and 1,1- diphenylethylene **(**Figure 12.4.1b**)** 43% yield was achieved. Our further goal was to improve this yield by design of experiment.

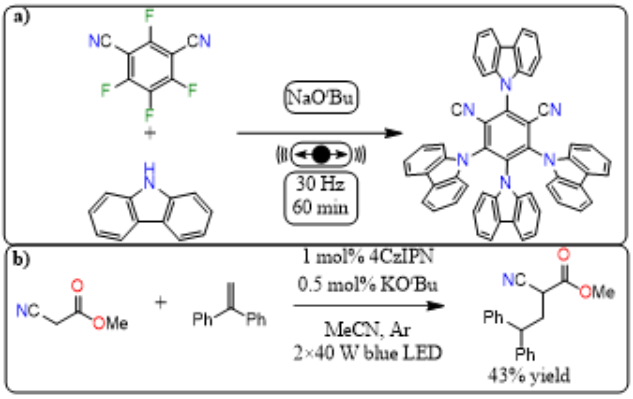

Figure 12.4.1 a) Synthesis of 4CzIPN by a mechanochemical method. b) Coupling reaction between methyl cianoacetate and 1,1- diphenylethylene

Acknowledgements

This research was funded by the National Research, Development, and Innovation Office (grant number FK138037), National Laboratories Programme (PharmaLab, RRF-2.3.1-21-2022-00015), the Richter Gedeon Excellence PhD Scholarship of the Richter Gedeon Talentum Foundation, Gedeon Richter Plc. (D. R.) and the University Research Scholarship Programme, Ministry for Culture and Innovation, National Research, Development and Innovation Fund (EKÖP-24-1-BME-226).

12.5 Assay of B_2 vitamin content in diary products using fluorescence spectroscopy method

Dominik Műller*,1, Agata Krakowska, Beata Paczosa-Bator

1. Department of Analytical Chemistry and Biochemistry, AGH University of Krakow, Krakow, Poland

e-mail: domul@agh.edu.pl

KEYWORDS: *riboflavin, fluorescence, vitamin B2, fluorescence spectrometry, dairy products*

Milk and dairy products have been a foundation for many Western countries since ancient times. As the main food source for developing mammals it provides mayny key nutrients including fats, proteins and vitamins, with vitamin B_2 being the main subject of the presented study. Over the years the more refined methods of dairy farming and processing required rigorous quality control to ensure the safety of the consumers and to provide the most nutritious addition to their diet. This gave raise to many simple, fast and cheap assay methods meant to be the basis for proper certifications that ensure that the dairy produce entering circulation meets all the necessary guidelines.

Vitamin B_2, known also under the name riboflavin, is a vitamin that plays a vital role in many biological processes in human body. Its deficiency may result in variety of dire consequences, including stunted growth, skin issues, cataracts, balding and fertility problems. Dairy products provide one of the simples, most straightforward sources of dietary riboflavin, though a rising concern with the loss of nutritional value through processes like pasteurization prompts diary producers to reevaluate their quality control methods to better fit the demand from the consumers.

One of the characteristic qualities of riboflavin is its ability to produce fluorescence spectra. Fluorescent qualities of substances have been a basis for assay using fluorescence spectroscopy method. This method uses the yielded fluorescent spectra and their changes, to quantify the concentration of fluorescent substance in the sample. Moreso, fluorescent substances display characteristic fluorescent spectra, which may be a basis for qualitative assay of samples with complex organic matrixes.

In this study a quantity control method has been created, using simple methods, like centrifugation of the samples, and widely available reagents, like acetic acid. The method has been validated and the data observed in the study proves processes like pasteurization have little effect on the content of riboflavin in the provided milk samples, with the fat content of the milk being much more important of a factor and with the highest concentration of riboflavin retained in unpasteurized milk.

Acknowledgements

Research project supported by program "Excellence initiative-research university" for the AGH University of Krakow.

Index of Authors

Index of keywords

Cover design
Maria Ziółkowska, mariamz11@wp.pl

Paper review team
Lead by Monika Klimek
Jakub Lewandowski, Aleksandra Pisarek, Amini Seyedshoja,

Typesetting team
Layout and formatting by Grzegorz Bernacki & Izabela Kazimierczak
Zuzanna Dąbała, Zuzanna Kupniewska, Adrian Malinowski, Karolina Traczyk

ISBN 978-83-953822-5-3